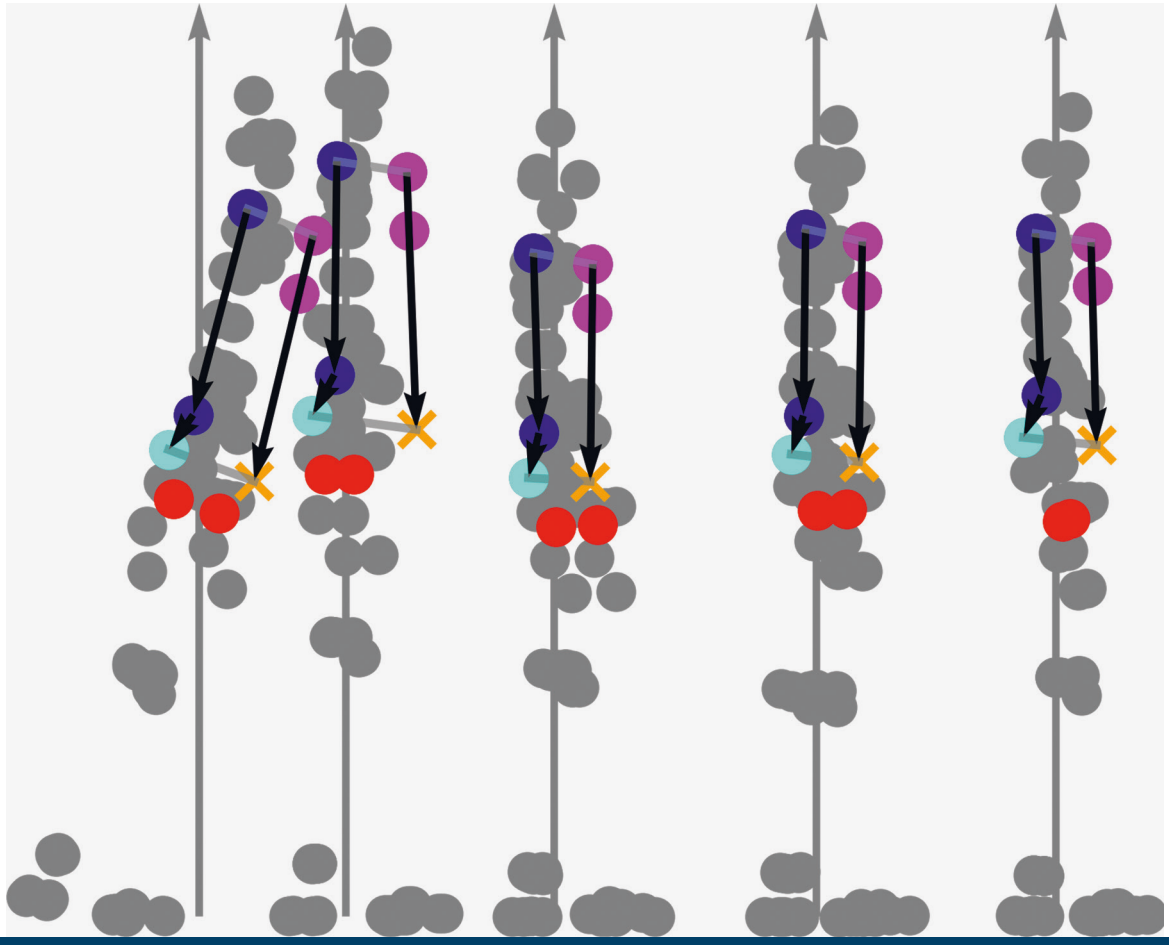

Towards Improved Civil Safety: Experimental Insights into Impulse Propagation through Crowds

Sina Feldmann

IAS Series
Band / Volume 70
ISBN 978-3-95806-828-5

Mitglied der Helmholtz-Gemeinschaft

JÜLICH
Forschungszentrum

Schriften des Forschungszentrums Jülich
IAS Series Band / Volume 70

Forschungszentrum Jülich GmbH
Institute for Advanced Simulation (IAS)
Zivile Sicherheitsforschung (IAS-7)

Towards Improved Civil Safety: Experimental Insights into Impulse Propagation through Crowds

Sina Feldmann

Schriften des Forschungszentrums Jülich
IAS Series

Band / Volume 70

ISSN 1868-8489

ISBN 978-3-95806-828-5

Bibliografische Information der Deutschen Nationalbibliothek.
Die Deutsche Nationalbibliothek verzeichnet diese Publikation in der
Deutschen Nationalbibliografie; detaillierte Bibliografische Daten
sind im Internet über http://dnb.d-nb.de abrufbar.

Herausgeber und Vertrieb:	Forschungszentrum Jülich GmbH Zentralbibliothek, Verlag 52425 Jülich Tel.: +49 2461 61-5368 Fax: +49 2461 61-6103 zb-publikation@fz-juelich.de www.fz-juelich.de/zb
Umschlaggestaltung:	Grafische Medien, Forschungszentrum Jülich GmbH
Druck:	Grafische Medien, Forschungszentrum Jülich GmbH
Copyright:	Forschungszentrum Jülich 2025

Schriften des Forschungszentrums Jülich
IAS Series, Band / Volume 70

D 468 (Diss. Wuppertal, Univ., 2024)

ISSN 1868-8489
ISBN 978-3-95806-828-5

Vollständig frei verfügbar über das Publikationsportal des Forschungszentrums Jülich (JuSER)
unter www.fz-juelich.de/zb/openaccess.

Abstract

Crowds range in size from a few dozen to thousands or even millions of people and convey a sense of community. However, they pose significant risks and dangers to individuals. Investigating the dynamics of crowds is therefore essential to minimise these hazards and avoid potential crowd accidents. Previous research has often neglected the propagation of impulses or the risk of losing balance, although both are considered high-risk scenarios. To address these challenges, laboratory experiments were conducted in which participants standing in crowds of different sizes were pushed forward. The resulting analyses of these experiments were published in three papers that comprise the main part of this dissertation.

The first publication provides a quantitative analysis of the relationship between the intensity of impulses and the distance and speed at which impulses propagate. The resulting mathematical equations serve as a valuable tool for understanding impulse propagation in a row of people. The second paper delves deeper into the participants' 3-dimensional movement during impulse propagation. Through analysis of the forward velocity, margin of stability, and distance between participants, individual reactions could be divided into three temporal phases: receiving or passing on the impulse as well as an intermediate phase between these two. The identification of these phases represents a significant contribution to understanding the emergence of various risks such as wave movements and individual falls. The third publication extends the concept of impulse propagation in crowds to a larger scale. It unveils novel information, demonstrating that the initial inter-person distance and impulse intensity are key factors influencing propagation speed. Additionally, it reveals the occurrence of an absorption effect along long rows. The study concludes with the introduction of heat maps that showcase the magnitude of impulse-induced impacts depending on the position within crowds.

Overall, the findings of these three papers provide valuable insights into impulses and 3D motion propagation in crowds. This enables a more accurate description of human behaviour and contributes to increasing the reliability of models for predicting dangerous situations, which can lead to a significant improvement in civil safety.

Zusammenfassung

Menschenmengen variieren in ihrer Größe von einigen Dutzend bis hin zu Tausenden oder sogar Millionen von Menschen und können ein Gefühl von Gemeinschaft vermitteln. Allerdings bergen sie auch erhebliche Risiken und Gefahren für den Einzelnen. Die Erforschung der Dynamik von Menschenmengen ist daher unerlässlich, um diese Gefahren zu minimieren und mögliche Unfälle zu vermeiden. Bisherige Untersuchungen haben die Ausbreitung von Kraftstößen oder das Risiko, das Gleichgewicht zu verlieren, oft vernachlässigt, obwohl beide als hochriskante Szenarien gelten. Um diese Herausforderungen anzugehen, wurden Experimente durchgeführt, bei denen Teilnehmende, die in Gruppen unterschiedlicher Größe standen, nach vorne geschubst wurden. Die daraus resultierenden Auswertungen wurden in drei Artikeln veröffentlicht, die den Hauptteil dieser Dissertation bilden.

Die erste Veröffentlichung liefert eine quantitative Analyse des Zusammenhangs zwischen der Intensität von Kraftstößen und der Entfernung sowie Geschwindigkeit, mit der sich Kraftstöße ausbreiten. Die sich daraus ergebenden mathematischen Gleichungen dienen als wertvolles Hilfsmittel zum Verstehen der Stoßausbreitung in einer Reihe von Personen. Der zweite Artikel befasst sich eingehender mit der 3-dimensionalen Bewegung der Teilnehmenden während der Stoßausbreitung. Durch die Analyse der Vorwärtsgeschwindigkeit, der Stabilitätsgrenze und des Abstands zwischen den Teilnehmenden konnten die individuellen Reaktionen in drei zeitliche Phasen unterteilt werden: Empfang oder Weitergabe des Kraftstoßes sowie eine Übergangsphase zwischen diesen beiden. Die Identifizierung dieser Phasen stellt einen wichtigen Beitrag zum Verständnis der Entstehung verschiedener Risiken wie z.B. Wellenbewegungen und individuelle Stürze dar. Die dritte Veröffentlichung erweitert das Konzept der Ausbreitung von Kraftstößen in Menschenmengen auf einen größeren Maßstab. Sie zeigt, dass der anfängliche Abstand zwischen Personen und die Intensität des Kraftstoßes Schlüsselfaktoren sind, die die Ausbreitungsgeschwindigkeit beeinflussen. Außerdem deckt sie das Auftreten eines Absorptionseffekts entlang langer Reihen auf. Die Untersuchung schließt mit der Einführung von Heatmaps, die das Ausmaß der stoßbedingten Auswirkungen abhängig von der Position veranschaulicht.

Insgesamt liefern die Ergebnisse dieser drei Arbeiten wertvolle Erkenntnisse über die Ausbreitung von Kraftstößen und 3D-Bewegungen in Menschenmengen. Dies ermöglicht eine genauere Beschreibung des menschlichen Verhaltens und trägt dazu bei, die Zuverlässigkeit von Modellen zur Vorhersage gefährlicher Situationen zu erhöhen, was zu einer erheblichen Verbesserung der zivilen Sicherheit beiträgt.

Acknowledgements

I am deeply grateful to all those who have contributed to the realisation of this dissertation.

First and foremost, I would like to thank my doctoral supervisor, Prof. Dr. Armin Seyfried, for his exceptional expertise, insightful discussions, and encouragement throughout my research. I would like to express my gratitude to Dr. Juliane Adrian for her excellent supervision and invaluable contributions. It was a delight to work with her, and her support and guidance have been key in helping me complete this dissertation. I would also like to thank Dr. Maik Boltes for the enthusiastic discussions and his advice. Especially, I am immensely grateful for his assistance in merging the 3D MoCap data with head trajectories.

I would like to acknowledge the support of the CrowdDNA project and all collaborators. I am particularly thankful to Anna Sieben and Helena Lügering for stimulating discussions from various perspectives and effective experiment planning. Furthermore, I am grateful to Jernej Čamernik for his knowledge regarding the pressure sensors and his commitment during the experiments. I would like to thank Marc Ernst for his ideas on the experimental setup and Thomas Chatagnon for his tips on biomechanics. I highly appreciate the opportunity to participate in numerous project meetings, which have been very beneficial to my professional development.

I would like to acknowledge the German Academic Exchange Service (DAAD) scholarship, which allowed me to spend two months with INRIA in Rennes, France. My special thanks go to Dr. Julien Pettré and The VirtUs group, who welcomed me warmly and made my stay worthwhile.

I am very grateful to my colleagues at IAS-7 for ensuring that my time in Jülich was so enjoyable. In particular, I would like to thank everyone who volunteered to participate in the experiments and all the helping hands. The experiments would not have been as successful without the help of Alica Kandler, Tobias Schrödter, and Ann Katrin Boomers. Many thanks also to Deniz Kilic for his assistance in processing and, most importantly, visualising the 3D data in Blender and PeTrack.

Finally, a huge thank you goes to my family and friends for their unwavering encouragement and understanding. I am extremely grateful to Florian; his constant support and advice have been essential. Without his help, I would not be where I am today.

List of Publications

Journal Publications included in this Thesis

Publication A
Feldmann, S., Adrian, J. (2023). Forward propagation of a push through a row of people. Safety Science, 164, 106173. doi: 10.1016/j.ssci.2023.106173

Publication B
Feldmann, S., Chatagnon, T., Adrian, J., Pettré, J., Seyfried, A. (2024). Temporal segmentation of motion propagation in response to an external impulse. Safety Science, 175, 106512. doi: 10.1016/j.ssci.2024.106512

Publication C
Feldmann, S., Adrian, J., Boltes, M. (2024). Propagation of Controlled Frontward Impulses Through Standing Crowds. Collective Dynamics, 9, 1-17.
doi: 10.17815/CD.2024.148

Other Journal Publications

Publication D
Boomers, A. K., Boltes, M., Adrian, J., Beermann, M., Chraibi, M., Feldmann, S., Fiedrich, F., Frings, N., Graf, A., Kandler, A., Kilic, D., Konya, K., Küpper, M., Lotter, A., Lügering, H., Müller, F., Paetzke, S., Raytarowski, A.-K., Sablik, O., Schrödter, T., Seyfried, A., Sieben, A., Üsten, E. (2023). Pedestrian Crowd Management Experiments: A Data Guidance Paper. Collective Dynamics, 8, 1–57. doi: 10.17815/CD.2023.141

Publication E
Chatagnon, T., Feldmann, S., Adrian, J., Olivier, A.-H., Pontonnier, C., Hoyet, L., Pettré, J. (2024). Standing Balance Recovery Strategies of Young Adults in a Densely Populated Environment Following External Perturbations. Safety Science, 177, 106601. doi: 10.1016/j.ssci.2024.106601

Table of Contents

Abstract i

Zusammenfassung iii

Acknowledgements v

List of Publications vii

Introduction 1

Bibliography 9

Publication A. Forward propagation of a push through a row of people . **17**

1. Introduction 19
2. Methods 20
   - 2.1 Experimental setup 20
   - 2.2 Procedure and variations 21
   - 2.3 Data sets 22
     - 2.3.1 Video recordings 22
     - 2.3.2 3-dimensional inertial motion capturing 22
     - 2.3.3 Pressure 23
     - 2.3.4 Accuracy 24
3. Results 25
   - 3.1 Pressure measurement 25
   - 3.2 Propagation distance of a push 27
   - 3.3 Propagation speed of a push 27
4. Discussion 30

S. Supplementary Information 36
   - S1 Pressure measurement 36
   - S2 Moderation analysis 37

Publication B. Temporal segmentation of motion propagation **39**
1. Introduction 41
2. Methods 43
2.1 Experiments 43
2.2 Analytical methods for the analysis of MoCap data 44
2.2.1 Distance between a point and a line in a 2D plane . . 44
2.2.2 Distance between a point and a line segment in a 2D plane 44
2.2.3 Distance between two line segments in a 2D plane . . 45
2.2.4 Forward speed and acceleration 45
2.2.5 Projection of 3D position to a plane 46
3. Analysis 46
3.1 Qualitative description of phases of motion 46
3.2 3D data from MoCap 47
3.2.1 Contact 48
3.2.2 Start of motion 50
3.2.3 Perturbation and loss of standing balance 51
4. Results and Discussion 53
4.1 Detection of the phases 53
4.2 Occurrence and duration of phases 56
4.3 Applicability 59
4.4 Limitations 60
5. Conclusion and Outlook 60
S. Supplementary Information 67
S1 Analysed points of MoCap data 67
S2 Identification of the threshold values 67
S2.1 Closest distance between participants 67
S2.2 Acceleration and velocity 68
S2.3 Perturbation and loss of standing balance 69
S3 Analysis of the duration of phases relative to the intensity of external impulses 70

Publication C. Propagation of controlled frontward impulses **75**
1. Introduction 76
2. Methods 77
2.1 Experiments 78
2.2 Data sets 79
2.3 Analysis 79
3. Results 84
3.1 Comparison to five-row experiments 84

3.1.1 Preparation 84
3.1.2 Propagation speed 84
3.1.3 Propagation distance 86
3.2 Comparison of the two detection methods 87
3.3 Extension to side 87
4. Discussion 88
4.1 Limitations 88
4.2 Conclusion 89
S. Supplementary Information 93
S1 Experimental Data 93
S2 Moderation analysis 93

Introduction

Motivation and State of the Art

With a growing population, larger events, and denser cities, crowd management is becoming increasingly important to ensure safety in public spaces. When we are out in public, we can often encounter crowds. People gather in bustling streets, train stations, or shopping centres. Individuals may have different destinations here, while in other scenarios, such as concerts, demonstrations, sporting events, or during the evacuation of a building, everyone has similar intentions. Crowds can vary in size, from a few dozen to thousands or even millions of individuals. These different settings and individual behaviours contribute to the variety of dynamics that can be observed. While crowds can create a sense of excitement and community, they can also pose significant risks and harm to individuals. Due to their high number of casualties, accidents in crowds are the subject of numerous reports in the media [1]. The Love Parade in Duisburg (2010), the Islamic pilgrimage to Mecca (2015), and the Halloween celebrations in Seoul (2022) that caused 21, 2431, and over 150 deaths, respectively, and left many more injured [2, 3] are, unfortunately, only a few examples. An essential step towards preventing similar tragedies from happening in the future is to investigate crowd dynamics and identify their causes and the associated risks.

The focus of this thesis lies on standing crowds in which physical contact between individuals occurs. In these dense crowds, e.g. in waiting queues or at festivals and concerts, a combination of falls and macroscopic waves has been found to pose an enormous risk [4]. Consequently, it is crucial to integrate both the *macroscopic* movements of the crowd as a whole as well as individual *microscopic* behaviour when studying pedestrian motion, and more experimental data, especially in 3D, is needed.

This distinction between a macroscopic and a microscopic point of view historically originates from model development, but can be applied equally well to empirical research. On the macroscopic level, no distinction is made between individuals and key figures, such as density and flow, can only be meaningfully defined within a group [5]. On the microscopic level, pedestrians are analysed individually, focusing, for example, on velocity and heading. Until a few years ago, these analyses were carried out in two dimensions considering only the xy-plane: When studying on-site observations [6, 7] or analysing accidents [8, 9], researchers focused on head trajectories as the main body is often occluded. Also in experimental settings, trajectories that track the head position in the xy-plane were usually recorded [10].

The same applies to pedestrian models where agents were frequently simplified as shapes like circles or ellipses [11, 12]. On the microscopic scale, the use of novel sensors and techniques additionally allows to investigate three-dimensional movements. This is an important improvement since the risk of falling down can naturally only be explained in 3D.

This description of crowd dynamics on varying degrees of spatial (but also temporal) resolution often draws parallels with physics [13]. For example, the velocity or flow through a facility or the density distribution of a crowd are employed as macroscopic features [10, 14, 15]. In the greatest simplification, the temporal average or the peak values of these characteristics are examined in order to determine the areas with a possible risk, e.g. with the highest density [16, 17]. However, in some scenarios, a more detailed description is required to identify potentially dangerous situations, as complex movement patterns are not captured otherwise. Therefore, it is necessary to consider additional aspects of spatial and temporal correlations.

Time-varying densities or velocities allow a more detailed view of the entire crowd, providing a deeper insight into macroscopic phenomena and sudden collective movements considered high-risk. These involve density waves [18], pressure waves [4, 19], or turbulences [8, 20] where the density periodically increases and decreases along the crowd. Such phenomena are comparable to fluids and can be described using hydrodynamics [21, 22]. Collective movements were investigated in experiments where pedestrians moved in a direction transverse to the desired direction [23, 24] or clogging occurred in front of bottlenecks [25, 26].

To better understand the emergence of these phenomena, we take a closer look at the microscopic scale, as individuals interacting with each other can be the cause of these macroscopic dynamics. One example of such a interaction is pushing with the aim of reaching a destination faster, whereby the density is increased [24, 27]. Pushing behaviour includes closing gaps, overtaking, and moving forward [28, 29]. Lack of space or limited freedom of movement at high densities can also lead to unintentional physical contact between people [30].

While established theoretical frameworks such as the Social Force Model [31] try to avoid contact between pedestrians due to repulsive forces, the process of how an impulse is transmitted during physical contact and how it affects body movements can only be explained in three dimensions when individual limb movements are additionally considered. In this way, the falling over of people forming a pile, another dangerous phenomenon observed in actual accidents, [4, 30] could also be investigated.

Nevertheless, pedestrian models are valuable tools for studying and managing crowds of people. They are versatile, cost-effective, and can test scenarios that cannot be replicated in real-life experiments. The suitability of predictive models depends on the particular application. For instance, 2D models are sufficient for evaluating evacuation times or determining potential traffic congestion. Although models continue to evolve, for example, to simulate escape behaviour [32], shock waves through a crowd [33], or physical contacts [34, 35], incorporate crowding forces [36], and model the propagation of disturbances [37], limitations still need to be addressed. In particular, the propagation of impulses and their effects are neglected in the models. While the "domino model" attempts to approach this issue,

it represents individuals as simplified dominoes and does not include individual limb movements [38]. To better understand the complex dynamics of dense crowds, more data should be collected to validate and improve models that can accurately capture these dynamics.

Forces and Loss of Balance

A force is defined as a physical quantity that changes the velocity of a body or deforms it. In pedestrian research, one distinguishes between external and internal (muscular) forces. Gravity as an external force keeps pedestrians firmly on the ground, and if they lose balance, it is the reason why they fall down. Other external forces can also lead to a change in posture. Internal muscular forces can either be a reaction to an external perturbation or exerted deliberately. Determining these different kinds of forces in a crowd can be challenging since multiple forces act from different directions and can change over time. As a simplification, pressure sensors can record the normal component of the resulting force on a given surface. For example, this method has been employed to measure pressure on the wall and the door jamb during crowd evacuation [39] and pressure between participants [40–43]. Alternatively, an individually perceived risk value has been used to estimate the experienced forces [44]. While these studies estimate the magnitude of contact forces, they do not link pressure data to motion data.

Given that forces change with time, it is better to compare impulses, which are defined as the transfer of a force over a specific time. An impulse in a crowd, also commonly understood as a push, can be an external perturbation for a person that causes a change in momentum. In small-scale experiments with the respect to the number of participants or size of the crowd, body postures and motions of maximal two people [45] or collision dynamics along a row of five people [38] are analysed as a response to a push. These findings are relatively limited when applied to larger crowds. Furthermore, the individual three-dimensional movement is not examined in detail, and the analysis of how people regain their balance and how this motion propagates is missing.

When an impulse is exerted, a person is displaced from their resting position, which can lead to a loss of balance. In the worst case, this means stumbling or falling. The balance in a stationary condition is maintained when the projected Centre of Mass (CoM) on the ground is within the Base of Support (BoS), corresponding to the area of contact with the supporting surface [46]. New methods were suggested to examine balance in dynamic situations, including the extrapolated Centre of Mass (XCoM) [47, 48], Margin of Stability (MoS) [47, 49, 50], or Time-to-boundary (Ttb) [51–53]. To regain balance, various strategies, such as ankle, hip, or stepping, were reported in single-participant studies [46, 54, 55]. Another change-in-support option is the use of arms, e.g. grasping a handle [56]. However, the influence of other people's presence on balance recovery was not investigated.

Own Contributions

The research for this dissertation was carried out within the framework of CrowdDNA, a collaborative project funded by the European Commission to bridge different

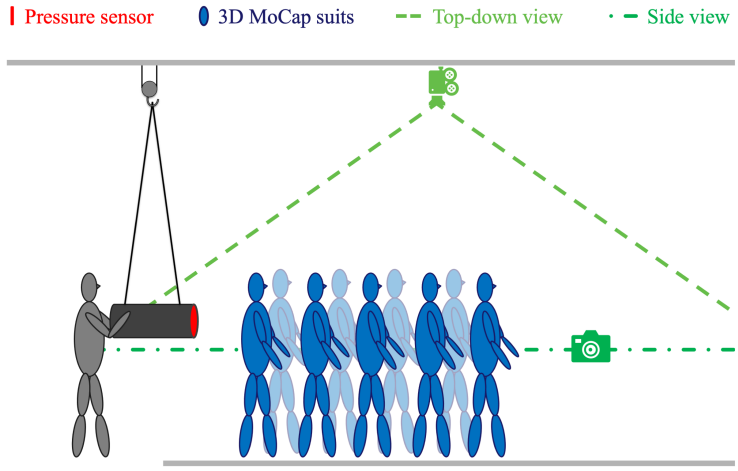

Figure 1: Schematic illustration of the experimental setup for this dissertation. Participants were pushed with a punching bag to which a pressure sensor was attached. Each trial was filmed from above and from the side. The individual body movements were recorded using 3D motion capturing (MoCap) suits. Taken together, this setup allowed to integrate all individual movement data into a common reference system. These fused 3D profiles could then be qualitatively compared with the recorded side view. Furthermore, the experiments link individual reactions following an external perturbation to quantitative pressure data.

crowd movements and provide new technologies for crowd management [57].

This dissertation aims to determine the propagation of impulses in a crowd and develop a method for investigating the 3D dynamics of an individual who loses balance and whose movements to recover balance are restricted by surrounding people. To this end, we designed, conducted, and analysed laboratory experiments with varying numbers of participants. Laboratory experiments have the advantage of being relatively precise and allowing for large amounts of data to be collected. Several parameters can be varied, while others are kept constant. In addition, starting with a small sample size and increasing the number of participants, as well as considering one direction at first, simplifies the scenario. These factors enable an isolated analysis of the effect impulses have on standing crowds. My analysis focuses on experiments in which the rearmost person of a standing crowd was pushed forward in a controlled manner (see Figure 1). Impulses were generated manually by one of the experimenters using a horizontally suspended punching bag. To begin this research, we started with a simplified scenario: A row of five people represented a small crowd, and only one pushing direction – a frontward impulse coming from behind – was considered [58]. In the next step, extended experiments were conducted with up to 36 participants standing in various formations [59].

The experiments were recorded from two perspectives, one from above and the other from the side. The purpose was to gather head trajectories [60, 61] and qualitative observations, respectively. Participants wore *Xsens* [62] full body motion-capturing (MoCap) suits consisting of 17 inertial measurement units (IMU). These

IMU sensors measure acceleration, angular rate, and magnetic field strength and are specifically placed on different body segments to capture individual limb movements. Using a biomechanical model, 3D motion profiles of various body segments for each participant are calculated separately. To align all individual 3D positions into a common reference system, a hybrid tracking algorithm projects the 3D MoCap data onto camera trajectories [63]. Additionally, a pressure sensor [64] was attached to the punching bag to measure the intensity of the impulses. These recorded data are innovative yet unique and allow new perspectives and analyses of crowd dynamics that were previously not possible, namely the observation of individual motion of limbs in dense crowds.

My analysis of these experiments has resulted in the three following papers that constitute the main part of this dissertation:

(A) Feldmann, S., Adrian, J. (2023). Forward propagation of a push through a row of people. Safety Science, 164, 106173. doi: 10.1016/j.ssci.2023.106173

(B) Feldmann, S., Chatagnon, T., Adrian, J., Pettré, J., Seyfried, A. (2024). Temporal segmentation of motion propagation in response to an external impulse. Safety Science, 175, 106512. doi: 10.1016/j.ssci.2024.106512

(C) Feldmann, S., Adrian, J., Boltes, M. (2024). Propagation of Controlled Frontward Impulses Through Standing Crowds. Collective Dynamics, 9, 1-17. doi: 10.17815/CD.2024.148

My contributions to each paper are stated in detail at the beginning of the corresponding chapter. Additionally, I have contributed to the following two papers that are not included in this thesis:

(D) Boomers, A. K., Boltes, M., Adrian, J., Beermann, M., Chraibi, M., Feldmann, S., Fiedrich, F., Frings, N., Graf, A., Kandler, A., Kilic, D., Konya, K., Küpper, M., Lotter, A., Lügering, H., Müller, F., Paetzke, S., Raytarowski, A.-K., Sablik, O., Schrödter, T., Seyfried, A., Sieben, A., Üsten, E. (2023). Pedestrian Crowd Management Experiments: A Data Guidance Paper. Collective Dynamics, 8, 1–57. doi: 10.17815/CD.2023.141

(E) Chatagnon, T., Feldmann, S., Adrian, J., Olivier, A.-H., Pontonnier, C., Hoyet, L., Pettré, J. (2024). Standing Balance Recovery Strategies of Young Adults in a Densely Populated Environment Following External Perturbations. Safety Science, 177, 106601. doi: 10.1016/j.ssci.2024.106601

Given the novelty of the data set and the planned experiments, we wanted to start small to test different parameters, reduce unintended effects, and ensure the safety of the participants. Also, in terms of the analysis, I started first examining familiar data, i.e., the head trajectories from the camera, before gradually examining more of the 3D positions, as this data set was new to our group. The experience gained from the short row experiments and the first data analyses simplified the planning of the extended experiments. This allowed us to decide which parameters to control

and which group formations to test, as well as reduce associated risks. Thus, each step of this work builds on established and gained knowledge, enhancing the overall quality and reliability of the research outcomes.

Publication A investigates the propagation of impulses in one dimension, specifically the push direction, for the short row experiments. The study aims to link the intensity of the push to the forward motion of the participants. To this end, the trajectories of the CoM and the impulse of the push derived from the pressure data are investigated. As a result, a propagation speed and a propagation distance are introduced as functions of the impulse intensity. Notably, the study finds no significant effect of the initial inter-person distance on the propagation speed. On the other hand, it reveals that a push propagates faster through the row for the same intensity if the participants keep their arms up from the start compared to their arms down or free.

The subsequent analysis in publication B focuses on the 3D reactions of each participant within the five-person rows. Based on observation of the side-view videos, the reactions are separated into temporal phases classified as (i) receiving, (ii) receiving and passing on, or (iii) passing on the impulse. Using the forward velocity, the MoS, and the distance between participants, these phases can be identified in the 3D data, allowing for a quantitative analysis. The number of occurring phases and their duration are influenced by the initial inter-person distance rather than the intensity of the impulses. A small initial inter-person distance shortens the first phase and prolongs the second. In some cases, the first phase may be omitted entirely, while the second phase may be skipped if people stand further apart. In future analyses, temporal phases can help distinguish between different physical interactions.

Publication C enhances impulse propagation to a larger scale by investigating the extended experiments. The study found that the propagation speed depends not only on the impulse intensity but also on the initial inter-person distance, which was not the case in the previous short row experiments. The preparation of the participants has no significant effect on impulse propagation. Furthermore, three cases can occur during impulse propagation: the impulse is transmitted linearly, the impulse is intensified, or the impulse is dampened. The impulse is passed on linearly for five people, whereas for 20 people, the impulse is dampened on average along the row. Finally, the paper presents heat maps of the participants' maximum displacement for different formations. The more intertwined people stand in a crowd, the more the impulse is distributed to the side. This means that more people with a smaller displacement are affected by the push.

Publication D describes the experiments and data collection carried out in collaboration with the CroMa project. Relevant to this thesis are the bottleneck experiments as part of the CrowdDNA project described in Chapter 3.7, which focus on dense crowds. To achieve close contact within these crowds, participants with a common goal walked through a bottleneck under various conditions. Data collected

includes head trajectories from top-down cameras, videos from side view cameras, pressure sensors mounted at the walls of the bottleneck, and 3D motion capturing profiles from 20 participants. In future analyses, the applicability of the results on impulse propagation and temporal phases to larger crowd, as well as movement strategies, effect of densities on 3D motion, emergence of collective phenomena such as wave movements, and magnitude of normal forces exerted by crowds can be examined.

Publication E further elaborates on the analysis of the extended experiments discussed in C, focusing on strategies to recover balance after an external perturbation. The study mainly examines the characteristics of first steps and compares them to trials in which single persons were pushed [53]. Being surrounded by people does not affect the duration of the first step, but it does reduce the step speed and length and causes the positioning of the steps to become scattered. In addition, the initial inter-person distance shifts the initialization of a step: With elbow distance, steps are set earlier, while with no distance, times are comparable to those for individuals. The observation of leaning strategies without steps and raising hands before taking steps to recover indicates the importance of physical interaction within crowds.

Discussion

This dissertation examines two different experiments regarding impulse propagation and individual 3D movements in dense crowds. Although this work was carried out in the context of events, the knowledge gained can be transferred to other situations where standing people predominate. Real-life applications include but are not limited to queueing systems, concerts, as well as train platforms, where waiting pedestrians are at risk of falling onto the rail tracks.

The novel data set presented here provides initial insights that are crucial for understanding crowd dynamics. For the first time, pressure data is linked to the movement of people in a group. As a result, we define the speed and distance of impulse propagation, accounting for different body positions and intensities. This can help us understand how people move each other and improve our comprehension of crowd dynamics, even in larger crowds. In the short row experiments, no significant effect of the initial inter-person distance on the propagation speed could be found, possibly due to limited repetitions with the same conditions and participants. The follow-up experiments showing the importance of the initial inter-person distance emphasise the scalability of the research design for a thorough investigation of these complicated relationships. In addition, the motion of participants in three dimensions is analysed for the first time within dense crowds. This is particularly relevant in the context of impulse propagation because people can lose their balance or even fall down, which can only be explained in 3D. Our results show that humans should not be represented by billiard balls, as this is not an elastic collision, nor by dominoes, as the propagation properties do not depend solely on the initial inter-person distance. Alternatively, an inverted pendulum might be a more suitable model, which takes the influence of the impulse intensity into account. Currently,

a novel 3D model [65] is developed against our data. Moreover, our evaluation regarding the propagation speed, as well as propagation distance and direction, uses the 3D data to draw conclusions in 2D. This information could be used to improve pedestrian models that rely on 2D representations.

In order to conduct a more realistic investigation of impulse propagation in future experimental studies, it would be beneficial to consider additional factors such as the direction of pushing, floor conditions, the level of awareness of participants, different formations of crowds, gaps within people, and people in motion.

Another new aspect of this work is the separation of individual movement when exerted to a push into quantitative temporal phases. As a result, different dynamics can be categorised on the basis of the individual phases which allows for a more rigorous assessment of risk levels: Either one person is strongly affected by the impulse, which can lead to a fall, or several people are simultaneously in the critical phase of losing their balance, causing a wave motion through the crowd. The fact that these phases can be detected using the 3D data makes it easier to investigate when and how the specific phenomena occur.

For future studies in this regard, one should take into account the order of the participants as their individual characteristics, e.g. height, weight and body tension, can heavily affect how an impulse is transmitted. Furthermore, people may exhibit different levels of preparedness or use different strategies to regain balance, and a quantitative classification of these strategies would improve the understanding of impulse propagation in crowds. To achieve this, step length, step width, number of steps, hip movements, and pendulum movements of the upper body should be analysed in more detail. Additional pressure sensors placed between the participants could help to detect physical contact and estimate normal forces.

As shown in this dissertation, it is essential to investigate crowds on all scales. The results presented here establish a link between movements of individual limbs and large scale, collective dynamics, providing an understanding of causality. The overall long term goal is to invert this approach, i.e. to identify individual risks based on observations of the crowd as a whole [57]. Real-life predictive analysis based on this technique could enable timely decision-making and crowd management interventions in order to avoid dangerous events.

Bibliography

[1] Claudio Feliciani, Alessandro Corbetta, Milad Haghani, and Katsuhiro Nishinari. "Trends in crowd accidents based on an analysis of press reports". en. In: *Safety Science* 164 (Aug. 2023), p. 106174. ISSN: 09257535. DOI: 10.1016/j.ssci.2023.106174.

[2] Claudio Feliciani. *List of crowd accidents from 1900 to 2019*. en. Jan. 2023. DOI: 10.5281/ZENODO.7523479.

[3] Virginia Harrison and Carly Earl. "A visual guide to how the Seoul Halloween crowd crush unfolded". en-GB. In: *The Guardian* (Oct. 2022). ISSN: 0261-3077. URL: https://www.theguardian.com/world/2022/oct/31/how-did-the-seoul-itaewon-halloween-crowd-crush-happen-unfolded-a-visual-guide (visited on 01/02/2023).

[4] Anna Sieben and Armin Seyfried. "Inside a life-threatening crowd: Analysis of the Love Parade disaster from the perspective of eyewitnesses". en. In: *Safety Science* 166 (Oct. 2023), p. 106229. ISSN: 09257535. DOI: 10.1016/j.ssci.2023.106229.

[5] Juliane Adrian, Nikolai Bode, Martyn Amos, Mitra Baratchi, Mira Beermann, Maik Boltes, Alessandro Corbetta, Guillaume Dezecache, John Drury, Zhijian Fu, Roland Geraerts, Steve Gwynne, Gesine Hofinger, Aoife Hunt, Tinus Kanters, Angelika Kneidl, Krisztina Konya, Gerta Köster, Mira Küpper, Georgios Michalareas, Fergus Neville, Evangelos Ntontis, Stephen Reicher, Enrico Ronchi, Andreas Schadschneider, Armin Seyfried, Alastair Shipman, Anna Sieben, Michael Spearpoint, Gavin Brent Sullivan, Anne Templeton, Federico Toschi, Zeynep Yücel, Francesco Zanlungo, Iker Zuriguel, Natalie Van der Wal, Frank Van Schadewijk, Cornelia Von Krüchten, and Nanda Wijermans. "A Glossary forResearch on Human Crowd Dynamics". In: *Collective Dynamics* 4 (Mar. 2019), A19. ISSN: 2366-8539. DOI: 10.17815/CD.2019.19.

[6] Arianna Bottinelli and Jesse L. Silverberg. *Can high-density human collective motion be forecasted by spatiotemporal fluctuations?* arXiv:1809.07875 [physics]. Sept. 2018. URL: http://arxiv.org/abs/1809.07875 (visited on 01/02/2023).

[7] Ramana Sundararaman, Cedric De Almeida Braga, Eric Marchand, and Julien Pettre. "Tracking Pedestrian Heads in Dense Crowd". In: *2021 IEEE/CVF Conference on Computer Vision and Pattern Recognition (CVPR)*. Nashville,

TN, USA: IEEE, June 2021, pp. 3864–3874. ISBN: 978-1-66544-509-2. DOI: 10.1109/CVPR46437.2021.00386.

[8] Dirk Helbing, Anders Johansson, and Habib Zein Al-Abideen. "Dynamics of crowd disasters: An empirical study". en. In: *Physical Review E* 75.4 (Apr. 2007), p. 046109. ISSN: 1539-3755, 1550-2376. DOI: 10.1103/PhysRevE.75.046109.

[9] Wang Jiayue, Weng Wenguo, and Zhang Xiaole. "Comparison of Turbulent Pedestrian Behaviors Between Mina and Love Parade". en. In: *Procedia Engineering* 84 (2014), pp. 708–714. ISSN: 18777058. DOI: 10.1016/j.proeng.2014.10.477.

[10] Maik Boltes, Jun Zhang, Antoine Tordeux, Andreas Schadschneider, and Armin Seyfried. "Empirical Results of Pedestrian and Evacuation Dynamics". en. In: *Encyclopedia of Complexity and Systems Science*. Ed. by Robert A. Meyers. Berlin, Heidelberg: Springer Berlin Heidelberg, 2018, pp. 1–29. ISBN: 978-3-642-27737-5. DOI: 10.1007/978-3-642-27737-5_706-1.

[11] Mohcine Chraibi, Antoine Tordeux, Andreas Schadschneider, and Armin Seyfried. "Modelling of Pedestrian and Evacuation Dynamics". en. In: *Encyclopedia of Complexity and Systems Science*. Ed. by Robert A. Meyers. Berlin, Heidelberg: Springer Berlin Heidelberg, 2018, pp. 1–22. ISBN: 978-3-642-27737-5. DOI: 10.1007/978-3-642-27737-5_705-1.

[12] Raphael Korbmacher and Antoine Tordeux. "Review of Pedestrian Trajectory Prediction Methods: Comparing Deep Learning and Knowledge-Based Approaches". In: *IEEE Transactions on Intelligent Transportation Systems* 23.12 (Dec. 2022), pp. 24126–24144. ISSN: 1524-9050, 1558-0016. DOI: 10.1109/TITS.2022.3205676.

[13] Alessandro Corbetta and Federico Toschi. "Physics of Human Crowds". en. In: *Annual Review of Condensed Matter Physics* 14.1 (Mar. 2023), pp. 311–333. ISSN: 1947-5454, 1947-5462. DOI: 10.1146/annurev-conmatphys-031620-100450.

[14] Yan Feng, Dorine Duives, Winnie Daamen, and Serge Hoogendoorn. "Data collection methods for studying pedestrian behaviour: A systematic review". en. In: *Building and Environment* 187 (Jan. 2021), p. 107329. ISSN: 03601323. DOI: 10.1016/j.buildenv.2020.107329.

[15] B. Steffen and A. Seyfried. "Methods for measuring pedestrian density, flow, speed and direction with minimal scatter". en. In: *Physica A: Statistical Mechanics and its Applications* 389.9 (May 2010), pp. 1902–1910. ISSN: 03784371. DOI: 10.1016/j.physa.2009.12.015.

[16] Jack Liddle, Armin Seyfried, Bernhard Steffen, Wolfram Klingsch, Tobias Rupprecht, Andreas Winkens, and Maik Boltes. "Microscopic insights into pedestrian motion through a bottleneck, resolving spatial and temporal variations". In: *Collective Dynamics* 7 (2022), pp. 1–23. DOI: https://doi.org/10.17815/CD.2022.139.

[17] Hongliu Li, Jun Zhang, Weiguo Song, and Kwok Kit Richard Yuen. "A comparative study on the bottleneck pedestrian flow under different movement motivations". en. In: *Fire Safety Journal* 120 (Mar. 2021), p. 103014. ISSN: 03797112. DOI: 10.1016/j.firesaf.2020.103014.

[18] Arianna Bottinelli, David T. J. Sumpter, and Jesse L. Silverberg. "Emergent Structural Mechanisms for High-Density Collective Motion Inspired by Human Crowds". en. In: *Physical Review Letters* 117.22 (Nov. 2016), p. 228301. ISSN: 0031-9007, 1079-7114. DOI: 10.1103/PhysRevLett.117.228301.

[19] Claudio Feliciani, Iker Zuriguel, Angel Garcimartín, Diego Maza, and Katsuhiro Nishinari. "Systematic experimental investigation of the obstacle effect during non-competitive and extremely competitive evacuations". en. In: *Scientific Reports* 10.1 (Sept. 2020), p. 15947. ISSN: 2045-2322. DOI: 10.1038/s41598-020-72733-w.

[20] Barbara Krausz and Christian Bauckhage. "Loveparade 2010: Automatic video analysis of a crowd disaster". en. In: *Computer Vision and Image Understanding* 116.3 (Mar. 2012), pp. 307–319. ISSN: 10773142. DOI: 10.1016/j.cviu.2011.08.006.

[21] Roger L. Hughes. "A continuum theory for the flow of pedestrians". en. In: *Transportation Research Part B: Methodological* 36.6 (July 2002), pp. 507–535. ISSN: 01912615. DOI: 10.1016/S0191-2615(01)00015-7.

[22] Nicolas Bain and Denis Bartolo. "Dynamic response and hydrodynamics of polarized crowds". en. In: *Science* 363.6422 (Jan. 2019), pp. 46–49. ISSN: 0036-8075, 1095-9203. DOI: 10.1126/science.aat9891.

[23] Angel Garcimartìn, Diego Maza, José Martìn. Pastor, Daniel R. Parisi, César Martìn-Gómez, and Iker Zuriguel. "Redefining the role of obstacles in pedestrian evacuation". In: *New Journal of Physics* 20.12 (Dec. 2018), p. 123025. ISSN: 1367-2630. DOI: 10.1088/1367-2630/aaf4ca.

[24] Juliane Adrian, Armin Seyfried, and Anna Sieben. "Crowds in front of bottlenecks at entrances from the perspective of physics and social psychology". en. In: *Journal of The Royal Society Interface* 17.165 (Apr. 2020), p. 20190871. ISSN: 1742-5689, 1742-5662. DOI: 10.1098/rsif.2019.0871.

[25] Helen C. Muir, David M. Bottomley, and Claire Marrison. "Effects of Motivation and Cabin Configuration on Emergency Aircraft Evacuation Behavior and Rates of Egress". en. In: *The International Journal of Aviation Psychology* 6.1 (Jan. 1996), pp. 57–77. ISSN: 1050-8414, 1532-7108. DOI: 10.1207/s15327108ijap0601_4.

[26] A Garcimartín, D R Parisi, J M Pastor, C Martín-Gómez, and I Zuriguel. "Flow of pedestrians through narrow doors with different competitiveness". In: *Journal of Statistical Mechanics: Theory and Experiment* 2016.4 (Apr. 2016), p. 043402. ISSN: 1742-5468. DOI: 10.1088/1742-5468/2016/04/043402.

[27] Milad Haghani, Majid Sarvi, and Zahra Shahhoseini. "When 'push' does not come to 'shove': Revisiting 'faster is slower' in collective egress of human crowds". en. In: *Transportation Research Part A: Policy and Practice* 122 (Apr. 2019), pp. 51–69. ISSN: 09658564. DOI: 10.1016/j.tra.2019.02.007.

[28] Ezel Üsten, Helena Lügering, and Anna Sieben. "Pushing and Non-pushing Forward Motion in Crowds: A Systematic Psychological Observation Method for Rating Individual Behavior in Pedestrian Dynamics". In: *Collective Dynamics* 7 (Aug. 2022), pp. 1–16. ISSN: 2366-8539. DOI: 10.17815/CD.2022.138.

[29] Ahmed Alia, Mohammed Maree, and Mohcine Chraibi. "A Hybrid Deep Learning and Visualization Framework for Pushing Behavior Detection in Pedestrian Dynamics". en. In: *Sensors* 22.11 (May 2022), p. 4040. ISSN: 1424-8220. DOI: 10.3390/s22114040.

[30] Dirk Helbing and Pratik Mukerji. "Crowd disasters as systemic failures: analysis of the Love Parade disaster". en. In: *EPJ Data Science* 1.1 (Dec. 2012), p. 7. ISSN: 2193-1127. DOI: 10.1140/epjds7.

[31] Dirk Helbing and Péter Molnár. "Social force model for pedestrian dynamics". en. In: *Physical Review E* 51.5 (May 1995), pp. 4282–4286. ISSN: 1063-651X, 1095-3787. DOI: 10.1103/PhysRevE.51.4282.

[32] Dirk Helbing, Illés Farkas, and Tamás Vicsek. "Simulating dynamical features of escape panic". en. In: *Nature* 407.6803 (Sept. 2000), pp. 487–490. ISSN: 0028-0836, 1476-4687. DOI: 10.1038/35035023.

[33] Wouter Van Toll, Thomas Chatagnon, Cédric Braga, Barbara Solenthaler, and Julien Pettré. "SPH crowds: Agent-based crowd simulation up to extreme densities using fluid dynamics". en. In: *Computers & Graphics* 98 (Aug. 2021), pp. 306–321. ISSN: 00978493. DOI: 10.1016/j.cag.2021.06.005.

[34] Sujeong Kim, Stephen J. Guy, Karl Hillesland, Basim Zafar, Adnan Abdul-Aziz Gutub, and Dinesh Manocha. "Velocity-based modeling of physical interactions in dense crowds". en. In: *The Visual Computer* 31.5 (May 2015), pp. 541–555. ISSN: 0178-2789, 1432-2315. DOI: 10.1007/s00371-014-0946-1.

[35] Chongyang Wang, Liangchang Shen, and Wenguo Weng. "Modelling physical contacts to evaluate the individual risk in a dense crowd". en. In: *Scientific Reports* 13.1 (Mar. 2023), p. 3929. ISSN: 2045-2322. DOI: 10.1038/s41598-023-31148-z.

[36] Jingni Song, Feng Chen, Yadi Zhu, Na Zhang, Weiyu Liu, and Kai Du. "Experiment Calibrated Simulation Modeling of Crowding Forces in High Density Crowd". In: *IEEE Access* 7 (2019), pp. 100162–100173. ISSN: 2169-3536. DOI: 10.1109/ACCESS.2019.2930104.

[37] Cuiling Li, Rongyong Zhao, Yan Wang, Ping Jia, Wenjie Zhu, Yunlong Ma, and Miyuan Li. "Disturbance Propagation Model of Pedestrian Fall Behavior in a Pedestrian Crowd and Elimination Mechanism Analysis". In: *IEEE Transactions on Intelligent Transportation Systems* (2023), pp. 1–11. ISSN: 1524-9050, 1558-0016. DOI: 10.1109/TITS.2023.3314072.

[38] Chongyang Wang, Shunjiang Ni, and Wenguo Weng. "Modeling human domino process based on interactions among individuals for understanding crowd disasters". en. In: *Physica A: Statistical Mechanics and its Applications* 531 (Oct. 2019), p. 121781. ISSN: 0378-4371. DOI: 10.1016/j.physa.2019.121781.

[39] Iker Zuriguel, Iñaki Echeverría, Diego Maza, Raúl C. Hidalgo, César Martín-Gómez, and Angel Garcimartín. "Contact forces and dynamics of pedestrians evacuating a room: The column effect". en. In: *Safety Science* 121 (Jan. 2020), pp. 394–402. ISSN: 09257535. DOI: 10.1016/j.ssci.2019.09.014.

[40] Chongyang Wang and Wenguo Weng. "Study on the collision dynamics and the transmission pattern between pedestrians along the queue". en. In: *Journal of Statistical Mechanics: Theory and Experiment* 2018.7 (July 2018), p. 073406. ISSN: 1742-5468. DOI: 10.1088/1742-5468/aace27.

[41] Xiaohong Li, Jianan Zhou, Feng Chen, and Zan Zhang. "Cluster Risk of Walking Scenarios Based on Macroscopic Flow Model and Crowding Force Analysis". en. In: *Sustainability* 10.2 (Feb. 2018), p. 385. ISSN: 2071-1050. DOI: 10.3390/su10020385.

[42] Xudong Li, Weiguo Song, Xuan Xu, Jun Zhang, Long Xia, and Congling Shi. "Experimental study on pedestrian contact force under different degrees of crowding". en. In: *Safety Science* 127 (July 2020), p. 104713. ISSN: 09257535. DOI: 10.1016/j.ssci.2020.104713.

[43] Xudong Li, Luciano Telesca, Michele Lovallo, Xuan Xu, Jun Zhang, and Weiguo Song. "Spectral and informational analysis of pedestrian contact force in simulated overcrowding conditions". en. In: *Physica A: Statistical Mechanics and its Applications* 555 (Oct. 2020), p. 124614. ISSN: 03784371. DOI: 10.1016/j.physa.2020.124614.

[44] Chongyang Wang, Liangchang Shen, and Wenguo Weng. "Experimental study on individual risk in crowds based on exerted force and human perceptions". In: *Ergonomics* 63.7 (July 2020). Publisher: Taylor & Francis, pp. 789–803. ISSN: 0014-0139. DOI: 10.1080/00140139.2020.1762933.

[45] Xudong Li, Xuan Xu, Jun Zhang, Kechun Jiang, Weisong Liu, Ruolong Yi, and Weiguo Song. "Experimental study on the movement characteristics of pedestrians under sudden contact forces". en. In: *Journal of Statistical Mechanics: Theory and Experiment* 2021.6 (June 2021). Publisher: IOP Publishing, p. 063406. ISSN: 1742-5468. DOI: 10.1088/1742-5468/ac02c7.

[46] Da Winter. "Human balance and posture control during standing and walking". en. In: *Gait & Posture* 3.4 (Dec. 1995), pp. 193–214. ISSN: 09666362. DOI: 10.1016/0966-6362(96)82849-9.

[47] A.L. Hof, M.G.J. Gazendam, and W.E. Sinke. "The condition for dynamic stability". en. In: *Journal of Biomechanics* 38.1 (Jan. 2005), pp. 1–8. ISSN: 00219290. DOI: 10.1016/j.jbiomech.2004.03.025.

[48] At L. Hof. "The 'extrapolated center of mass' concept suggests a simple control of balance in walking". en. In: *Human Movement Science* 27.1 (Feb. 2008), pp. 112–125. ISSN: 01679457. DOI: 10.1016/j.humov.2007.08.003.

[49] Noah J. Rosenblatt and Mark D. Grabiner. "Measures of frontal plane stability during treadmill and overground walking". en. In: *Gait & Posture* 31.3 (Mar. 2010), pp. 380–384. ISSN: 09666362. DOI: 10.1016/j.gaitpost.2010.01.002.

[50] Laura Hak, Han Houdijk, Peter J. Beek, and Jaap H. Van Dieën. "Steps to Take to Enhance Gait Stability: The Effect of Stride Frequency, Stride Length, and Walking Speed on Local Dynamic Stability and Margins of Stability". en. In: *PLoS ONE* 8.12 (Dec. 2013). Ed. by Amir A. Zadpoor, e82842. ISSN: 1932-6203. DOI: 10.1371/journal.pone.0082842.

[51] Brian W. Schulz, James A. Ashton-Miller, and Neil B. Alexander. "Can initial and additional compensatory steps be predicted in young, older, and balance-impaired older females in response to anterior and posterior waist pulls while standing?" en. In: *Journal of Biomechanics* 39.8 (2006), pp. 1444–1453. ISSN: 00219290. DOI: 10.1016/j.jbiomech.2005.04.004.

[52] Amber R. Emmens, Edwin H. F. Van Asseldonk, Vera Prinsen, and Herman Van Der Kooij. "Predicting reactive stepping in response to perturbations by using a classification approach". en. In: *Journal of NeuroEngineering and Rehabilitation* 17.1 (Dec. 2020), p. 84. ISSN: 1743-0003. DOI: 10.1186/s12984-020-00709-y.

[53] Thomas Chatagnon, Anne-Hélène Olivier, Ludovic Hoyet, Julien Pettré, and Charles Pontonnier. "Stepping strategies of young adults undergoing sudden external perturbation from different directions". en. In: *Journal of Biomechanics* 157 (Aug. 2023), p. 111703. ISSN: 00219290. DOI: 10.1016/j.jbiomech.2023.111703.

[54] Brian E. Maki and William E. McIlroy. "Control of rapid limb movements for balance recovery: age-related changes and implications for fall prevention". en. In: *Age and Ageing* 35.suppl_2 (Sept. 2006), pp. ii12–ii18. ISSN: 1468-2834, 0002-0729. DOI: 10.1093/ageing/afl078.

[55] Dario Tokur, Martin Grimmer, and André Seyfarth. "Review of balance recovery in response to external perturbations during daily activities". en. In: *Human Movement Science* 69 (Feb. 2020), p. 102546. ISSN: 01679457. DOI: 10.1016/j.humov.2019.102546.

[56] Brian E Maki and William E McIlroy. "The Role of Limb Movements in Maintaining Upright Stance: The "Change-in-Support" Strategy". In: *Physical Therapy* 77.5 (May 1997), pp. 488–507. ISSN: 0031-9023. DOI: 10.1093/ptj/77.5.488.

[57] CrowdDNA Project. *Website CrowdDNA Project*. https://crowddna.eu/. July 3, 2022. URL: https://crowddna.eu/ (visited on 07/03/2024).

[58] Sina Feldmann, Juliane Adrian, Ann Katrin Boomers, Maik Boltes, Jernej Čamernik, Marc Ernst, Alica Kandler, Helena Lügering, Tobias Schrödter, Armin Seyfried, and Anna Sieben. *Forward propagation of a push through a row of five people*. Pedestrian Dynamics Data Archive, Institute for Advanced Simulation 7: Civil Safety Research, Forschungszentrum Jülich. 2023. DOI: 10.34735/ped.2022.2.

[59] Sina Feldmann, Juliane Adrian, Maik Boltes, Jernej Čamernik, Thomas Chatagnon, Marc Comino-Trinidad, Alica Kandler, and Armin Seyfried. *Impulse propagation through a small standing crowd*. Pedestrian Dynamics Data Archive, Institute for Advanced Simulation 7: Civil Safety Research, Forschungszentrum Jülich. 2024. DOI: 10.34735/ped.2022.6.

[60] Maik Boltes and Armin Seyfried. "Collecting pedestrian trajectories". In: *Neurocomputing* 100 (2013). Special issue: Behaviours in video, pp. 127–133. ISSN: 0925-2312. DOI: https://doi.org/10.1016/j.neucom.2012.01.036.

[61] Maik Boltes, Ann Katrin Boomers, Juliane Adrian, Ricardo Martin Brualla, Arne Graf, Paul Häger, Daniel Hillebrand, Deniz Kilic, Paul Lieberenz, Daniel Salden, and Tobias Schrödter. *PeTrack*. Version v0.9. July 2021. DOI: 10.5281/zenodo.5126562.

[62] Martin Schepers, Matteo Giuberti, and Giovanni Bellusci. "Xsens MVN: Consistent Tracking of Human Motion Using Inertial Sensing". en. In: (2018). DOI: 10.13140/RG.2.2.22099.07205.

[63] Maik Boltes, Juliane Adrian, and Anna-Katharina Raytarowski. "A Hybrid Tracking System of Full-Body Motion Inside Crowds". en. In: *Sensors* 21.6 (Mar. 2021), p. 2108. ISSN: 1424-8220. DOI: 10.3390/s21062108.

[64] Xsensor LX210:50.50.05. *Datasheet: Xsensor SENSORS LX210:50.50.05*. 2019. URL: https://www.xsensor.de/wp-content/uploads/2015/11/LX210_50_50_05-2500-Sensoren-508mm-Aufl%C3%B6sung-Gr%C3%B6sse-25x25cm-Messbereich-014-11Ncm2-Anwendung-Sitze_Rollst%C3%BChle.pdf (visited on 10/13/2022).

[65] Jiangbei Yue, Baiyi Li, Julien Pettré, Armin Seyfried, and He Wang. "Human Motion Prediction Under Unexpected Perturbation". In: *Proceedings of the IEEE/CVF Conference on Computer Vision and Pattern Recognition (CVPR)*. June 2024, pp. 1501–1511.

PUBLICATION A

Forward propagation of a push through a row of people

This article was published as Feldmann, S., Adrian, J. (2023). Forward propagation of a push through a row of people. Safety Science, 164, 106173. doi: 10.1016/j.ssci.2023.106173

Author Contributions

Conceptualization: Sina Feldmann and Juliane Adrian
Data curation: Sina Feldmann
Formal analysis: Sina Feldmann
Investigation: Sina Feldmann
Methodology: Sina Feldmann and Juliane Adrian
Supervision: Juliane Adrian
Validation: Sina Feldmann
Visualization: Sina Feldmann
Writing–original draft preparation: Sina Feldmann
Writing–review and editing: Sina Feldmann and Juliane Adrian

Forward propagation of a push through a row of people

Sina Feldmann[1] [2] and Juliane Adrian[1]

[1] Institute for Advanced Simulation 7: Civil Safety Research, Forschungszentrum Jülich, Jülich, Germany

[2] Faculty of Architecture and Civil Engineering, University of Wuppertal, Wuppertal, Germany

Highlights

- Pressure data of a push was linked to motion data of pedestrians.
- Unlike a domino effect, pushes propagate further in the row with stronger impacts.
- The propagation speed depends on the pushing strength and the initial arm posture.

Abstract

Security plays a crucial role when it comes to planning large events such as concerts, sporting tournaments, pilgrims, or demonstrations. Monitoring and controlling pedestrian dynamics can prevent dangerous situations from occurring. However, little is known about the specific factors that contribute to harmful situations. For example, the individual response of a person to external forces in dense crowds is not well studied. In order to address this gap in knowledge, we conducted a series of experiments to examine how a push propagates through a row of people and how it affects the participants. We recorded 2D head trajectories and 3D motion capturing data. To ensure that different trials can be compared to one another, we measured the force at the impact. We find that that the propagation distance as well as the propagation speed of the push are mainly functions of the strength of the push and in particular the latter depends on the initial arm posture of the pushed participants. Our results can contribute to a deeper understanding of the microscopic causes of macroscopic phenomena in large groups, and can be applied to inform models of pedestrian dynamics or validate them, ultimately improving crowd safety.

Keywords: Pushing; Propagation; Pedestrian; Experiment; Motion Capturing; Pressure

1 Introduction

Pedestrian dynamics play a crucial role in the safety of large events, such as concerts, sporting tournaments, and demonstrations. Crowded gatherings can easily lead to pushing and jostling, which can not only cause discomfort but also dangerous situations. A recent example of this is the Halloween celebrations in Seoul in 2022, in which over 150 people died and several dozen more were injured in a narrow, crowded street [1]. To help prevent such tragedies, it is essential to better understand the dynamics of dense crowds and to identify potential measures to improve safety.

When many people gather closely together, they interact and exchange forces, leading to various dynamics that influence the behaviour and movements of pedestrians as well as collective phenomena of the entire crowd. For example, turbulence can develop in dense crowds, causing pedestrian movements to become irregular and chaotic [2, 3]. This in turn can lead to a domino effect [4, 5], whereby a small disturbance starts a chain reaction spreading through the crowd. Dense crowds can also exhibit 'density waves' where the density periodically increases and decreases [6]. In addition, collective movements where pedestrians move in a direction lateral to the desired direction have been studied in experiments [7, 8].

One attempt to investigate these collective movements further is computer-based simulations based on pedestrian models. Such models have the advantage of being cost-effective and allowing scenarios to be tested that cannot be studied in real experiments. Modelling escape behaviour [9], recreating a shock-wave through a crowd [10] or incorporating crowding forces [11] are just a few examples. However, these studies mainly manipulate model parameters to visualise specific situations in dense crowds without investigating real-life causes of such macroscopic phenomena.

What can be macroscopically observed as transversal waves or large collective dynamics corresponds on a microscopic level to a transfer of momentum and forces acting between individuals. Pushing is an example of a microscopic behaviour and can cause pedestrians to change their direction of motion or even fall. In experiments, for example, pushing is used as a strategy to get to the target faster, which can result in a higher density [12]. This often involves closing gaps, overtaking and pulling forward, which are assessed as pushing behaviour [13], [14]. However, high densities in crowds can also be the cause for unintentional pushing because pedestrians touch each other due to the lack of space or moving in a confined space [5].

The way people react to an external force and how this force is propagated within a crowd have not yet been thoroughly investigated. Previous studies on this topic have mainly focused on pressure measurement at the wall and doorjamb during an evacuation of a crowd [15], pressure measurement between participants [16, 17], the development of a 'domino model' [18], or the definition of an individually perceived risk value [19]. While these studies have provided valuable insights into contact forces and collision dynamics, they have limitations in terms of accounting for

individual differences in pedestrian responses, and linking pressure data to motion data. Small-scale experiments with one or two participants [20] analyse body postures and behaviours as a reaction to a force, but it is difficult to transfer these results to larger crowds.

In our research, we want to contribute to a deeper knowledge of the processes of pushing by conducting a range of experiments. The aim of the study was to determine the propagation of a push within a crowd. For this purpose, head position, 3-dimensional motion data as well as pressure collected during small-scale experiments are analysed. As a simplification, only one row of five people and one direction, i.e. forward movement are taken into account. This allows us to break down reality to the smallest and simplest level and to investigate the effect of the push in an isolated way. Thereby, the five people represent a small crowd occurring for example during waiting queues. The overall objective of this study is to categorise pushes to compare the strength of the impact with the forward motion of the participants. In the following, we will present our results in detail. We hope that our work can contribute to a deeper understanding of pushing in a crowd and provide useful information for the further development of pedestrian models and their application in practice.

2 Methods

2.1 Experimental setup

The experimental area of three meters by five meters (see Figure 1) was covered with mats, that are also used in martial arts, to minimise injuries in case of falls. One side of the area was limited by a solid wall, while on the other side a punching bag, stabilised with a wooden plank, was suspended horizontally from the ceiling.

Figure 1: The Experimental area covered with mats has a size of 3 m × 5 m. On the left side, a punching bag was suspended from the ceiling to push the participants forward. The right side of the area was limited by a solid wall.

2.2 Procedure and variations

A total of 14 volunteers aged 19 - 55 years were recruited. Prior to the experiments, each participant signed a written informed consent and assured that they felt physically fit enough to take part in the experiments. The participants were informed beforehand about the procedure and possible risks. At any time, participants were able to stop the experiments or skip individual experimental trials without giving any reason or any disadvantage.

In order to push the participants the punching bag was manually moved forward by the same person in all trials. Therefore, preliminary tests were carried out, in which pushes were classified into three categories: weak, medium and strong. To this end, four different participants were pushed individually determining the intensity of the pushes based on personal perception. During this process, the person who moved the punching bag learned to push in the three defined categories.

Before each trial, five participants were lined up in front of the punching bag without touching it and facing the wall. The conditions of the trial were read aloud and the distance between the participants were adjusted with the individual arm length. The person at the end of the line was pushed forward in a controlled manner.

The intensity of the push, the height of the push, the initial inter-person distance, the initial arm position and the body posture were varied (see Table 1). In addition, the participants were positioned either directly in front of the wall with the first person keeping the same inter-person distance to the wall (i.e. with boundary), or far enough away from the wall to allow the first person to move freely to the front (i.e. without boundary), as shown in Figure 2. Each variation was carried out firstly with a weak push and then the intensity of the push increased from medium to strong. Upon request some runs were omitted.

Table 1: Overview of variations. Only variations in bold are analysed further.

Parameter	Variations		
intensity of push	**weak**	**medium**	**strong**
initial inter-person distance	**arm**	**elbow**	**none**
initial arm posture	**free**	**down**	**up**
body posture	**body tension**	relaxed	
height of push	**shoulder**	lower back	
boundary	**none**	**wall**	

For further analysis, only experiments in which participants stood with tension in the body, i.e. feet were placed hip-width apart, and were pushed at shoulder height are considered. The series of experiments with and without boundary are considered separately. Within a series, the order of the participants remained the same, but the intensity of the push, initial inter-person distance, and the initial arm posture were varied. In total, 42 pushes without wall and 55 pushes with wall are analysed.

Trials in which persons stood relaxed could not be carried out in a standardised way, because individual interpretations of this condition were possible. The person

at the end of the line moved quite differently when pushed at the lower back rather than the shoulder, which made it difficult to compare these trials with each other. In order to simplify the experiments, not all variations, e.g. arm postures or interperson distances, were included in the case of standing relaxed or being pushed at lower back. Therefore, these trials are only used for a qualitative description.

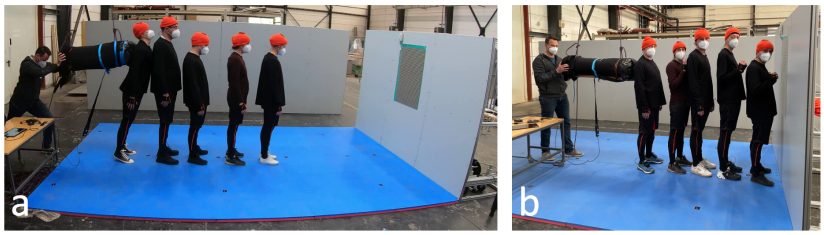

Figure 2: Setup of the experiments (a) without wall and (b) with wall. Five people lined up in a queue and were pushed forward in a controlled manner.

2.3 Data sets

During the experiments, various data sets were recorded.

2.3.1 Video recordings

The experiments were filmed with 25 fps from a top-down as well as from a lateral perspective. The side-view ensures a qualitative analysis of the trials. During the experiments, each participant had to wear an orange hat with an attached Aruco-Code which is linked to individual characteristics such as body measurements and gender in an anonymised way. These hats with codes are automatically detected and tracked using the video recordings from above in the Software PeTrack[21, 22]. The so derived individual head trajectories give information on the position within the experimental area (Figure 3) and can be used to calculate other quantities, e.g. the velocity of the individual participants.

2.3.2 3-dimensional inertial motion capturing

All participants were dressed in a 3-dimensional motion capturing (MoCap) suit from Xsens [23], which in turn was equipped with 17 inertial measurement units (IMU). In order to record movements of each individual limb, the IMU sensors, measuring acceleration, the angular rate and the magnetic field strength, are placed on specific body segments, that can move separately from each other. The advantage of this MoCap system, in contrast to other e.g. optical MoCap techniques, is that no full view of all body parts is necessary and therefore the Xsens suits can also be used in crowds.

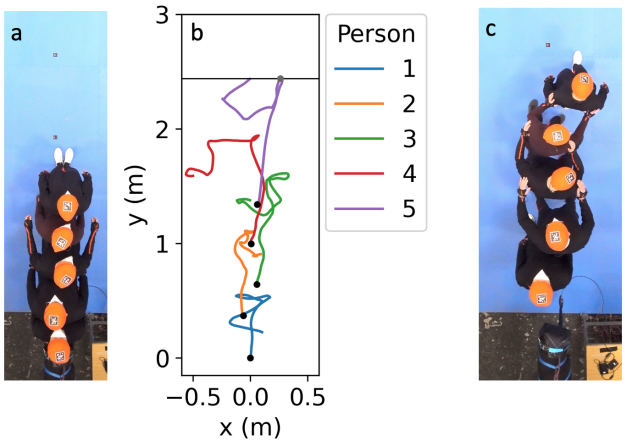

Figure 3: (a) The snapshot from the overhead video recordings shows the participants at the beginning of the trial. (b) For all five participants, the start positions are represented as black dots and extracted head trajectories are plotted as coloured lines. It was pushed along the positive y-direction. (c) The snapshot from the overhead video recordings shows the position, when all participants have regained balance. This is set as end position for a push.

A calibration is required prior to the actual data recording. For this purpose, detailed body measurements for all participants were taken. By applying a biomechanical model in the MVN Analyze software, the orientation, position, velocity, acceleration, angular velocity and angular acceleration of every segment in addition to the joint angles and the position of the center of mass (CoM) are determined. Each Xsens suit is connected wirelessly to the software MVN Analyze allowing a simultaneous start of the measurements. All data is recorded with 240 fps and stored on a local body pack in each suit. To synchronise camera recordings with one another and with the motion data in time, a timecode generator Tentacle Sync E [24] is used to impose time-codes on the measured data sets.

However, the resulting 3D position data are considered for each individual separately and are not aligned to the global coordinate system of the experimental area, because the IMU sensors rely on relative measurements. To ensure a correct spatial placement and orientation of all participants to each other, the 3D MoCap data are projected onto the camera trajectories (Figure 4) by employing a hybrid tracking algorithm [25]. This allows the trajectories of the CoM to be used for further analysis of the motion initiated by a push, thereby neglecting large head movements.

2.3.3 Pressure

The pressure sensor Xsensor LX210:50.50.05 [26] was attached to the punching bag and connected to the software Xsensor Pro V8. Covering an area of 25.4 cm × 25.4 cm, 2500 measuring cells record pressure at a framerate of 34 fps. The pressure range is

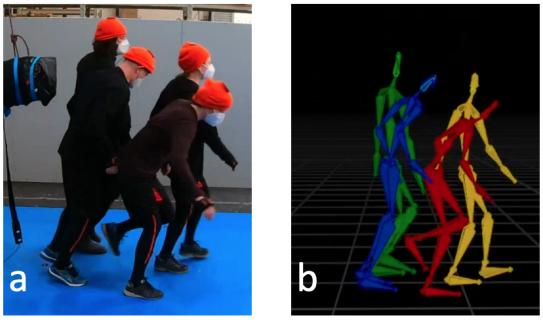

Figure 4: (a) Participants wearing a 3D MoCap suit are pushed forward. (b) Combining 3D MoCap data with trajectories provides accurate positioning in the experimental area.

set to $0.14\,\mathrm{Ncm}^{-2}$ – $10.3\,\mathrm{Ncm}^{-2}$, because the sensor has been pre-calibrated by the manufacturer.

In addition, the Pressure Mapping Sensor 5400N from TekScan [27] was mounted on the wall vertically and covered with Teflon foil. This sensor measures the pressure with 1768 cells on an area of $57.8\,\mathrm{cm} \times 88.4\,\mathrm{cm}$ at 90 fps using the I-Scan software. For a preliminary calibration, weights of 120 kg and 185 kg were placed on the horizontally lying sensor and mapped to pressure values with a sensitivity of S-30. The sensitivity is a measure of how responsive the pressure sensor reacts. We used a higher sensitivity than the default value to increase the resolution of the pressure measurements between the range of $0\,\mathrm{Ncm}^{-2}$ – $8\,\mathrm{Ncm}^{-2}$.

An instantaneous recording of the pressure sensor indicates the contact area of the punching bag with the first person pushed as well as the pressure on the sensor surface. The pressure recordings P are integrated over the area of the sensor A for each time frame. This results in a normal force F_n acting on the back of the first person pushed. The temporal development of this force provides information about other quantities such as the maximum force or the duration of a push (Figure 5). The integral of F_n over time determines an impulse of the push J.

$$F_n(t) = \int_A P \,\mathrm{d}A$$

$$J = \int_t F_n(t) \,\mathrm{d}t$$

2.3.4 Accuracy

In the coordinate system of the experimental area, the head trajectories have an error of 1.54 cm and 1.20 cm for the experiments with and without wall, respectively, as a result of the calibration in PeTrack and the consideration of the correct body heights for each participant. In addition, there is an error of approximately 3 cm because the correct position of the top of head, as also given in the 3D MoCap data, is important mainly for combining 3D MoCap data with trajectories.

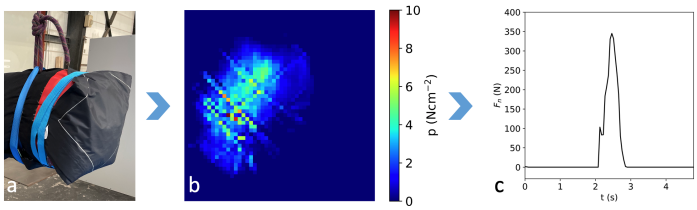

Figure 5: (a) A pressure sensor measures the pushing intensities at the punching bag. (b) Spatial image of a single time frame recorded by the pressure sensor. (c) Time series of the normal force $F_n(t)$.

The 3D MoCap data has a positional drift over time increasing the error of the positioning, which can be neglected because of the hybrid tracking algorithm. Within one motion capturing suit, the accuracy of the individual limbs to each other have a dynamic error of 1 ° RMS. The static accuracy of the trackers have an error for roll and pitch of 0.2 ° and for heading 0.5 ° [28]. It should be noted that taking body measurements contribute an estimated error of 2 cm to the biomechanical model.

The pressure sensor from Xsensor used at the punching bag has an accuracy of 5 % [26] at full scale. Based on the performed calibration, we assume that the accuracy of the pressor sensor from TekScan is 7 %.

3 Results

In the following, the trajectories of the CoM which result from the hybrid tracking algorithm are analysed because the head trajectories can show large movements. Furthermore, we only consider movements in the pushing direction, i.e. in y-direction, because only a normal component can be measured at the pressure sensor. This breaks down the experiment, which already represents a simplification of the reality e.g. a waiting queue, to the smallest and simplest level. Thus, an isolated observation of how much of the push is really transmitted forward into the movement of participants without the influence of people standing around can be made.

3.1 Pressure measurement

One of the objectives of this study was to categorise the strength of the impact in order to achieve comparable pushes. Considering that the strength of the impact is difficult to estimate for the manual pusher and the values cannot be read immediately at the pressure sensor, we aimed to obtain three different pushing intensities. According to the announcement, the punching bag was manually pushed forward in the categories: weak, medium and strong. Absolut values for these three categories were not achieved and therefore the measured impulses are used for further analysis. A detail comparison of the measured impulse of each push with the three categories (weak, medium and strong) can be found in S1.

Different impulses were measured for the three initial inter-person distances, which

contradicts the expectation that the strength of a push only depends on the person who pushed. This might be explained by the fact, that the pressure sensor responds to a resistance. When the participants stand close to each other, the first person might already touch the second person while being pushed and thus increasing the resistance. It should be further noted, that the pusher could have unknowingly adjusted the pushes according to the resistance or experimental condition (with or without wall). With the wall, the probability of injuries is more likely, so perhaps the pushing intensity was reduced for these trials. Differences in the measured values for different initial inter-person distances as well as the conditions with and without wall can be seen in Figures S1 b and S1 a.

When the measured impulses on the wall are compared with the values measured on the punching bag, a certain correlation can be seen for different inter-person distances (Figure 6). Here, the values on the wall for elbow distance are noticeable higher compared to no or arm distance. This corresponds to the perception of the participants who rated the trials with elbow distance as most dangerous.

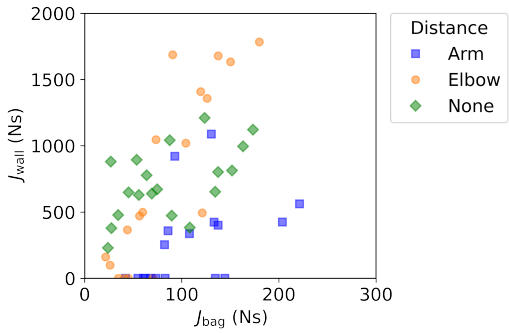

Figure 6: Impulse measured at the wall compared to impulses measured at punching bag. Please note: Data recorded at the wall cannot be quantitatively compared to data recorded at the punching bag.

Furthermore, it has to be noted that the impulses measured at the wall are significantly higher than the impulses calculated at the punching bag. The reason is that the two measurements were carried out using different sensors with different frame-rates and sensels sizes. The sensor on the punching bag has better surface resolution and a higher sensitivity while the sensor on the wall has a higher resolution in time. Furthermore, the contact surfaces varied since it makes a difference if the back of a person is pushed with a deformable punching bag or bony elbows of a person touch a solid wall. Most importantly, the contact time on the punching bag is limited whereas the contact time on the wall can exceed several seconds. This makes the comparison of the data from the two pressure sensors difficult (Figure 6). However, the data from the same sensor can be compared for different trials.

3.2 Propagation distance of a push

An analysis is made of how far a push propagates through a row of five people. First, the number of participants who were affected by the push, i.e. who moved forward, is counted (Figure 7).

The number of people moving forward due to the push depends on the initial distance of the participants to each other and on the strength of the push. At no distance, all five persons are affected by the push regardless of the magnitude of the impulse. At elbow distance, all participants move forward when the exerted impulse reaches over 75 Ns. At arm distance, the push propagates through the entire row of people starting at a value of 90 Ns.

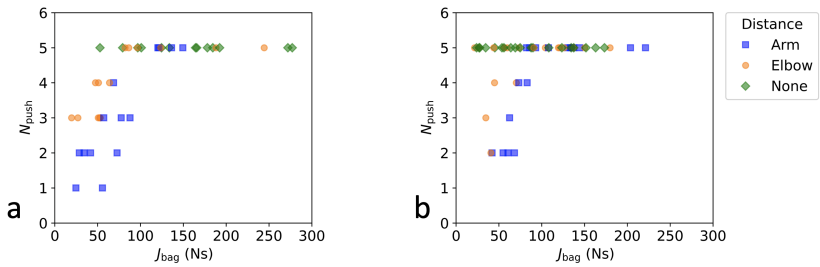

Figure 7: Number of persons affected by the push in relation to the impulse at the punching bag for (a) experiments without wall and (b) experiments with wall. If the initial inter-person distance is small and the impulse is large, more people move forward due to the push.

To define a propagation distance of the push, the distance between the initial position of the person standing at the punching bag and the end position of the last person moving forward is calculated. This takes two factors into account: The number of persons affected by the push (Figure 7) as well as the distance the last person needed to regain balance. In doing so, several steps could have been taken forward (Figure 3 c). As an example, Figure 3 b indicates the distance of the push by a black horizontal line.

For the experiments without wall, there is a linear relation between the propagation distance of the push and the impulse given into the system for impulses below 110 Ns (Figure 8 a). Above 110 Ns a maximum of 3 m as the propagation distance is reached. That could be related to the fact that the push passes through the entire row and the last person steps forward the same regardless of the intensity of the push. Perhaps the wall at the end of the experimental area could also have an influence on this behaviour. In the experiments with wall, the boundary is clearly visible (Figure 8 b) and corresponds well to the findings in Figure 7 b.

3.3 Propagation speed of a push

For the definition of a speed at which the push propagates through the row, the forward motion of each participant is considered (Figure 9). The elbow point of the

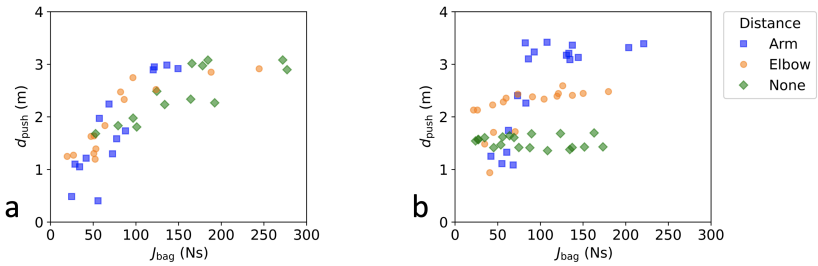

Figure 8: Propagation distance of the push for (a) experiments without wall and (b) experiments with wall. (a) The propagation distance increases with stronger pushes before reaching a maximum. (b) The propagation distance is often the same as the distance to the wall.

y-t-curve (black dot) between a fixed start and end time of the push indicates the start time of the motion which corresponds to the time the push affects this person. These points are aligned on a linear regression very well. Therefore, we define the propagation speed as the gradient of the regression line.

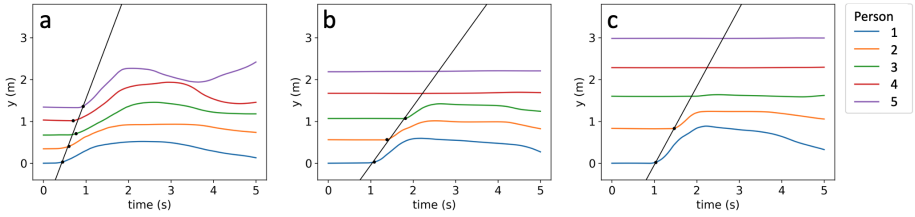

Figure 9: Forward motion of CoM used to define a propagation speed of the push through the row of five persons for exemplary trials with different initial inter-person distances: (a) none, (b) elbow and (c) arm. The y-axis is aligned along the pushing direction. The regression lines (black) of the elbow points (black point) determine the propagation speed. When a person is not affected by the push, no elbow point is assigned.

Figure 10 shows that the propagation speed depends on the intensity of the push. There is a linear relation between the propagation speed and the impulse of the push. However, the initial arm posture of the participants makes a difference, whereas inter-person distances have no effect on the propagation speed. For the three initial arm postures (up, free, down), a multiple linear regression with interaction terms (moderation analysis) was performed in R. The analysis did not show a significant difference between arms down and arms free. Arms up has a significant effect on the propagation speed with $p < 0.001$ (between up and down) and $p = 0.01$ (between up and free). However, there is no significant interaction between arms up and the intensity of the push, as we found a p value of 0.055. The fact that the result is just not significant could also be caused by the small sample size. The complete output of the moderation analysis can be found in S2. We conclude that there are two equations for the propagation speed:

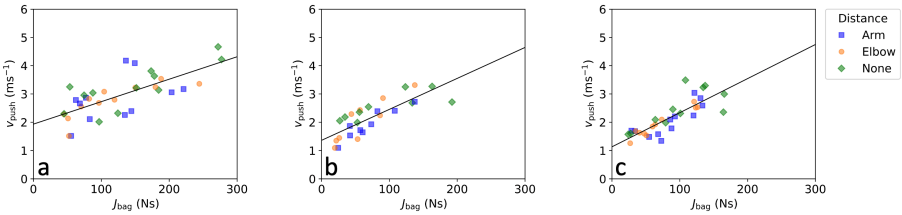

Figure 10: Propagation speed of the push through a row of five persons for different initial arm positions: (a) up, (b) free, (c) down. In this case, trials with and without wall are considered together. A linear fit is indicated by a black line. The propagation speed increases with larger impulses.

$$v_{\text{push, up}} = 0.012 \frac{\text{m}}{\text{Ns}^2} \cdot J_{\text{bag}} + 1.933 \frac{\text{m}}{\text{s}}$$

$$v_{\text{push, down}} = 0.012 \frac{\text{m}}{\text{Ns}^2} \cdot J_{\text{bag}} + 1.130 \frac{\text{m}}{\text{s}}$$

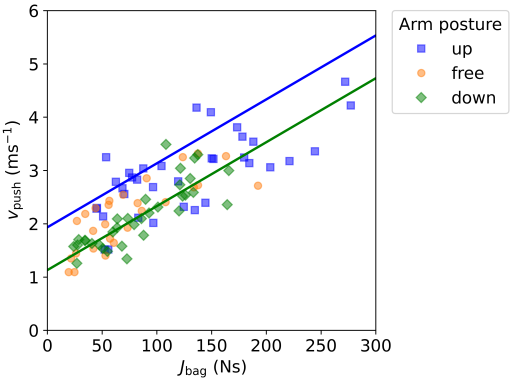

Figure 11: Propagation speed of the push through a row of five persons for different initial arm postures (up, free, down). In this case, trials with and without wall are considered together. The propagation speed increases with larger impulses. For arms up or arms down/free, two linear fits can be obtained, shown as blue and green lines

A comparison of the two linear equations can be seen in Figure 11. Through the effect of arms up there are different y-intercepts, but because we cannot assume an interaction the lines are parallel. This means, a push propagates faster through the row if the participants keep their arms up from the start. The results are consistent with the qualitative observation of the experiments, as people behaved very similarly with arms down and free. With arms up, the participants already touched each other from the start and were thus also able to pass on the push more quickly.

4 Discussion

In this article, experiments were performed to investigate how pushes propagate through a crowd. For this purpose, a crowd was simplified as a row of five people, and only one pushing as well as one propagation direction were considered. As soon as a person standing in a queue is pushed forward, the impact is passed on. Thereby, it depends on the strength of the push, the initial inter-person distance and the initial arm posture how far or how fast the push propagates. From a modelling perspective, this implies that the "dominoes" approach could be problematic, since in the naive concept of dominoes, the propagation of the push merely depends on the initial distance. Therefore, it might be more appropriate to model pedestrians as inverted pendulums when they are exposed to an external force.

In our experiments we tried to classify the intensities of the pushes. It is difficult to estimate forces in a crowd, because only the normal component of a force vector was measured with a pressure sensor and muscle forces of participants were neglected. In addition, one person manually pushed the participants for all trials leading to a less reliable repeatability. Based on different situations, the pushes can be adjusted. For example a high resistance on the punching bag can intensify the measured impulses. A wall at the end of the row, on the other hand, may reduce the pushing intensity, because the person manually pushing aims to avoid injuries at the wall.

The trials with elbow distance were rated as being most dangerous by the participants. These trials also often involved the highest impulses being measured at the wall, especially in the case of strong pushes. The factors of space and time are probably important in explaining this. It could be assumed that at elbow distance participants may have not enough space for their reaction (e.g. setting steps) and interact with one another very quickly, whereas at arm distance more space and time is available. This can lead to more collision of the feet, which in turn increases the risk of tripping or even falling. At no distance, the interaction between participants already starts before the push and they can be better aware of the available space for their own feet. Another factor that may contribute to the increased danger at elbow distance is the speed with which interactions between participants occur. At elbow distance, each participant can accelerate more compared to no distance. But compared to arm distance, there might be hardly no time to slow down or restore their own balance before colliding with the person in front. This would also result in more people reaching the wall at higher speed and thus increasing the measured impulses at the wall. However, this is just an assumption and has to be further investigated for example by analysing the 3D MoCap data in more detail.

The results presented in this article provide valuable information on propagation distance and speed of a push taking into account different body positions as well as pushing intensities. This in turn can give insight into how people move one another, intentionally or unintentionally, and thereby help to better understand dynamics even in larger crowds. These information can be used to validate and improve pedestrian models as well as to help assess risk levels and prevent potentially

dangerous situations. In our analysis, it is especially interesting to observe, that the initial inter-person distance has no effect on the propagation speed. This means that the propagation speed is not dependent on the quasi 1D density. However, just applying this concept to a larger crowd with 2D density seems a bit tricky. This analysis should be investigated on a larger sample size to draw a statistically significant conclusion. Besides, the propagation speed needs to be analysed for 2D densities, for example in experiments where several rows are standing next to each other.

Furthermore, other factors such as individual characteristics, body tension, and also preparedness can play an important role in how a push propagates. People can respond in individual ways by choosing different strategies (ankle, hip, steps [29], [30], [31]) to regain balance. This could result in either absorbing or intensifying the impact. Individual motion strategies and associated factors that influence the transmission will be investigated in more detail in the future using the 3D motion data. We will focus on the evaluation of the steps (step length, step width and number of steps), movements of the hips as well as pendulum movements of the upper body.

The small-scale experiments presented here examined a total of 97 pushes on eight different participants. This is a small sample size that may not allow for a reliable statistical analysis. Therefore, the proposed analysis will be applied to larger experiments including up to thirty participants. So far, only a very simplified representation of the crowd in form of a row of people have been considered, which can limit the generalisability of the findings. Our results can mainly be applied to real-world situations where people are standing along a line, e.g. a waiting queue as observed at the entrance of a concert.

But in real-world situations, people are often distributed in a random and irregular order. Especially in larger crowds, it is important to consider the arrangement of people in order to investigate the propagation of a push more accurately. In upscaled experiments, positioning of the participants will be varied in order to obtain a more realistic representation of crowds. The persons will stand either in a long row, in several rows next to each other or staggered as a group. Thus, not only the propagation of the push to the front will be investigated, but also how the push propagates to the side and therefore including density into the analysis. Furthermore, the analysis will focus on the extent to which the transmission of an impulse differs from how the participants were prepared.

Data Availability

The raw data from the experiments are freely accessible at the Pedestrian Dynamics Data Archive of the Research Centre Jülich, doi: 10.34735/ped.2022.2.

Acknowledgements

We would like to thank Jernej Čamernik, Marc Ernst, Helena Lügering, Armin Seyfried and Anna Sieben who supported us in the conception, planning and realisation of the experiments. Furthermore, we are grateful to Alica Kandler, Maik Boltes, Ann Katrin Boomers and Tobias Schrödter for their help in setting up the experiments and curating the data.

Funding

This research was supported by the European Unions Horizon 2020 research and innovation program within the project CrowdDNA [project number 899739].

Ethical Review

The experiments were approved by the ethics board of the University of Wuppertal in April 2021 (Reference: MS/BBL 210409 Seyfried).

References

[1] Virginia Harrison and Carly Earl. "A visual guide to how the Seoul Halloween crowd crush unfolded". en-GB. In: *The Guardian* (Oct. 2022). ISSN: 0261-3077. URL: https://www.theguardian.com/world/2022/oct/31/how-did-the-seoul-itaewon-halloween-crowd-crush-happen-unfolded-a-visual-guide (visited on 01/02/2023).

[2] Dirk Helbing, Anders Johansson, and Habib Zein Al-Abideen. "Dynamics of crowd disasters: An empirical study". en. In: *Physical Review E* 75.4 (Apr. 2007), p. 046109. ISSN: 1539-3755, 1550-2376. DOI: 10.1103/PhysRevE.75.046109.

[3] Barbara Krausz and Christian Bauckhage. "Loveparade 2010: Automatic video analysis of a crowd disaster". en. In: *Computer Vision and Image Understanding* 116.3 (Mar. 2012), pp. 307–319. ISSN: 10773142. DOI: 10.1016/j.cviu.2011.08.006.

[4] John J Fruin. "THE CAUSES AND PREVENTION OF CROWD DISASTERS". en. In: (1993).

[5] Dirk Helbing and Pratik Mukerji. "Crowd disasters as systemic failures: analysis of the Love Parade disaster". en. In: *EPJ Data Science* 1.1 (Dec. 2012), p. 7. ISSN: 2193-1127. DOI: 10.1140/epjds7.

[6] Arianna Bottinelli and Jesse L. Silverberg. *Can high-density human collective motion be forecasted by spatiotemporal fluctuations?* arXiv:1809.07875 [physics]. Sept. 2018. URL: http://arxiv.org/abs/1809.07875 (visited on 01/02/2023).

[7] Angel Garcimartìn, Diego Maza, José Martìn. Pastor, Daniel R. Parisi, César Martìn-Gómez, and Iker Zuriguel. "Redefining the role of obstacles in pedestrian evacuation". In: *New Journal of Physics* 20.12 (Dec. 2018), p. 123025. ISSN: 1367-2630. DOI: 10.1088/1367-2630/aaf4ca.

[8] Claudio Feliciani, Iker Zuriguel, Angel Garcimartín, Diego Maza, and Katsuhiro Nishinari. "Systematic experimental investigation of the obstacle effect during non-competitive and extremely competitive evacuations". en. In: *Scientific Reports* 10.1 (Sept. 2020), p. 15947. ISSN: 2045-2322. DOI: 10.1038/s41598-020-72733-w.

[9] Dirk Helbing, Illés Farkas, and Tamás Vicsek. "Simulating dynamical features of escape panic". en. In: *Nature* 407.6803 (Sept. 2000), pp. 487–490. ISSN: 0028-0836, 1476-4687. DOI: 10.1038/35035023.

[10] Wouter van Toll, Cédric Braga, Barbara Solenthaler, and Julien Pettré. "Extreme-Density Crowd Simulation: Combining Agents with Smoothed Particle Hydrodynamics". en. In: *Motion, Interaction and Games*. Virtual Event SC USA: ACM, Oct. 2020, pp. 1–10. ISBN: 978-1-4503-8171-0. DOI: 10.1145/3424636.3426896.

[11] Jingni Song, Feng Chen, Yadi Zhu, Na Zhang, Weiyu Liu, and Kai Du. "Experiment Calibrated Simulation Modeling of Crowding Forces in High Density Crowd". In: *IEEE Access* 7 (2019), pp. 100162–100173. ISSN: 2169-3536. DOI: 10.1109/ACCESS.2019.2930104.

[12] Juliane Adrian, Armin Seyfried, and Anna Sieben. "Crowds in front of bottlenecks at entrances from the perspective of physics and social psychology". en. In: *Journal of The Royal Society Interface* 17.165 (Apr. 2020), p. 20190871. ISSN: 1742-5689, 1742-5662. DOI: 10.1098/rsif.2019.0871.

[13] Ezel Üsten, Helena Lügering, and Anna Sieben. "Pushing and Non-pushing Forward Motion in Crowds: A Systematic Psychological Observation Method for Rating Individual Behavior in Pedestrian Dynamics". In: *Collective Dynamics* 7 (Aug. 2022), pp. 1–16. ISSN: 2366-8539. DOI: 10.17815/CD.2022.138.

[14] Ahmed Alia, Mohammed Maree, and Mohcine Chraibi. "A Hybrid Deep Learning and Visualization Framework for Pushing Behavior Detection in Pedestrian Dynamics". en. In: *Sensors* 22.11 (May 2022), p. 4040. ISSN: 1424-8220. DOI: 10.3390/s22114040.

[15] Iker Zuriguel, Iñaki Echeverría, Diego Maza, Raúl C. Hidalgo, César Martín-Gómez, and Angel Garcimartín. "Contact forces and dynamics of pedestrians evacuating a room: The column effect". en. In: *Safety Science* 121 (Jan. 2020), pp. 394–402. ISSN: 09257535. DOI: 10.1016/j.ssci.2019.09.014.

[16] Chongyang Wang and Wenguo Weng. "Study on the collision dynamics and the transmission pattern between pedestrians along the queue". en. In: *Journal of Statistical Mechanics: Theory and Experiment* 2018.7 (July 2018), p. 073406. ISSN: 1742-5468. DOI: 10.1088/1742-5468/aace27.

[17] Xudong Li, Weiguo Song, Xuan Xu, Jun Zhang, Long Xia, and Congling Shi. "Experimental study on pedestrian contact force under different degrees of crowding". en. In: *Safety Science* 127 (July 2020), p. 104713. ISSN: 09257535. DOI: 10.1016/j.ssci.2020.104713.

[18] Chongyang Wang, Shunjiang Ni, and Wenguo Weng. "Modeling human domino process based on interactions among individuals for understanding crowd disasters". en. In: *Physica A: Statistical Mechanics and its Applications* 531 (Oct. 2019), p. 121781. ISSN: 0378-4371. DOI: 10.1016/j.physa.2019.121781.

[19] Chongyang Wang, Liangchang Shen, and Wenguo Weng. "Experimental study on individual risk in crowds based on exerted force and human perceptions". In: *Ergonomics* 63.7 (July 2020). Publisher: Taylor & Francis, pp. 789–803. ISSN: 0014-0139. DOI: 10.1080/00140139.2020.1762933.

[20] Xudong Li, Xuan Xu, Jun Zhang, Kechun Jiang, Weisong Liu, Ruolong Yi, and Weiguo Song. "Experimental study on the movement characteristics of pedestrians under sudden contact forces". en. In: *Journal of Statistical Mechanics: Theory and Experiment* 2021.6 (June 2021). Publisher: IOP Publishing, p. 063406. ISSN: 1742-5468. DOI: 10.1088/1742-5468/ac02c7.

[21] Maik Boltes and Armin Seyfried. "Collecting pedestrian trajectories". In: *Neurocomputing* 100 (2013). Special issue: Behaviours in video, pp. 127–133. ISSN: 0925-2312. DOI: https://doi.org/10.1016/j.neucom.2012.01.036.

[22] Maik Boltes, Ann Katrin Boomers, Juliane Adrian, Ricardo Martin Brualla, Arne Graf, Paul Häger, Daniel Hillebrand, Deniz Kilic, Paul Lieberenz, Daniel Salden, and Tobias Schrödter. *PeTrack*. Version v0.9. July 2021. DOI: 10.5281/zenodo.5126562.

[23] Martin Schepers, Matteo Giuberti, and Giovanni Bellusci. "Xsens MVN: Consistent Tracking of Human Motion Using Inertial Sensing". en. In: (2018). DOI: 10.13140/RG.2.2.22099.07205.

[24] Tentacle Sync GmbH. *Tentacle Sync E - Operating Manual v1.0*. 2020. URL: https://tentaclesync.com/files/documents/Tentacle_Sync_E_Operating_Manual_ENG.pdf.

[25] Maik Boltes, Juliane Adrian, and Anna-Katharina Raytarowski. "A Hybrid Tracking System of Full-Body Motion Inside Crowds". en. In: *Sensors* 21.6 (Mar. 2021), p. 2108. ISSN: 1424-8220. DOI: 10.3390/s21062108.

[26] Xsensor LX210:50.50.05. *Datasheet: Xsensor SENSORS LX210:50.50.05*. 2019. URL: https://www.xsensor.de/wp-content/uploads/2015/11/LX210_50_50_05-2500-Sensoren-508mm-Aufl%C3%B6sung-Gr%C3%B6sse-25x25cm-Messbereich-014-11Ncm2-Anwendung-Sitze_Rollst%C3%BChle.pdf (visited on 10/13/2022).

[27] Tekscan PMS5400N. *Datasheet: Tekscan Pressure Mapping Sensor 5400N*. 2019. URL: https://www.tekscan.com/sites/default/files/resources/IDL-Pressure-Mapping-Sensor-5400N-Datasheet_0.pdf (visited on 10/13/2022).

[28] Xsens. *MVN User Manual, Revision Z, 20 04 2022*. 2022. URL: https://www.xsens.com/hubfs/MVN_User_Manual.pdf.

[29] Da Winter. "Human balance and posture control during standing and walking". en. In: *Gait & Posture* 3.4 (Dec. 1995), pp. 193–214. ISSN: 09666362. DOI: 10.1016/0966-6362(96)82849-9.

[30] Brian E. Maki and William E. McIlroy. "Control of rapid limb movements for balance recovery: age-related changes and implications for fall prevention". en. In: *Age and Ageing* 35.suppl_2 (Sept. 2006), pp. ii12–ii18. ISSN: 1468-2834, 0002-0729. DOI: 10.1093/ageing/afl078.

[31] Dario Tokur, Martin Grimmer, and André Seyfarth. "Review of balance recovery in response to external perturbations during daily activities". en. In: *Human Movement Science* 69 (Feb. 2020), p. 102546. ISSN: 01679457. DOI: 10.1016/j.humov.2019.102546.

S Supplementary Information

S1 Pressure measurement

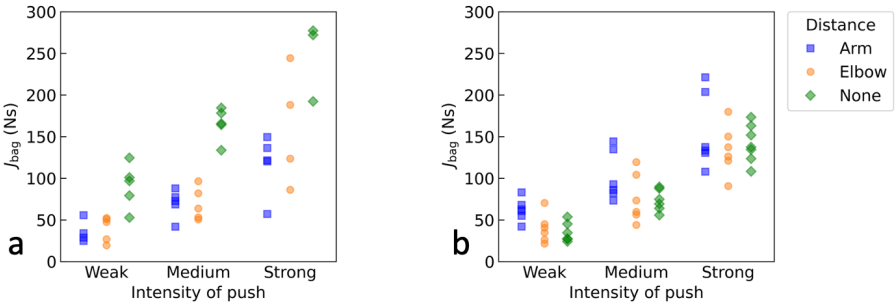

Figure S1: Impulse of the push measured at the punching bag for (a) experiments without wall and (b) experiments with wall. There is a general correlation between the perceived strength and the recorded values, but the impulse is affected by the initial inter-person distance as well as the experimental condition (with or without wall).

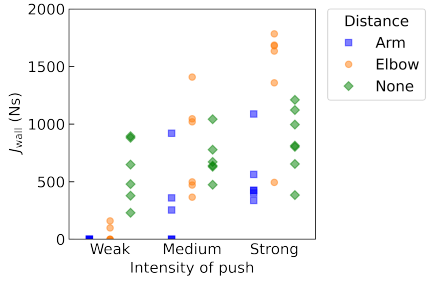

Figure S2: Impulse measured at the wall compared to perception of push.Please note: Data recorded at the wall cannot be quantitatively compared to data recorded at the punching bag.

The measured impulse of each push, which is differentiated according to the initial inter-person distances, is compared with the three categories (weak, medium and strong) based on the perception of intensity for the first pushed person in Figure S1. Thereby, the experimental series with wall (Figure S1 b) and without (Figure S1 a) are considered separately.

Within the same perceived strength, the measured impulses show a large variation, comparable to the range between the different categories (weak, medium, strong). Although there is a general correlation between the perceived strength and the recorded values, it is noticeable that the initial inter-person distance as well as the experimental condition (with or without wall) have an influence. In the experiments without a wall the values for no distance are often larger than for elbow or arm

distance, whereas in the experiments with a wall it is vice versa. We conclude that the participants' perception is not a good measure for estimating the strength of an impact. Therefore, the measured impulses are used for further analysis.

The same analysis as well as the comparison of calculated impulse to the three categories is conducted for the pressure values measured at the wall (Figure S2). In case of weak pushes, there is no impact on the wall at arm distance and only a small impact at elbow distance. For all other conditions, the impulse data has a high scatter. When the participants were standing with no distance to each other, there is no significant difference in the calculated impulses among the three perceptions.

S2 Moderation analysis

A moderation analysis was conducted in R version 4.3.2. The results are shown in Table S1 for the comparison of arm postures up, free and down.

Table S1: Moderation analysis comparing arms up and arms free to arms down

Residuals:	Min	1Q	Median	3Q	Max
	-0.8591	-0.2509	0.0002	0.2561	1.1630
Coefficients	**Estimate**	**Std. Error**	**t**	**p**	**Signif.**
intercept	1.1303	0.1701	6.644	2.3e-09	***
impulse of push	0.0121	0.0018	6.695	1.8e-09	***
arm posture free	0.2296	0.2319	0.990	0.32476	
arm posture up	0.8025	0.2328	3.447	0.00086	***
impulse : arm posture free	-0.0011	0.0025	-0.437	0.66305	
impulse : arm posture up	-0.0041	0.0021	-1.944	0.05502	.
Signif. codes: 0 '***' 0.001 '**' 0.01 '*' 0.05 '.' 0.1 ' ' 1					
Residual standard error: 0.4288 on 90 degrees of freedom Multiple R-squared: 0.6952, Adjusted R-squared: 0.6782 F-statistic: 41.05 on 5 and 90 DF, p-value: < 2.2e-16					

PUBLICATION B

Temporal segmentation of motion propagation in response to an external impulse

This article was published as Feldmann, S., Chatagnon, T., Adrian, J., Pettré, J., Seyfried, A. (2024). Temporal segmentation of motion propagation in response to an external impulse. Safety Science, 175, 106512. doi: 10.1016/j.ssci.2024.106512

Author Contributions

CONCEPTUALIZATION: Sina Feldmann, Juliane Adrian, Julien Pettré and Armin Seyfried
DATA CURATION: Sina Feldmann
FORMAL ANALYSIS: Sina Feldmann
INVESTIGATION: Sina Feldmann
METHODOLOGY: Sina Feldmann, Thomas Chatagnon, Juliane Adrian, Julien Pettré and Armin Seyfried
SUPERVISION: Juliane Adrian, Julien Pettré and Armin Seyfried
VALIDATION: Sina Feldmann
VISUALIZATION: Sina Feldmann
WRITING–ORIGINAL DRAFT PREPARATION: Sina Feldmann
WRITING–REVIEW AND EDITING: Sina Feldmann, Thomas Chatagnon, Juliane Adrian, Julien Pettré and Armin Seyfried

Temporal segmentation of motion propagation in response to an external impulse

Sina Feldmann[1] [2] , Thomas Chatagnon[3] , Juliane Adrian[1] , Julien Pettré[3] , and Armin Seyfried[1] [2]

[1] Institute for Advanced Simulation 7: Civil Safety Research, Forschungszentrum Jülich, Jülich, Germany
[2] Faculty of Architecture and Civil Engineering, University of Wuppertal, Wuppertal, Germany
[3] Univ Rennes, Inria, CNRS, IRISA, M2S, France

Highlights

- 3D motion as response to an external impulse is segmented into temporal phases.
- Three phases of motion involve different physical interactions.
- Reception and transmission of an impulse are separated.
- Development of a method to detect the phases in 3D motion data.

Abstract

In high-density crowds, local motion can propagate, amplify, and lead to macroscopic phenomena, including "density waves". These density waves only occur when individuals interact, and impulses are transferred to neighbours. How this impulse is passed on by the human body and which effects this has on individuals is still not fully understood. To further investigate this, experiments focusing on the propagation of a push were conducted. In the experiments the crowd is greatly simplified by five people lining up in a row. The rearmost person in the row was pushed forward in a controlled manner with a punching bag. The intensity of the push, the initial distance between participants and the initial arm posture were varied. Collected data included side view and top view video recordings, head trajectories, 3D motion using motion capturing (MoCap) suits as well as pressure measured at the punching bag. With a hybrid tracking algorithm, the MoCap data are combined with the head trajectories to allow an analysis of the motion of each limb in relation to other persons.

The observed motion of the body in response to the push can be divided into three phases. These are (i) receiving an impulse, (ii) receiving and passing on an impulse, and (iii) passing on an impulse. Using the 3D MoCap data, we can identify

the start and end times of each phase. To determine when a push is passed on, the forward motion of the person in front has to be considered. The projection of the center of mass relative to the initial position of the feet is a measure of the extent to which a person is displaced from the rest position. Specifying the timing of these phases is particularly important to distinguish between different types of physical interactions. Our results contribute to the development and validation of a pedestrian model for identifying risks due to motion propagation in dense crowds.

Keywords: External Impulse; Motion Propagation; Pedestrian; Experiment; Motion Capturing; Balance

1 Introduction

Motion is a fundamental concept in physics and refers to the change in position of an object, either in terms of its distance from a point or its displacement from an initial position. Studying the motion of pedestrians is relevant for applications such as public space design, traffic engineering, and crowd safety. Especially in large crowds, pedestrian safety is of great importance, and crowd accidents are widely reported in the media ([1]). To better understand the causes of these accidents and the associated risks, it is necessary to analyse crowd motions.

The motion of a crowd (macroscopic scale) results from the motion of multiple individuals and, in particular, from the motion of their three-dimensional bodies (submicroscopic scale). Macroscopic phenomena are caused by the propagation of motion in a crowd, which occur when individuals interact and impulses are transmitted. The motion of people in crowds is generally described by points in terms of their velocity or flow through a facility or characterised by their density distributions ([2, 3]). In this context, the motion of pedestrians is assessed in two dimensions, either when trajectories are recorded in experiments (e.g. [4]) or when pedestrians are represented as circles or ellipses in models ([5, 6]). Videos of crowds are also evaluated during on-site observations ([7, 8]) or when analysing actual crowd accidents (e.g. [9, 10]), considering mainly the motion of heads as the main body is occluded. For a detailed list of accidents that occurred over the years see [1]. In this way, macroscopic phenomena and collective movements of a crowd that are considered high risk can be characterised. These include, for example, clogging in front of bottlenecks ([11, 12]), density waves ([13]), pressure waves ([14, 15]), turbulences ([9, 16]), or transversal waves ([4, 17]). There are approaches to simulate contact forces ([18, 19]), but how exactly impulses propagate in a crowd is not yet fully understood. Furthermore, the exact motion of people is disregarded and three dimensional movement patterns cannot be described sufficiently. One example of this is the risk of people falling over and forming a pile on the ground ([15, 20]).

The risk of losing balance, stumbling or falling down results from challenges that individuals face at the sub-microscopic scale. Previous research on human standing balance has focused on different recovery strategies for single individuals following external perturbations, e.g. the ankle, hip or stepping strategies to regain balance

([21–23]). In this context, the critical point for static human balance has been defined as the time at which the projected centre of mass (CoM) on the ground passes the base of Support (BoS) in static conditions ([21]). Later on, the use of the extrapolated center of mass (XCoM) was proposed to study standing balance in dynamic conditions ([24, 25]). Further indicators for human standing balance such as the Margin of Stability (MoS) ([24, 26, 27]) or the Time-to-boundary ([28–30]), have also been introduced. The aforementioned studies are limited to single individuals and do not consider how the presence of others restricts the torso and limb movements, thus affecting the recovery of balance. On the one hand, the lack of space may alter the strategies chosen and foster stumbling; on the other hand, individuals may also use other change-in-support options, such as contact with their neighbours, to increase their BoS ([31]). Both possibilities were mentioned in witness statements at the Loveparade ([15]).

First experimental studies in which people were pushed and unbalanced in a crowd have been conducted only on small groups. They mainly examine the collision dynamics ([32]), contact forces ([33]) and pressure measurements ([34]) in groups of people or the motion of only two participants ([35]). This does not resolve the difficulty of understanding individual three-dimensional motion, the way people regain balance and how this motion propagates in a crowd. Furthermore, [15] concluded that both, falls and macroscopic waves, cause the greatest risk in dense crowds. Therefore, it is essential to connect the macroscopic with the submicroscopic analysis, when studying the motion of pedestrians.

With our research, we aim to develop a methodology to comprehend the dynamics of a human body when losing balance while the movement of the torso and limbs are restricted by surrounding people. Therefore, we conducted a series of experiments to investigate the propagation of a push and the balance recovery in a standing crowd. This experimental campaign was carried out as part of the EU-funded project CrowdDNA ([36]). For a starting point of this research direction, we simplified the crowd to a row of five people and varied specific parameters, such as the intensity of the impulses and the initial inter-person distance in order to study their effect on the impulse propagation ([37]). We collected head trajectories and 3D motion capturing data of each individual, which we then combined to one data-set to get an insight into how the individuals interact with each other by describing the movement of their body in three dimensions. In a first analysis of the macroscopic characteristics, the propagation of pushes in terms of distance and speed were investigated in one dimension (the direction of the push) without considering the individual limb motions of the participants. Now we take the analysis a step further and examine the same experiments in more detail for the 3D reactions of each participant.

To gain a deeper understanding into how impulses propagate through a row of people and how this is influenced by individual behaviour, we have to consider not only reactions to the external impulse, but also the interactions between people. In this context, the term "impulse" refers to the transfer of a force over a period of time causing an external perturbation to the participants. Dividing what happens into

different phases facilitates a detailed analysis in the future, especially to distinguish between various types of physical interactions that occur in each phase. This allows us to better compare differences between single person trials (as conducted by [30]) with the row experiments, to separate between reactions of unintended displacement from the resting position caused by external impulses and the intended balance recovery strategy, as well as to investigate whether an impulse is reduced or intensified along the row. By studying the propagation of motion, insights into how pedestrians behave in response to various forces and conditions can be obtained. This understanding allows pedestrian behaviour to be more accurately described and helps to develop three-dimensional models of pedestrian dynamics also in high density scenarios, in order to hopefully predict and identify potentially dangerous situations in the future.

2 Methods

2.1 Experiments

To investigate motion propagation in crowds, we are analysing the same 97 trials from the pushing experiments as described in [37]. External impulses were delivered by one of the experimenters manually pushing a punching bag, that was suspended horizontally from the ceiling, towards the upper back of the last participant in a line of five people. All participants standing with feet hip-width apart and facing in the direction of the push.

In the experiment, certain factors were manipulated, including the intensity of the impulses. The inter-person distance, measured by individual arm length, was set as arm, elbow or as close as possible (none). At the beginning of a trial, participants held their arms either up, down, or in an arm position of their choice. The first person of the queue either had enough space to move forward freely or was standing in front of a wall with the specified distance.

The experiments were recorded from the side to enable a visual qualitative analysis as well as from above to collect individual head trajectories with the help of PeTrack ([38, 39]). In addition, each participant wore a Xsens ([40]) motion capture (MoCap) suit containing 17 inertial measurement units. This allowed us to record individual 3D motion data, and then integrate them into a common reference system by fusing the 3D data with the head trajectories ([41]). This 3D MoCap data is in the c3d format and contains the positions of 64 points, 22 joints, and the calculated center of mass (CoM) of the human skeleton. Furthermore, we used a pressure sensor from Xsensor ([42]) to measure the strength of the impulses at the punching bag and a sensor from TekScan ([43]) to estimate the impact of the foremost person on the wall.

For the analysis, we went for a two method approach: First the side-view videos were qualitatively described and three temporal phases observed. As a second step, the 3D MoCap data were analysed to define the start and end points of each phase. We will focus our analysis only on specific points of the human skeleton, which can be found in the Supplementary Information.

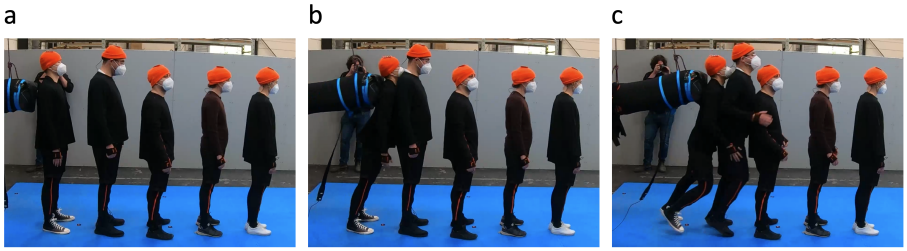

Figure 1: Snapshots of the experiments from the side-view camera. Five people lined up along the y-axis in front of a punching bag. (a) At the beginning of the trial, all participants stand at rest. (b) The last person in the row is pushed forward by the punching bag and touches the next person. (c) The impulse reaches the third person of the row.

2.2 Analytical methods for the analysis of MoCap data

For the analysis of the MoCap data, various analytical methods were applied.

2.2.1 Distance between a point and a line in a 2D plane

To describe the loss of standing balance, the distance between the projected CoM on the ground, represented as a trajectory, and a line passing through the two toe points is used. In three dimensions, the distance between a point and a line can be calculated using the cross product. The projection on a 2D plane is simplified as follows.

Let $\mathbf{a}, \mathbf{b}, \mathbf{c} \in \mathbb{R}^2$ and the line, that passes through the points $\mathbf{a}, \mathbf{b}$, is defined as $\mathbf{ab} = \mathbf{a} + t \cdot \mathbf{n}$ with unit vector $\mathbf{n} = \frac{(\mathbf{b}-\mathbf{a})}{\|(\mathbf{b}-\mathbf{a})\|}$ along the line and $t \in \mathbb{R}$. Then the distance $d(\mathbf{ab}, \mathbf{c})$ between point $\mathbf{c}$ and line $\mathbf{ab}$ is given by:

$$d(\mathbf{ab}, \mathbf{c}) = n_1 \cdot (a_2 - c_2) - n_2 \cdot (a_1 - c_1) \tag{1}$$

2.2.2 Distance between a point and a line segment in a 2D plane

The point - line segment distance is used to estimate the distance between hands and the back of the person in front. A line segment is a special case of a line whereby the segment is limited by two specified endpoints and includes every point on the line that lies between its endpoints. The distance between a point and the segment is defined as the length of the shortest connecting line between that point and a point on the segment.

Let $\mathbf{a}, \mathbf{b}, \mathbf{c} \in \mathbb{R}^2$ as discussed above. The line segment $\overline{\mathbf{ab}}$ with its two endpoints $\mathbf{a}$ and $\mathbf{b}$ is defined similarly to a line $\overline{\mathbf{ab}} = \mathbf{a} + \tilde{t} \cdot \mathbf{n}$. Here, $\mathbf{n}$ is again the unit vector $\mathbf{n} = \frac{(\mathbf{b}-\mathbf{a})}{\|(\mathbf{b}-\mathbf{a})\|}$, but this time $\tilde{t} \in [0, \|(\mathbf{b} - \mathbf{a})\|]$. The distance of point $\mathbf{c}$ to the line

segment can be calculated using equation 1:

$$d(\overline{\mathbf{ab}}, \mathbf{c}) = \begin{cases} d(\mathbf{ab}, \mathbf{c}) & \text{if } 0 \leq (\mathbf{c}-\mathbf{a}) \cdot \mathbf{n} \leq \|(\mathbf{b}-\mathbf{a})\| \\ \min(\|(\mathbf{c}-\mathbf{a})\|, \|(\mathbf{c}-\mathbf{b})\|), & \text{otherwise} \end{cases} \tag{2}$$

2.2.3 Distance between two line segments in a 2D plane

To investigate the distance between the chest of a participant and the back of the next person, the distance between two line segments is used. The distance of two line segments $\overline{\mathbf{ab}}$ and $\overline{\mathbf{cd}}$ is considered as the shortest connecting line between an endpoint of one segment to a point of the other segment. Therefore, equation 2 can be used for each endpoint of the segments to determine $d(\overline{\mathbf{ab}}, \overline{\mathbf{cd}})$:

$$d(\overline{\mathbf{ab}}, \overline{\mathbf{cd}}) = \min[d(\overline{\mathbf{ab}}, \mathbf{c}), d(\overline{\mathbf{ab}}, \mathbf{d}), d(\overline{\mathbf{cd}}, \mathbf{a}), d(\overline{\mathbf{cd}}, \mathbf{b})] \tag{3}$$

2.2.4 Forward speed and acceleration

Velocities $\mathbf{v}_i^p(t)$ and accelerations $\mathbf{a}_i^p(t)$ can be calculated from the position data of individual body parts $\mathbf{r}_i^p(t)$ as follows:

$$\mathbf{v}_i^p(t) = \frac{\mathbf{r}_i^p(t+\Delta t) - \mathbf{r}_i^p(t-\Delta t)}{2 \cdot \Delta t} \tag{4}$$

$$\mathbf{a}_i^p(t) = \frac{\mathbf{v}_i^p(t+\Delta t) - \mathbf{v}_i^p(t-\Delta t)}{2 \cdot \Delta t} \tag{5}$$

Hereby, i indicates the number of the person in the row ($i \in [1, 5]$) and p is a point corresponding to an anatomical landmark of the human body reconstructed from the MoCap data. We used $\Delta t = 0.05\,\text{s}$ to better detect rapid changes in the motion of participants, because the duration of the external impulses were quite short with 0.69 s on average. This time step is also shorter than the typical reaction time of young adults, i.e. from 0.18 s to 0.3 s for reactions to haptic or visual stimuli ([44, 45]). Furthermore, we want to investigate mainly the forward motion of participants which is the same as the pushing direction, because we are particularly interested in the effect of the impulse on the motion. To determine the forward component, we calculate the unit vector $\mathbf{u}_i$ in the xy-plane that is perpendicular to the hip vector at the beginning of the trial ($\mathbf{r}_i^{\text{LHIP}}(0) - \mathbf{r}_i^{\text{RHIP}}(0)$). Then the forward speed $v_i^p(t)$ results from:

$$v_i^p(t) = \mathbf{v}_i^p(t) \cdot \mathbf{u}_i \tag{6}$$

The same applies for the acceleration $\mathbf{a}_i^p(t)$.

2.2.5 Projection of 3D position to a plane

The projection of a 3D vector corresponds to a Matrix-Vector multiplication with the projection matrices

$$P_{xy} = \begin{pmatrix} 1 & 0 & 0 \\ 0 & 1 & 0 \\ 0 & 0 & 0 \end{pmatrix}, P_{yz} = \begin{pmatrix} 0 & 0 & 0 \\ 0 & 1 & 0 \\ 0 & 0 & 1 \end{pmatrix}, P_{xz} = \begin{pmatrix} 1 & 0 & 0 \\ 0 & 0 & 0 \\ 0 & 0 & 1 \end{pmatrix}$$

for the xy, yz and xz plane respectively.

3 Analysis

3.1 Qualitative description of phases of motion

In the experiments, the body of a participant receives an external impulse and the person is displaced from their rest position as a result of the push. Muscles and skeleton can dampen this impulse, direct it into the ground or transfer it to the person in front. To manage the impact and to regain a stable position, participants can choose different strategies, for instance, transferring forces into the ground by taking a step, transferring forces through arms and hands to the person in front with and without a step, or dampening the impulse by moving the hips backwards. These are just a few examples, and due to the complexity of the human body, there are even more possible reactions. Consequently, various physical interactions can occur along the row. In order to study impulse propagation in more detail and detect these strategies, it is important to first separate and divide the motions and interactions into different temporal phases.

For each person within the row, multiple phases of impulse propagation can be identified, although the number of applicable phases may vary. In the following, the most detailed version, which consists of three phases, is explained. These phases are (0) initial position at rest, (i) receiving an impulse, (ii) receiving and passing on an impulse, and (iii) passing on an impulse (Figure 2). From an observational analysis of the side-view videos, we obtained different individual behaviours within the three phases. In this context, touching refers to any contact that may occur between two people, for example, with hands or with the upper body. In the first phase, the blue person in the middle of the row is touched from behind, i.e. they receive the impulse, and are consequently displaced from the rest position which can lead to losing balance. The second phase differs from the first phase by the fact that the person now additionally touches the next person in the row and therefore passes on the impulse. When the person is no longer touched from behind, the third phase begins. They are not receiving the push anymore, but are still passing it on. This phase lasts until the person has regained balance or does not touch the person in front anymore.

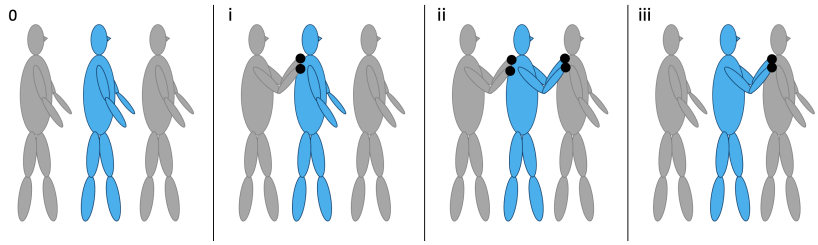

Figure 2: Overview of the phases of impulse propagation for the blue person in the middle: (0) no external impact (i) receiving an impulse, (ii) receiving and passing on an impulse, and (iii) passing on an impulse. The black dots represent a contact.

Table 1: Overview of the investigated times.

Description	Variable	Time	Condition	Derived time
Start of motion	$a_i^{\mathrm{CoM}}(t_1) > 0.3\,\frac{\mathrm{m}}{\mathrm{s}^2}$ $v_i^{\mathrm{CoM}}(t_2) > 0.05\,\frac{\mathrm{m}}{\mathrm{s}}$ $v_i^{\mathrm{C7}}(t_2) > 0.05\,\frac{\mathrm{m}}{\mathrm{s}}$ $v_i^{\mathrm{HIP}}(t_2) > 0.05\,\frac{\mathrm{m}}{\mathrm{s}}$ $a_i^{\mathrm{CoM}}(t_0) > 0.15\,\frac{\mathrm{m}}{\mathrm{s}^2}$	t_1 t_2 t_2 t_2 t_0	$< t_2$ $> t_1$ $> t_1$ $> t_1$ $< t_2$	$t_{\mathrm{start}}[i]$
Unstable position	$\arg\min_t MoS_i(t)$	t_{min}	/	$t_{\mathrm{min}}[i]$
Stabilised position	$MoS_i(t_2) \geq 0.87 \cdot MoS_i(0)$ $\arg\max_{t_3} MoS_i(t_3)$	$\min[t_2]$ t_3	$> t_{\mathrm{min}}[i]$ $> t_{\mathrm{min}}[i]$ $< t_{\mathrm{min}}[i] + 2\,\mathrm{s}$	$t_{\mathrm{stable}}[i]$
End of contact	$d_{\mathrm{min}}[i, i+1](t_4) > 0.12\,\mathrm{m}$	$\min[t_4]$	$> t_{\mathrm{start}}[i+1]$	$t_{\mathrm{touch}}[i]$
End of phases	$\min[t_{\mathrm{stable}}[i], t_{\mathrm{touch}}[i]]$	/	/	$t_{\mathrm{end}}[i]$

3.2 3D data from MoCap

The second analysis aims to identify characteristics in the 3D MoCap data that represent the different phases in order to accurately determine the start and end times of each phase. Following the reconstruction from the MoCap data, only certain points corresponding to anatomical landmarks of the human skeleton will be examined. The points and the abbreviations used as well as the index to find these points in the reconstructed MoCap data are listed in the Supplementary Information. The analysis was performed in python with the *ezc3d* library ([46]). To detect the phases, several variables, namely the forward velocity, the margin of stability and the distance between two participants, have to be investigated in combination. In this section, each variable is first explained separately, and then the phases are defined based on the combination. For temporal segmentation of the phases, we examine several times to derive the actual start and end times of the phases. A list of the studied times is given in Table 1 as an overview and will be explained in more detail in the following section.

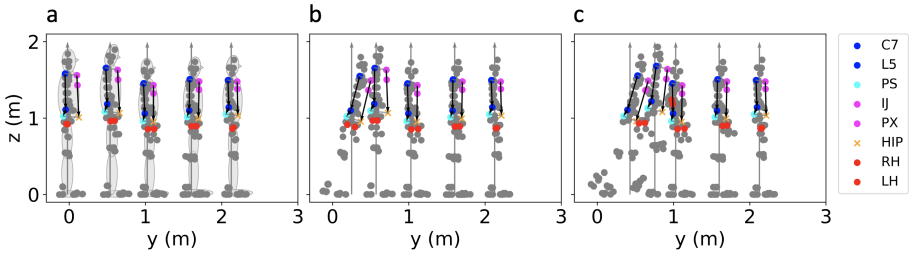

Figure 3: MoCap data for the same experiment and times as in Figure 1. The points of the MoCap data for all five participants are shown in grey. The upper body of each participant is approximated by the two points of the sternum IJ and PX (magenta), the height of the hip HIP (yellow), the sacrum PS (cyan) and two points of the spine C7 and L5 (blue). The hands RH and LH are shown as red points and the segments of the chest, upper back and lower back are represented as black arrows. (a) All participants stand at rest. (b) The impulse is passed on to the second person. (c) The second person in the row receives and passes on the impulse.

3.2.1 Contact

As observed in the videos, whether there is a contact or not is a measure of receiving and passing on the impulse. This can be analysed by looking at the distance between different points of the individual MoCap data. In most cases, people are touched at the back either by hands or the upper body. Contacts that were observed in the videos include hands on upper back, hands on lower back, chest on upper back, belly on lower back and hands on the side of the arms. It is also possible for multiple contacts to occur at the same time, for example the chest on the upper back and hands on the lower back, or the belly on the lower back and hands on the upper back.

In order to find contacts, we estimate the extent of the torso using the 3D MoCap data, which corresponds to the approximate positions of anatomical landmarks on the human skeleton. The upper body of each participant is therefore approximated by the two points of the sternum (IJ, PX), the height of the hip (HIP), the sacrum (PS) and two points of the spine C7 and L5 as plotted in Figure 3. This results in three line segments: the segment of the chest (CH) from the upper sternum through the lower sternum to the projected hip point, the upper back (UB) from C7 to L5 and the lower back (LB) from L5 to the sacrum. For the hands, the points of the right as well as the left palm are considered (RH, LH).

For simplification and because all participants are lined up along the y-axis of the experimental area, the x-component of the MoCap data was not considered. To calculate the shortest distance $d_{\min}[i, i+1]$ between the two participants i and $i+1$ with $i \in [1, 4]$, equations 2 and 3 are used for the segments in the yz-plane as follows:

$$\begin{aligned} d_{\min}[i, i+1] = \min[&d(P_{yz}\mathbf{r}_i^{\mathrm{CH}}, P_{yz}\mathbf{r}_{i+1}^{\mathrm{UB}}), d(P_{yz}\mathbf{r}_i^{\mathrm{CH}}, P_{yz}\mathbf{r}_{i+1}^{\mathrm{LB}}), \\ &d(P_{yz}\mathbf{r}_i^{\mathrm{RH}}, P_{yz}\mathbf{r}_{i+1}^{\mathrm{UB}}), d(P_{yz}\mathbf{r}_i^{\mathrm{RH}}, P_{yz}\mathbf{r}_{i+1}^{\mathrm{LB}}), \\ &d(P_{yz}\mathbf{r}_i^{\mathrm{LH}}, P_{yz}\mathbf{r}_{i+1}^{\mathrm{UB}}), d(P_{yz}\mathbf{r}_i^{\mathrm{LH}}, P_{yz}\mathbf{r}_{i+1}^{\mathrm{LB}})] \end{aligned}$$

For the shortest inter-person distance to be as accurate as possible, the correct positioning in the experimental area is crucial. In addition, to an error of the trajectory data of 1.54 cm and the 3D MoCap data of approximately 3 cm, an error resulting from the fusion of both data-sets has to be considered. The simplified representation of a person by three segments further decreases the accuracy. Therefore, we define a touch if the distance falls below a certain threshold, which has been set to 0.12 m by an initial estimation (see Supplementary Information). An example of the closest distance between two people changing over time is shown in Figure 4. According to our definition, contact occurs when the distance drops below the dotted line, which can be confirmed by the video. It can be seen that the two people approach each other and touch between 1 s and 2.4 s of the trial.

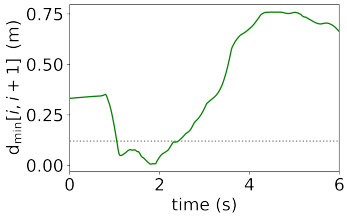

Figure 4: An example of the closest distance $d_{\min}[i, i+1]$ changing over time. As a limit for touching, the threshold value of 0.12 m is represented as dotted line.

Furthermore, individual differences might be relevant, as the MoCap data only gives a reconstruction of the skeleton meaning that the exact body dimension cannot be taken into account when calculating the distance. To find appropriate thresholds, we assume that a person is touched from behind when they start moving forward, and therefore we analyse the closest distance at the time the motion starts (Figure 5). For the definition of the start of motion see Section 3.2.2.

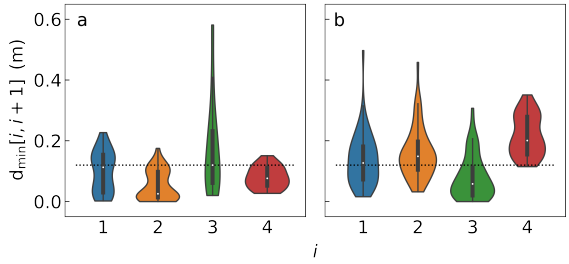

Figure 5: Closest distance between two persons i and $i+1$ at the time the motion starts. (a) Series of experiments without a wall and (b) with wall. Within a series, the order of participants remained the same. The person who receives the push first has number one. The dotted line represents a threshold value of 0.12 m

Figure 5 illustrates that the distances between the same participants vary considerably across trials and there is no significant difference between individuals. Our conclusions are this: The calculated distances are too imprecise for a definition of a phase and touching cannot be reliably detected in the MoCap data. Nevertheless, the distance can be used subsequently to describe whether people are moving towards or away from each other and to find an overall minimal distance.

3.2.2 Start of motion

In order to define the phases, the start time of the motion is considered for further analysis and the overall definition of the phases has to be adjusted. The aim of this section is to find the time at which a person starts moving forward because of the external impulse and thus determine the start time of the first phase. The analysis of the 3D motion of a human body is complex, because the body consists of several limbs that can move individually. Furthermore, participants can react differently when they are pushed. To investigate the motion propagation due to an external impulse more uniformly, the motion of the center of mass (CoM) can be compared. However, the CoM will also move when, for example, only the arms are raised upwards and the person does not receive the push. Participants can in addition move independently, e.g. looking down, turning around or swaying on the spot while waiting. Therefore, it is necessary to develop a method that captures only the motion in response to the external impulse. In order to include all movements that are initiated by the external impulse, but at the same time exclude movements that do not relate to it, multiple criteria have to be fulfilled. We investigate the forward velocities of the three body parts C7, Hip and the CoM and the acceleration of the CoM with equation 6.

We want to find the time t_0 at which the velocity of the participants is still zero. But since only motions should be counted that exceed a threshold value, prospective events will be firstly investigated. We assume that the CoM is considerably accelerated by the impulse, i.e. it is larger than $0.3\,\mathrm{ms}^{-2}$. If shortly afterwards the velocities of all three body parts C7, Hip and the CoM are greater than $0.05\,\mathrm{ms}^{-1}$ simultaneously, it will be counted as motion due to the push. This results in the Boolean variable motion$[i,t]$ that is true if the following condition occurs.

$$\text{motion}[i,t] : a_i^{\text{CoM}}(t_1) > 0.3\,\tfrac{\text{m}}{\text{s}^2} \wedge v_i^{\text{CoM}}(t_2) > 0.05\,\tfrac{\text{m}}{\text{s}} \wedge v_i^{\text{C7}}(t_2) > 0.05\,\tfrac{\text{m}}{\text{s}} \wedge v_i^{\text{HIP}}(t_2) > 0.05\,\tfrac{\text{m}}{\text{s}}, \text{ for } t_2 > t_1$$

The thresholds defining motion$[i,t]$ exclude minor movements that are not initiated by the external impulse. For the exact definition of the start of a phase, it is important to identify the point in time at which the participants are still at rest but will move in the next time step. The time detected by motion$[i,t]$ deviates from the actual start time of motion. Therefore, a backward search is performed to find the previous point in time at which the participant has not yet moved. A participant stands definitely at rest, when the acceleration of the CoM is less than $0.15\,\mathrm{ms}^{-2}$. Using this threshold value, the start time $t_{\text{start}}[i]$ can be found as follows:

$$t_{\text{start}}[i] = t_0, \quad \text{if } a_i^{\text{CoM}}(t_0) > 0.15\,\frac{\text{m}}{\text{s}^2}, \quad \text{for } t_0 < t_2$$

The determined threshold values were found by comparing the output of the analysis with the side-view videos qualitatively to best represent the experiments (see Supplementary Information for more detail). Figure 6 a shows the forward acceleration, the threshold value of $0.3\,\mathrm{ms}^{-2}$ as well as the start time $t_{\mathrm{start}}[i]$. The forward velocities of C7, Hip and the CoM are plotted as an example in Figure 6 b. The threshold value of $0.05\,\mathrm{ms}^{-1}$ is shown as dotted grey line and the detected start time as dotted black line. In this example, the following times were detected: $t_1 = 0.68\,\mathrm{s}$, $t_2 = 0.73\,\mathrm{s}$ and $t_0 = t_{\mathrm{start}}[i] = 0.67\,\mathrm{s}$.

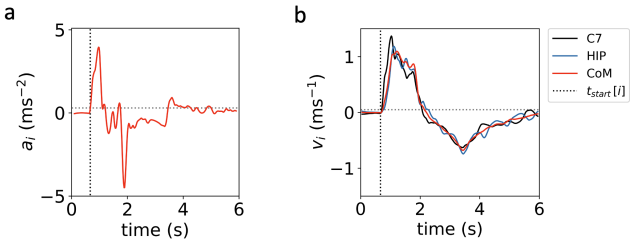

Figure 6: (a) The forward acceleration of the CoM with a threshold value of $0.3\,\mathrm{ms}^{-2}$. (b) Example of the velocity of C7, HIP and CoM with the threshold value of $0.05\,\mathrm{ms}^{-1}$. The start time of the motion $t_{\mathrm{start}}[i]$ is shown as dotted black vertical line.

3.2.3 Perturbation and loss of standing balance

As response to the external impulse, the participants are displaced from their rest position and potentially lose balance. One way to measure standing balance is to consider the position of the projection of the CoM to the xy-plane in relation to the position of the feet. The external points of both feet create the base of support (BoS). In general static conditions, a person is considered in balance when the CoM lies inside the BoS and out of balance when the CoM is located outside of the BoS. However, the CoM of individuals does not remain static following an external perturbation. In such dynamic conditions, the velocity of the CoM should also be considered to study standing balance. Therefore, the margin of stability MoS as proposed by [24], which is the shortest distance of the extrapolated CoM to the boundary of the BoS, is analysed.

The extrapolated centre of mass XCoM takes the velocity into account and can be calculated with the pendulum equation $\omega_0 = \sqrt{g/l}$. Here, g is the gravitational acceleration and l the leg length of the participant.

$$\mathbf{r}_i^{\mathrm{XCoM}}(t) = \mathbf{r}_i^{\mathrm{CoM}}(t) + \frac{\mathbf{v}_i^{\mathrm{CoM}}(t)}{\omega_0}$$

For the calculation of the $MoS_i(t)$, we only consider the forward boundary of the BoS, i.e. the line TOE that passes through the two toe points (LT and RT), because we mainly investigate the effect of the impulse to the front. With equation 1, $MoS_i(t)$ is calculated as follows:

$$MoS_i(t) = d(P_{xy}\mathbf{r}_i^{\mathrm{TOE}}(t), P_{xy}\mathbf{r}_i^{\mathrm{XCoM}}(t))$$

This definition gives a negative distance when the XCoM lies ahead of the TOE line of the BoS and a positive distance when lying behind it. An example of the $MoS_i(t)$ during one trial is shown in Figure 7.

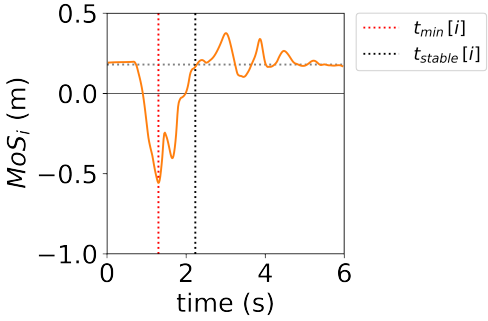

Figure 7: Example of the MoS, which is the distance of the XCoM to the TOE line. The MoS is positive when the XCoM lies behind the TOE line of the BoS and negative when lying ahead of the TOE line. The most unstable position at $t_{\mathrm{min}}[i]$ is shown as dotted red vertical line and the time at which the person is in balance again $t_{\mathrm{stable}}[i]$ is shown as dotted black vertical line.

Our goal is to distinguish between receiving and passing on the impulse. However, that is a very challenging task, because we have to differentiate between passive and active actions. We assume that a participant is unintentionally displaced from their rest position and then takes action to regain a stable position. Therefore, we can define the most critical state of standing balance corresponding to the smallest MoS. This gives the time $t_{\mathrm{min}}[i]$ until the person reaches the most unstable position. After that, the person uses strategies to regain balance and thus may pass on the impulse. To obtain an end time for potentially passing on the impulse, the actions of the participants need to be divided, in terms of what is a necessary reaction to the impulse and what is not. Since the MoS also takes into account the velocity of the CoM as well as the positioning of the feet, we propose the time at which the MoS reaches a threshold value as the end time. For our experiments, we define the threshold value as being 87% of the initial MoS_i value. In the cases when this value is not reached, the time at which MoS_i value is at a maximum within 2 s after $t_{\mathrm{min}}[i]$ is considered as end time. However, these threshold values are just a starting point of the analysis that must be tested critically in further experiments (see Supplementary Information).

This results in the following definitions for both times.

$$t_{\mathrm{min}}[i] = \arg\min_t MoS_i(t)$$

$$t_{\text{stable}}[i] = \begin{cases} \min[t_2], & \text{if } MoS_i(t_2) \geq 0.87 \cdot MoS_i(0), \text{ for } t_2 > t_{\min}[i] \\ \arg\max_{t_3} MoS_i(t_3), & \text{for } t_{\min}[i] < t_3 < t_{\min}[i] + 2\,\text{s} \end{cases}$$

We estimate that at t_{stable} the person has regained a stable position and no further motion is required to counteract the impulse. Therefore, this is set as the time until the impulse could potentially be passed on, although this does not ensure whether this is actually the case. Additionally including the closest distance $d_{\min}[i, i+1]$, as shown in Figure 4, can give information on how close people are to each other and provide an indication of whether or not people are touching and thus passing on the impulse. In order to find the time when people are out of contact again, we use the threshold as proposed in Section 3.2.1. There is no longer a contact at time t_{touch}, when $d_{\min} > 0.12\,\text{m}$.

$$t_{\text{touch}}[i] = \min[t_4], \quad \text{if } d_{\min}[i, i+1](t_4) > 0.12\,\text{m} \quad \text{for } t_4 > t_{\text{start}}[i+1]$$

As a result, the end time t_{end} of the last phase is given as the smallest time of t_{stable} and t_{touch}.

$$t_{\text{end}}[i] = \min[t_{\text{stable}}[i], t_{\text{touch}}[i]]$$

4 Results and Discussion

4.1 Detection of the phases

Precisely detecting the defined phases of impulse propagation in the 3D MoCap data is a challenging task. For this purpose, we used the following two methods, observation of the side-view videos as well as investigation of the 3D MoCap data. We distinguished three phases, (0) initial position at rest, (i) receiving an impulse, (ii) receiving and passing on an impulse, and (iii) passing on an impulse. In the videos, it is easier to see when people are touching each other rather than when each individual starts moving forward. For the 3D MoCap data, the opposite is the case: the start of motion is more reliably detected than the time people touch each other. However, touching does not necessarily involve passing on the impulse. Participants can grab the person in front instead of pushing forward, as sometimes seen in the videos. Furthermore, people can move in a variety of ways and of their own choice and not every behaviour is a response to the impulse. Therefore, it is important to evaluate which motions are counted for defining the phases and investigate various parameters simultaneously.

We come to the conclusion that mainly three variables are needed to identify the phases. These are the velocity in the same direction as the external impulse, i.e. the forward direction, the margin of stability in the forward direction and the estimated distance between two participants. Figure 8 presents a summary of the variables

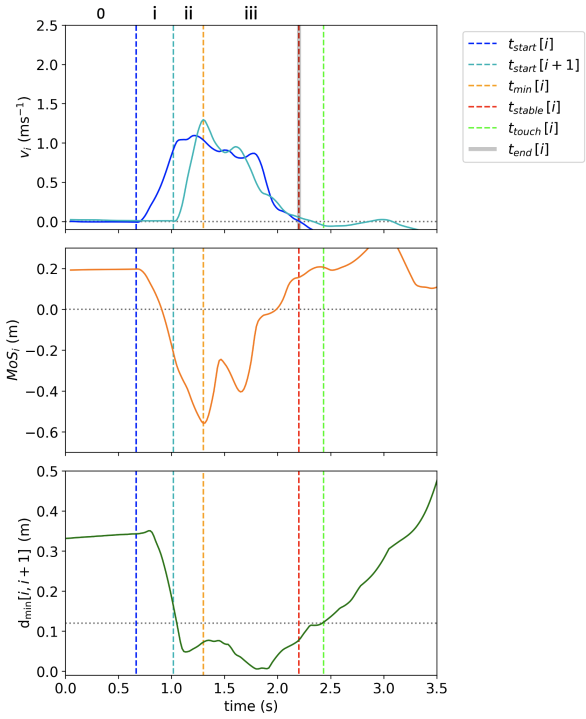

Figure 8: Three variables are needed to identify the phases of motion for one person with the 3D MoCap data. The start time of the first phase is defined by the time the forward motion starts $t_{\text{start}}[i]$ and ends when the next person in the row starts moving forward $t_{\text{start}}[i+1]$. The second phase ends with the minimal MoS at time $t_{\text{min}}[i]$. The end time of the third phase $t_{\text{end}}[i]$ is set by using the MoS as well as the closest distance between two participants.

Table 2: Overview of the phases of motion for each person in the middle of the row.

Phase	Impulse	Behaviour	Start	End
0	None	In balance	–	$t_{\text{start}}[i]$
i	Receiving	Moving forward, Displacement from rest position	$t_{\text{start}}[i]$	$t_{\text{start}}[i+1]$
ii	Receiving and passing on	Moving forward, Person in front moves, Displacement from rest position	$t_{\text{start}}[i+1]$	$t_{\text{min}}[i]$
iii	Passing on	Person in front moves, Regaining rest position	$t_{\text{min}}[i]$	$t_{\text{end}}[i]$
iv	None	In balance	$t_{\text{end}}[i]$	–

as a function of time, and shows the start and end times of each phase for a trial without wall, in which the initial inter-person distance is set to elbow and the initial arm posture is free. Based on this example, the following times are obtained for the first person pushed. Person $i = 1$ receives the impulse and thus enters the first phase when they start moving forward ($t_{\text{start}}[1] = 0.67\,\text{s}$) . The second phase begins when the next person $i = 2$ in the row moves ($t_{\text{start}}[2] = 1.02\,\text{s}$). The start of the third phase $t_{\text{min}}[1] = 1.30\,\text{s}$ corresponds to the most unstable position, and it ends when the person reaches either a certain stability in the MoS ($t_{\text{stable}}[1] = 2.20\,\text{s}$) or a certain distance to the person in front ($t_{\text{touch}}[1] = 2.43\,\text{s}$). The phases continue smoothly into one another. A general overview of these start and end times with the corresponding phases are listed in Table 2.

Determining a time at which a person receives the impulse is relatively clear and the detection works well. The beginning of our experiments represents a stationary crowd for example in a waiting scenario. This means that participants do not move that much and there is a correspondingly significant motion, when they receive the impulse. In order to capture only the motion in response to the external impulse, small as well as slow motions are not considered. This ensures that independent movements, such as swaying on the spot, are excluded, but it also implies that slight effects on the body due to the impact are not taken into account. Since the three body parts CoM, Hip and C7 have to move forward simultaneously to be included, movements like raising hands or looking down are neglected, and the forward component of the velocity causes rotations or moving backwards to remain undetected. When comparing the identified start of motion with the videos, only one person is falsely detected (false positive) in one trial because they show a very similar motion pattern to a pushed person. Furthermore, there are four cases of false negative detections. These occur mainly when the persons are already touching each other while waiting for the impulse.

On the contrary, it is difficult to identify when a person is no longer receiving or passing on an impulse. One can argue that touching as observed in the videos is

an indicator, but on the other hand, this is no guarantee that forces are actually exchanged. For example, one person could be holding the person in front of them instead of passing on the external impulse by pushing that person forward. Therefore, we choose to use a measure of stability for the definition. We are confident that up to the lowest MoS ($t_{\min}[i]$), which corresponds to a most unstable position, the impulse is received. However, this does not necessarily mean that the person cannot continue to be affected by the impulse past this moment. Since $t_{\min}[i]$ sets the end of receiving in our definition, we may underestimate phase 2 and overestimate phase 3. The experiments are designed in such a way that the subjects move forward due to the impulse, regain their balance and usually return to their starting position immediately afterwards. This returning is not caused by the impulse and should not be included as part of the phases. Detecting the time $t_{\text{stable}}[i]$ when a person regained stability works quite well. In our definition, we assume that no further action is necessary at this time to achieve a stable standing position, other than maybe placing the heels of the foot fully on the ground. This outcome also agrees with the viewing of the videos, and only for a few single cases the time is specified a little late.

4.2 Occurrence and duration of phases

The three phases defined in Table 2 are not always applicable to all persons. By default, the last person to receive the impulse only goes through the first phase. To investigate this, we examined the data for all four individuals within the row. The data for the furthermost person is ignored because, by definition, they can only undergo the first phase if at all and cannot pass on the impulse. This means that a total of 420 pushed persons can be examined. In 28 cases, the person is not affected by the push when the initial inter-person distance is large (either arm or elbow) and therefore does not go through any phase. A further 28 people were the last person to be pushed and hence only experienced phase 1. Of the remaining 364 pushed persons, 306 persons completed all three phases.

It could happen that there are sometimes just two phases. If people touch each other directly at the beginning, which is particularly the case with arms up, but can also occur at no distance, people are able to transfer the impulse faster and thus shorten the time of the first phase. For 7 persons, only phases 2 and 3 are detected and in extreme cases, only phase 2 is observed (9 persons). This means the difference of the start time of both participants $t_{\text{start}}[i]$ and $t_{\text{start}}[i+1]$ is smaller than the time resolution of the sensors. Consequently, there are only phase 2 (receiving and passing on) and phase 3 (passing on the impulse).

By contrast, standing further apart at the beginning increases the probability that a person is already in the process of regaining a stable position by the time they reach the next person. At large inter-person distances (elbow or arm), phase 2 is omitted (32 times) and therefore, only phases 1 and 3 are detected, which results in the phases (i) receiving and (iii) passing on the impulse. In this scenario, there could be a gap between phases when $t_{\min}[i] < t_{\text{start}}[i+1]$. For a total of 10 persons, only phases 1 and 2 were identified, because the closest distance $d_{\min}[i, i+1]$ never

drops below the threshold of 0.12 m.

In the next step of the analysis, the duration of each phase is investigated in relation to the initial distances and the arm position up or not up, whereby we distinguish between experiments with and without a wall. Figure 9 shows the duration of the phases Δt for trials where the initial arm posture were either down or free and Figure 10 for trials with arms up.

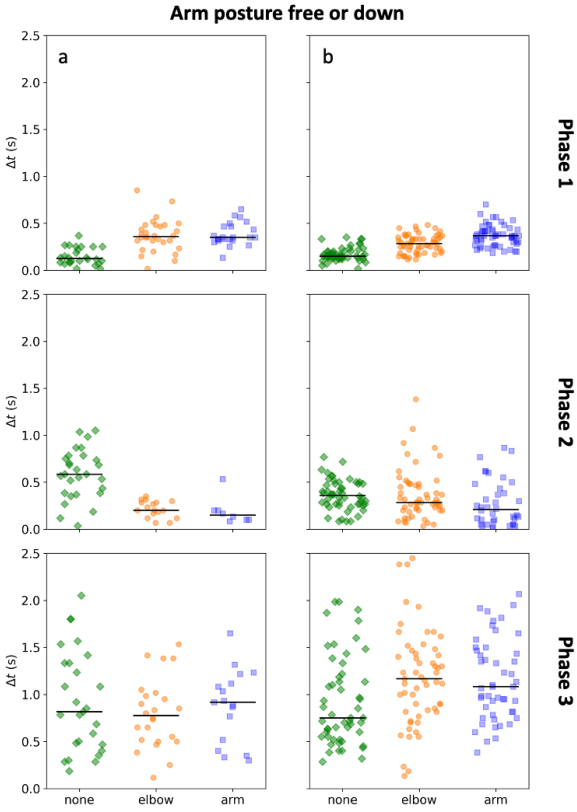

Figure 9: Duration Δt of phases 1, 2 and 3 according to different initial inter-person distances none, elbow and arm. The arm posture of participants were either free or down for trials (a) without a wall and (b) with wall. The median is shown as black horizontal line.

We find that the duration of phases 1 and 2 correlate with the initial inter-person distance which corresponds to our assumption. The closer the people stand to each other, the shorter is the first phase and the longer the second phase, as people interact with each other more quickly and therefore pass on the impulse sooner. In addition, the options for motion strategies in phase 1 increase with the initial inter-person distance. This is shown by the fact that the variance in phase duration is low for short distances and greater for longer distances. No clear statement can

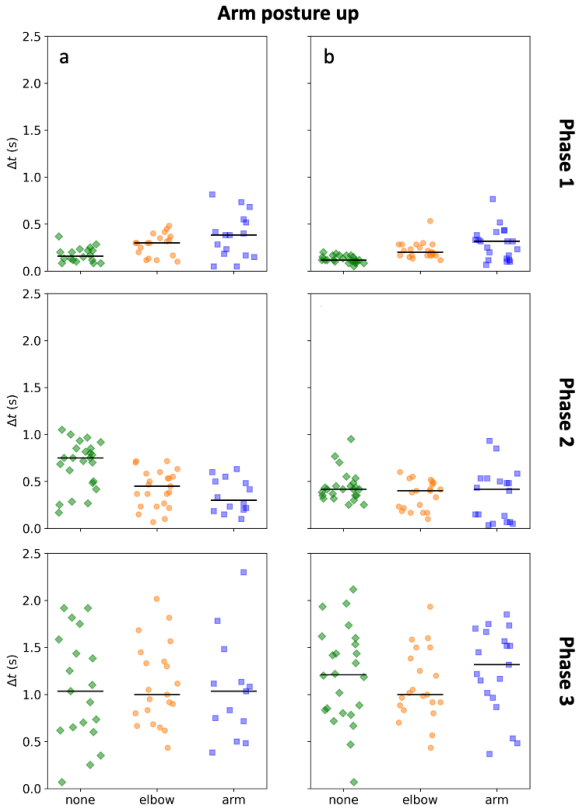

Figure 10: Duration Δt of phases 1, 2 and 3 according to different initial inter-person distances none, elbow and arm. The arm posture of participants were up for trials (a) without a wall and (b) with wall. The median is shown as black horizontal line.

be made about the third phase, because the duration is widely distributed across all intervals. In Phase 3, strategies to regain balance vary, and this variation is reflected in the variance of the phase duration, regardless of the initial inter-person distance. Another reason could be the fact that the end of the third phase is difficult to determine (both in the qualitative analysis of the videos and on the basis of the data) and thus hard to detect.

All trends in the duration of the phases are given for both arm posture conditions (up or not up) and there is no significant difference between experiments with and without wall. Furthermore, we did not find a correlation between the duration of the phases and the intensity of the impulses. Figures of this analysis can be found in the Supplementary Information.

4.3 Applicability

First of all, the aim of our research is to investigate how external impulses propagate in a crowd. It is important to note that people behave differently from billiard balls (elastic impact) and that the displacement of an individual can occur in various ways. This means that different characteristics of impulse transfer and strategies to regain balance can occur in a crowd. To investigate this in more detail and identify different characteristics, we divide the impulse transfer between people into different temporal phases. We hope that these findings will be helpful in developing a physical model for impulse propagation in a crowd.

Furthermore, it is of great importance to understand and characterise risks in a crowd. Previously, there have been different concepts when talking about these risks. For example, a single person could fall down ([15]), several people could move in one direction within the crowd leading to density waves ([13]), or the interactions between multiple people are described with a domino model ([32]). The temporal segmentation of motion propagation into three phases can contribute to an understanding how these different types of movement can emerge and help to identify the conditions under which they occur.

Phase 1 corresponds primarily to the fact that only one person is severely affected by the impulse. Particularly in cases where phase 2 is skipped, i.e. when a person moves from phase 1 to phase 3, there could be a risk of a single person falling down. In phase 2, a person is not only receiving the impulse but also passes it on. This could fit well with a domino model, as at least three people are simultaneously affected by the impulse. To this end, the duration of the second phase could be investigated in more detail. If the times of the second phase of several people overlap, it is possible to determine how many people are in the critical phase of losing balance at the same time and to examine wave movements of the crowd. The third phase indicates the time in which people regain their balance. Identifying this time could enable different movement strategies to be determined and automatically detected. In addition, applying this method to rows with more people could identify the conditions under which an impulse may be intensified or dampened, allowing a more accurate description of impulse propagation in crowds.

4.4 Limitations

It is interesting to note that there are differences in the closest inter-person distances between trials with and without a wall, as shown in Figure 5. For the trials without wall, all medians are below the determined 0.12 m threshold, while for the trials with a wall, three out of the four medians exceed the threshold. The reason for this could be that the wall may cause people to change their strategies to transfer more of the impulse to the ground instead of passing it on to the next person. As a result, participants keep more distance to their neighbours in this situation. The contact detection method proposed in this study has a few weaknesses and could be improved. Especially to investigate whether hands enclose arms or touch the shoulders at the back, the xy-plane must be considered in addition to the yz-plane. This is also necessary for experiments that are extended to two dimensions. The approximation by segments in the xy-plane, for example for the shoulders, can be useful as well. It would also be interesting to compare different methods that represent the participants differently. These would be for example point cloud, line segments or the convex hull.

Another limitation of this study is the accuracy of the data. If the 3D MoCap data are not well enough aligned with each other due to combining the data with the head trajectories, it results in a significant error especially when calculating the distance between two people. To minimise this error for the forward motion, we have calculated the forward direction for each person individually using the hip vector and did not use the y-direction as standard for all. Even within one person, the 3D MoCap data can contain some errors, for example if sensors are displaced during trials or if the body measurements, on which the articulation of the skeleton are based, are taken imprecisely. Furthermore, this study [47] comes to the conclusion that the BoS calculated with Xsens showed a high error.

5 Conclusion and Outlook

In this study, the 3D motion of the human body as response to an external impulse is separated into temporal phases. These phases can be detected based on the MoCap data by investigating the forward velocity, the margin of stability and the estimated distance between two participants. A maximum of three phases can occur, which are characterised by receiving, receiving and passing on or passing on the impulse.

Each phase should be further investigated in terms of their specific characteristics, physical interactions that occur, and the differences between the phases. More research is also needed on the relation of the initial inter-person distance as well as the intensity of the impulse to the phases of motion and the factors that influence them. Possible factors include individual characteristics (e.g. height or weight of the participants), body tension, or also preparedness and reaction time. The age

of the participants should also be taken into account, as age may induce a number of changes in these characteristics. As mentioned in [23] people choose different strategies, i.e. ankle, hip or steps, to regain a stable position. As a result, the impulse might be transmitted differently or perhaps even be intercepted, leading to a general intensification or mitigation of the impulse along the row. We could observe different movement strategies in the videos and it would be helpful to classify these strategies into individual movement types. Thereby, the analysis could focus on pendulum movements of the upper body, the exact hip motions, the placement of the feet, and the use of the hands.

The experiments presented in this study could be enhanced to capture physical contacts by using additional pressure sensors on the hands and backs of the participants. This would also facilitate the estimation of normal forces acting between individuals and hence improve the analysis of whether an impulse is passed on. Furthermore, these experiments were conducted on a small scale corresponding to only a few real-life scenarios, such as queues. Therefore, the analysis of the phases should be extended to larger experiments in which people are standing in multiple rows or groups.

Data Availability

The raw data from the experiments are freely accessible at the Pedestrian Dynamics Data Archive of the Research Centre Jülich, doi: 10.34735/ped.2022.2.. The data include videos in mp4 format, head trajectories as txt files, combined MoCap data as c3d files, pressure data as txt files and information about participants.

Acknowledgements

We would like to thank Jernej Čamernik, Marc Ernst, Helena Lügering and Anna Sieben who supported us in the conception, planning and realisation of the experiments. Furthermore, we are grateful to Alica Kandler, Maik Boltes, Ann Katrin Boomers and Tobias Schrödter for their help in setting up the experiments and curating the data.

Funding

This study was funded by the European Unions Horizon 2020 research and innovation program within the project CrowdDNA [grant number 899739]. SF was additionally supported by a scholarship from the German Academic Exchange Service (DAAD).

Ethical Review

The experiments were approved by the ethics board of the University of Wuppertal in April 2021 (Reference: MS/BBL 210409 Seyfried).

References

[1] Claudio Feliciani, Alessandro Corbetta, Milad Haghani, and Katsuhiro Nishinari. "Trends in crowd accidents based on an analysis of press reports". en. In: *Safety Science* 164 (Aug. 2023), p. 106174. ISSN: 09257535. DOI: 10.1016/j.ssci.2023.106174.

[2] Maik Boltes, Jun Zhang, Antoine Tordeux, Andreas Schadschneider, and Armin Seyfried. "Empirical Results of Pedestrian and Evacuation Dynamics". en. In: *Encyclopedia of Complexity and Systems Science*. Ed. by Robert A. Meyers. Berlin, Heidelberg: Springer Berlin Heidelberg, 2018, pp. 1–29. ISBN: 978-3-642-27737-5. DOI: 10.1007/978-3-642-27737-5_706-1.

[3] Yan Feng, Dorine Duives, Winnie Daamen, and Serge Hoogendoorn. "Data collection methods for studying pedestrian behaviour: A systematic review". en. In: *Building and Environment* 187 (Jan. 2021), p. 107329. ISSN: 03601323. DOI: 10.1016/j.buildenv.2020.107329.

[4] Juliane Adrian, Armin Seyfried, and Anna Sieben. "Crowds in front of bottlenecks at entrances from the perspective of physics and social psychology". en. In: *Journal of The Royal Society Interface* 17.165 (Apr. 2020), p. 20190871. ISSN: 1742-5689, 1742-5662. DOI: 10.1098/rsif.2019.0871.

[5] Mohcine Chraibi, Antoine Tordeux, Andreas Schadschneider, and Armin Seyfried. "Modelling of Pedestrian and Evacuation Dynamics". en. In: *Encyclopedia of Complexity and Systems Science*. Ed. by Robert A. Meyers. Berlin, Heidelberg: Springer Berlin Heidelberg, 2018, pp. 1–22. ISBN: 978-3-642-27737-5. DOI: 10.1007/978-3-642-27737-5_705-1.

[6] Raphael Korbmacher and Antoine Tordeux. "Review of Pedestrian Trajectory Prediction Methods: Comparing Deep Learning and Knowledge-Based Approaches". In: *IEEE Transactions on Intelligent Transportation Systems* 23.12 (Dec. 2022), pp. 24126–24144. ISSN: 1524-9050, 1558-0016. DOI: 10.1109/TITS.2022.3205676.

[7] Arianna Bottinelli and Jesse L. Silverberg. *Can high-density human collective motion be forecasted by spatiotemporal fluctuations?* arXiv:1809.07875 [physics]. Sept. 2018. URL: http://arxiv.org/abs/1809.07875 (visited on 01/02/2023).

[8] Ramana Sundararaman, Cedric De Almeida Braga, Eric Marchand, and Julien Pettre. "Tracking Pedestrian Heads in Dense Crowd". In: *2021 IEEE/CVF Conference on Computer Vision and Pattern Recognition (CVPR)*. Nashville, TN, USA: IEEE, June 2021, pp. 3864–3874. ISBN: 978-1-66544-509-2. DOI: 10.1109/CVPR46437.2021.00386.

[9] Dirk Helbing, Anders Johansson, and Habib Zein Al-Abideen. "Dynamics of crowd disasters: An empirical study". en. In: *Physical Review E* 75.4 (Apr. 2007), p. 046109. ISSN: 1539-3755, 1550-2376. DOI: 10.1103/PhysRevE.75.046109.

[10] Wang Jiayue, Weng Wenguo, and Zhang Xiaole. "Comparison of Turbulent Pedestrian Behaviors Between Mina and Love Parade". en. In: *Procedia Engineering* 84 (2014), pp. 708–714. ISSN: 18777058. DOI: 10.1016/j.proeng.2014.10.477.

[11] Helen C. Muir, David M. Bottomley, and Claire Marrison. "Effects of Motivation and Cabin Configuration on Emergency Aircraft Evacuation Behavior and Rates of Egress". en. In: *The International Journal of Aviation Psychology* 6.1 (Jan. 1996), pp. 57–77. ISSN: 1050-8414, 1532-7108. DOI: 10.1207/s15327108ijap0601_4.

[12] A Garcimartín, D R Parisi, J M Pastor, C Martín-Gómez, and I Zuriguel. "Flow of pedestrians through narrow doors with different competitiveness". In: *Journal of Statistical Mechanics: Theory and Experiment* 2016.4 (Apr. 2016), p. 043402. ISSN: 1742-5468. DOI: 10.1088/1742-5468/2016/04/043402.

[13] Arianna Bottinelli, David T. J. Sumpter, and Jesse L. Silverberg. "Emergent Structural Mechanisms for High-Density Collective Motion Inspired by Human Crowds". en. In: *Physical Review Letters* 117.22 (Nov. 2016), p. 228301. ISSN: 0031-9007, 1079-7114. DOI: 10.1103/PhysRevLett.117.228301.

[14] Claudio Feliciani, Iker Zuriguel, Angel Garcimartín, Diego Maza, and Katsuhiro Nishinari. "Systematic experimental investigation of the obstacle effect during non-competitive and extremely competitive evacuations". en. In: *Scientific Reports* 10.1 (Sept. 2020), p. 15947. ISSN: 2045-2322. DOI: 10.1038/s41598-020-72733-w.

[15] Anna Sieben and Armin Seyfried. "Inside a life-threatening crowd: Analysis of the Love Parade disaster from the perspective of eyewitnesses". en. In: *Safety Science* 166 (Oct. 2023), p. 106229. ISSN: 09257535. DOI: 10.1016/j.ssci.2023.106229.

[16] Barbara Krausz and Christian Bauckhage. "Loveparade 2010: Automatic video analysis of a crowd disaster". en. In: *Computer Vision and Image Understanding* 116.3 (Mar. 2012), pp. 307–319. ISSN: 10773142. DOI: 10.1016/j.cviu.2011.08.006.

[17] Angel Garcimartìn, Diego Maza, José Martìn. Pastor, Daniel R. Parisi, César Martìn-Gómez, and Iker Zuriguel. "Redefining the role of obstacles in pedestrian evacuation". In: *New Journal of Physics* 20.12 (Dec. 2018), p. 123025. ISSN: 1367-2630. DOI: 10.1088/1367-2630/aaf4ca.

[18] Sujeong Kim, Stephen J. Guy, Karl Hillesland, Basim Zafar, Adnan Abdul-Aziz Gutub, and Dinesh Manocha. "Velocity-based modeling of physical interactions in dense crowds". en. In: *The Visual Computer* 31.5 (May 2015), pp. 541–555. ISSN: 0178-2789, 1432-2315. DOI: 10.1007/s00371-014-0946-1.

[19] Wouter Van Toll, Thomas Chatagnon, Cédric Braga, Barbara Solenthaler, and Julien Pettré. "SPH crowds: Agent-based crowd simulation up to extreme densities using fluid dynamics". en. In: *Computers & Graphics* 98 (Aug. 2021), pp. 306–321. ISSN: 00978493. DOI: 10.1016/j.cag.2021.06.005.

[20] Dirk Helbing and Pratik Mukerji. "Crowd disasters as systemic failures: analysis of the Love Parade disaster". en. In: *EPJ Data Science* 1.1 (Dec. 2012), p. 7. ISSN: 2193-1127. DOI: 10.1140/epjds7.

[21] Da Winter. "Human balance and posture control during standing and walking". en. In: *Gait & Posture* 3.4 (Dec. 1995), pp. 193–214. ISSN: 09666362. DOI: 10.1016/0966-6362(96)82849-9.

[22] Brian E. Maki and William E. McIlroy. "Control of rapid limb movements for balance recovery: age-related changes and implications for fall prevention". en. In: *Age and Ageing* 35.suppl_2 (Sept. 2006), pp. ii12–ii18. ISSN: 1468-2834, 0002-0729. DOI: 10.1093/ageing/afl078.

[23] Dario Tokur, Martin Grimmer, and André Seyfarth. "Review of balance recovery in response to external perturbations during daily activities". en. In: *Human Movement Science* 69 (Feb. 2020), p. 102546. ISSN: 01679457. DOI: 10.1016/j.humov.2019.102546.

[24] A.L. Hof, M.G.J. Gazendam, and W.E. Sinke. "The condition for dynamic stability". en. In: *Journal of Biomechanics* 38.1 (Jan. 2005), pp. 1–8. ISSN: 00219290. DOI: 10.1016/j.jbiomech.2004.03.025.

[25] At L. Hof. "The 'extrapolated center of mass' concept suggests a simple control of balance in walking". en. In: *Human Movement Science* 27.1 (Feb. 2008), pp. 112–125. ISSN: 01679457. DOI: 10.1016/j.humov.2007.08.003.

[26] Noah J. Rosenblatt and Mark D. Grabiner. "Measures of frontal plane stability during treadmill and overground walking". en. In: *Gait & Posture* 31.3 (Mar. 2010), pp. 380–384. ISSN: 09666362. DOI: 10.1016/j.gaitpost.2010.01.002.

[27] Laura Hak, Han Houdijk, Peter J. Beek, and Jaap H. Van Dieën. "Steps to Take to Enhance Gait Stability: The Effect of Stride Frequency, Stride Length, and Walking Speed on Local Dynamic Stability and Margins of Stability". en. In: *PLoS ONE* 8.12 (Dec. 2013). Ed. by Amir A. Zadpoor, e82842. ISSN: 1932-6203. DOI: 10.1371/journal.pone.0082842.

[28] Brian W. Schulz, James A. Ashton-Miller, and Neil B. Alexander. "Can initial and additional compensatory steps be predicted in young, older, and balance-impaired older females in response to anterior and posterior waist pulls while standing?" en. In: *Journal of Biomechanics* 39.8 (2006), pp. 1444–1453. ISSN: 00219290. DOI: 10.1016/j.jbiomech.2005.04.004.

[29] Amber R. Emmens, Edwin H. F. Van Asseldonk, Vera Prinsen, and Herman Van Der Kooij. "Predicting reactive stepping in response to perturbations by using a classification approach". en. In: *Journal of NeuroEngineering and Rehabilitation* 17.1 (Dec. 2020), p. 84. ISSN: 1743-0003. DOI: 10.1186/s12984-020-00709-y.

[30] Thomas Chatagnon, Anne-Hélène Olivier, Ludovic Hoyet, Julien Pettré, and Charles Pontonnier. "Stepping strategies of young adults undergoing sudden external perturbation from different directions". en. In: *Journal of Biomechanics* 157 (Aug. 2023), p. 111703. ISSN: 00219290. DOI: 10.1016/j.jbiomech.2023.111703.

[31] Brian E Maki and William E McIlroy. "The Role of Limb Movements in Maintaining Upright Stance: The "Change-in-Support" Strategy". In: *Physical Therapy* 77.5 (May 1997), pp. 488–507. ISSN: 0031-9023. DOI: 10.1093/ptj/77.5.488.

[32] Chongyang Wang, Shunjiang Ni, and Wenguo Weng. "Modeling human domino process based on interactions among individuals for understanding crowd disasters". en. In: *Physica A: Statistical Mechanics and its Applications* 531 (Oct. 2019), p. 121781. ISSN: 0378-4371. DOI: 10.1016/j.physa.2019.121781.

[33] Xudong Li, Weiguo Song, Xuan Xu, Jun Zhang, Long Xia, and Congling Shi. "Experimental study on pedestrian contact force under different degrees of crowding". en. In: *Safety Science* 127 (July 2020), p. 104713. ISSN: 09257535. DOI: 10.1016/j.ssci.2020.104713.

[34] Chongyang Wang and Wenguo Weng. "Study on the collision dynamics and the transmission pattern between pedestrians along the queue". en. In: *Journal of Statistical Mechanics: Theory and Experiment* 2018.7 (July 2018), p. 073406. ISSN: 1742-5468. DOI: 10.1088/1742-5468/aace27.

[35] Xudong Li, Xuan Xu, Jun Zhang, Kechun Jiang, Weisong Liu, Ruolong Yi, and Weiguo Song. "Experimental study on the movement characteristics of pedestrians under sudden contact forces". en. In: *Journal of Statistical Mechanics: Theory and Experiment* 2021.6 (June 2021). Publisher: IOP Publishing, p. 063406. ISSN: 1742-5468. DOI: 10.1088/1742-5468/ac02c7.

[36] CrowdDNA Project. *Website CrowdDNA Project*. https://crowddna.eu/. July 3, 2022. URL: https://crowddna.eu/ (visited on 07/03/2024).

[37] Sina Feldmann and Juliane Adrian. "Forward propagation of a push through a row of people". en. In: *Safety Science* 164 (Aug. 2023), p. 106173. ISSN: 09257535. DOI: 10.1016/j.ssci.2023.106173.

[38] Maik Boltes and Armin Seyfried. "Collecting pedestrian trajectories". In: *Neurocomputing* 100 (2013). Special issue: Behaviours in video, pp. 127–133. ISSN: 0925-2312. DOI: https://doi.org/10.1016/j.neucom.2012.01.036.

[39] Maik Boltes, Ann Katrin Boomers, Juliane Adrian, Ricardo Martin Brualla, Arne Graf, Paul Häger, Daniel Hillebrand, Deniz Kilic, Paul Lieberenz, Daniel Salden, and Tobias Schrödter. *PeTrack*. Version v0.9. July 2021. DOI: 10.5281/zenodo.5126562.

[40] Martin Schepers, Matteo Giuberti, and Giovanni Bellusci. "Xsens MVN: Consistent Tracking of Human Motion Using Inertial Sensing". en. In: (2018). DOI: 10.13140/RG.2.2.22099.07205.

[41] Maik Boltes, Juliane Adrian, and Anna-Katharina Raytarowski. "A Hybrid Tracking System of Full-Body Motion Inside Crowds". en. In: *Sensors* 21.6 (Mar. 2021), p. 2108. ISSN: 1424-8220. DOI: 10.3390/s21062108.

[42] Xsensor LX210:50.50.05. *Datasheet: Xsensor SENSORS LX210:50.50.05*. 2019. URL: https://www.xsensor.de/wp-content/uploads/2015/11/LX210_50_50_05-2500-Sensoren-508mm-Aufl%C3%B6sung-Gr%C3%B6sse-25x25cm-Messbereich-014-11Ncm2-Anwendung-Sitze_Rollst%C3%BChle.pdf (visited on 10/13/2022).

[43] Tekscan PMS5400N. *Datasheet: Tekscan Pressure Mapping Sensor 5400N*. 2019. URL: https://www.tekscan.com/sites/default/files/resources/IDL-Pressure-Mapping-Sensor-5400N-Datasheet_0.pdf (visited on 10/13/2022).

[44] Adrian Ramos Peon and Domenico Prattichizzo. "Reaction times to constraint violation in haptics: comparing vibration, visual and audio stimuli". In: *2013 World Haptics Conference (WHC)*. 2013, pp. 657–661. DOI: 10.1109/WHC.2013.6548486.

[45] Aditya Jain, Ramta Bansal, Avnish Kumar, and K. D. Singh. "A comparative study of visual and auditory reaction times on the basis of gender and physical activity levels of medical first year students". In: *International Journal of Applied and Basic Medical Research* 5.2 (2015). DOI: https://doi.org/10.4103/2229-516X.157168.

[46] Benjamin Michaud and Mickaël Begon. "ezc3d: An easy C3D file I/O cross-platform solution for C++, Python and MATLAB". In: *Journal of Open Source Software* 6.58 (Feb. 2021), p. 2911. ISSN: 2475-9066. DOI: 10.21105/joss.02911.

[47] Liangjie Guo and Shuping Xiong. "Accuracy of Base of Support Using an Inertial Sensor Based Motion Capture System". en. In: *Sensors* 17.9 (Sept. 2017), p. 2091. ISSN: 1424-8220. DOI: 10.3390/s17092091.

S Supplementary Information

S1 Analysed points of MoCap data

Table S1: Overview of points of the human skeleton from the MoCap data that are analysed

Description	c3d points	
Sternum	**11**	pIJ
	14	pPX
Hip	**0**	pHipOrigin
	78	jRightHip
	82	jLeftHip
Spine	**15**	pC7SpinalProcess
	8	pL5SpinalProcess
Sacrum	**7**	pSacrum
Hands	**34**	pRightBallHand
	37	pLeftBallHand
Feet	**52**	pRightHeelFoot
	54	pRightFifthMetatarsal
	57	pRightToe
	63	pLeftToe
	60	pLeftFifthMetatarsal
	58	pLeftHeelFoot
CoM	**86**	CenterOfMass

S2 Identification of the threshold values

S2.1 Closest distance between participants

In general, an impulse is passed from one person to the next when they touch each other. This observation can also be seen in the video recordings of the experiments. At this moment of contact, the closest distance between these two participants should theoretically be zero. In practice, however, there is no guarantee that a calculated distance of zero will be reached, as we are only looking at skeletal data in which the extension of the body is neglected. In addition, the calculated distances are superimposed by measurement errors and inaccuracies in the data fusion. Nevertheless, we assume that the smallest distance between the participants will reach a minimum value over time at which a contact is very likely. In order to determine a threshold value, we consider the minimum of the closest distance ($\min(d_{\min}[i, i+1])$) of all trials in which both participants i and $i+1$ have moved forward (see Figure S1). These trials represent the correct positive cases of passing

the motion. It can be seen, that in most cases the smallest distance is close to zero. To include as many trials as possible and keep the threshold as small as possible, we choose the threshold of 0.12 m, which is plotted as black vertical line. This threshold value retains 98% of the cases.

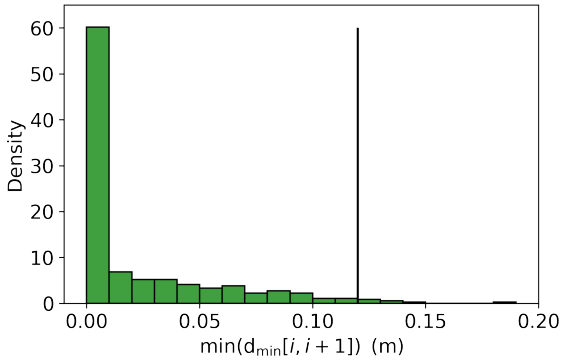

Figure S1: Distribution of the global minima of the closest distances ($\min(d_{\min}[i, i+1])$) if the two participants i and $i+1$ have moved forward. The threshold value of 0.12 m is indicated as black vertical line.

S2.2 Acceleration and velocity

People can move individually and independently, so that velocities and accelerations are measured continuously, even if usually within a small range. However, larger values can also be achieved if, for example, participants look down at the floor, turn around or sway on the spot while waiting. Since we assume that the participants are accelerated quite strongly by an external impulse, the acceleration should differ from the resting movements. In order to be able to better estimate how large values become in a stable waiting position, the accelerations of the CoM of the first 0.5 s are examined for all trials, as there was no external impulse at that time. Based on the distribution of these accelerations in Figure S2, we assume that the acceleration should be greater than $0.25\,ms^{-2}$ in order to ensure a reliable and at the same time not too sensitive detection of motion.

In a next step, we compare different threshold values of the acceleration and the velocity with the side-view videos. The videos observation do not provide a ground truth in the sense of a quantitative measurement, but rather a qualitative yes or no observation. From watching the videos, the start times of motion can not be precisely determined. Instead, the number of participants that are affected by the impulse can be easily and quickly identified. Furthermore, this value can be compared to the Boolean variable motion[i, t] from section 3.2.2 to estimate false positive and false negative detections. Various threshold values for the acceleration a_{THR} and the velocity v_{THR} are tested and all false detections are summed up without

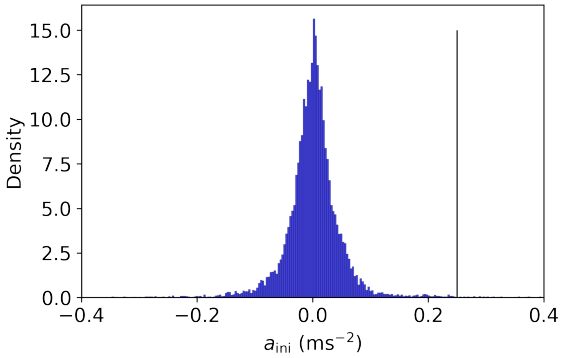

Figure S2: Distributions of all measured accelerations in the first 0.5 seconds of a trial The participants were not yet pushed and were standing on the same spot.

distinguishing between false negative and false positive. Theses false detections are shown in red in Figure S3 indicating a more accurate detection in a lighter colour. For further analysis, the highest acceleration and the lowest velocity with the best detection rate are choosen resulting in threshold values of $a_{\text{THR}} = 0.3\,ms^{-2}$ and $v_{\text{THR}} = 0.05\,ms^{-1}$. The latter threshold value $v_{\text{THR}} = 0.05\,ms^{-1}$ is in accordance with the adopted threshold in perturbation experiments of single persons ([1]).

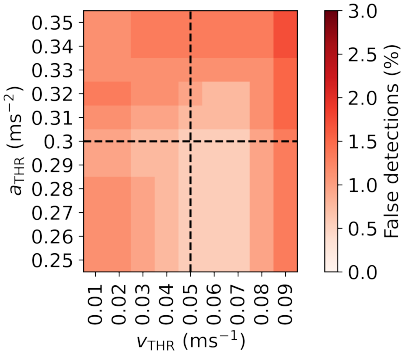

Figure S3: False detections for different threshold values for the acceleration a_{THR} and the velocity v_{THR} when compared to the side-view videos. For further analysis, we choose the combination of the highest acceleration ($a_{\text{THR}} = 0.3\,ms^{-2}$) and the smallest velocity ($v_{\text{THR}} = 0.05\,ms^{-1}$) which has the best detection rate.

S2.3 Perturbation and loss of standing balance

The search for the end of phase 3 turned out to be very challenging. During this phase, the participants try to regain their balance by using different strategies, such

as taking steps forward, leaning on the person in front and straightening up again, etc.. This results in different movement patterns. Furthermore, participants usually returned to their starting position immediately after regaining their balance. It is therefore also necessary to differentiate which movements were made in response to the impulse and which movements are no longer absolutely necessary, which makes it even more difficult. The challenge here is to find a coherent parameter that includes as many strategies as possible, but at the same time is not too large to find a suitable ending. In addition, losing and regaining balance cannot be precisely recognised in the videos. In our investigation, no set of external characteristics could be found to determine this in a standardised way.

We have decided to investigate the MoS, as not only the position of the CoM in relation to the feet but also the velocity of the CoM is taken into account. Thus, a certain value of MoS can only be achieved when the person is upright and the feet and CoM move slightly. Moreover, it is a measure that is then calculated the same for everyone and simplifies a comparison. A maximum value of the MoS is not very sufficient, as participants can slowly regain balance and not always a local maximum is reached. To simplify the analysis, we wanted to use the initial value of the MoS as the threshold value, because we assume that the chosen starting position of each participant is a stable standing position. However, people do not necessarily have to return to their original state, so this value is not always reached after having received the push. On the other hand, the threshold value should not be set too low, as the displacement was sometimes small. From an observational analysis, the 87% of the MoS was chosen to include as most participants as possible. Alternatively, 2 s were selected to give participants enough time (typical reaction time of young adults ranges from 0.18 s to 0.3 s ([2, 3]) to regain their balance and determine an end. This threshold is just a starting point of the analysis that must be tested critically in further experiments.

S3 Analysis of the duration of phases relative to the intensity of external impulses

The duration of the three phases is investigated in relation to the intensity of the external impulses and differentiated between experimental conditions. No significant correlation in terms of intensity was found for any of the phases.

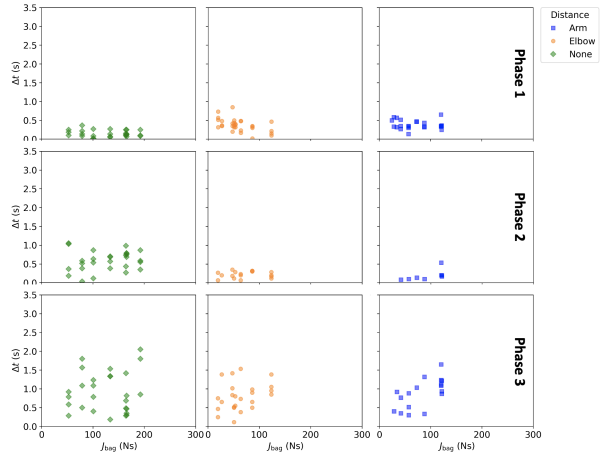

Figure S4: Duration Δt of phases 1, 2 and 3 in relation to the intensity of the impulses for the different initial inter-person distances none, elbow and arm. The arm posture of participants were either free or down for trials without a wall.

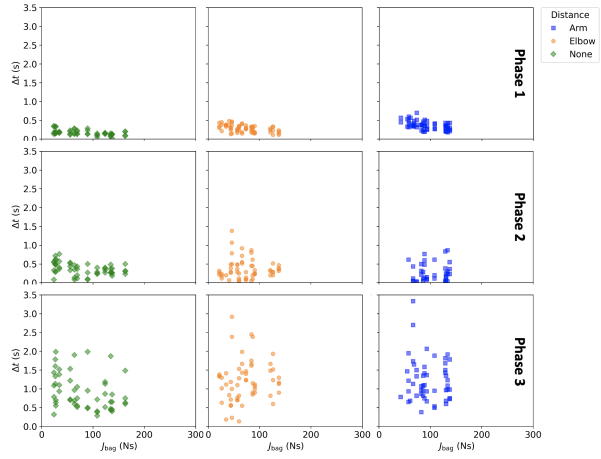

Figure S5: Duration Δt of phases 1, 2 and 3 in relation to the intensity of the impulses for the different initial inter-person distances none, elbow and arm. The arm posture of participants were either free or down for trials with a wall.

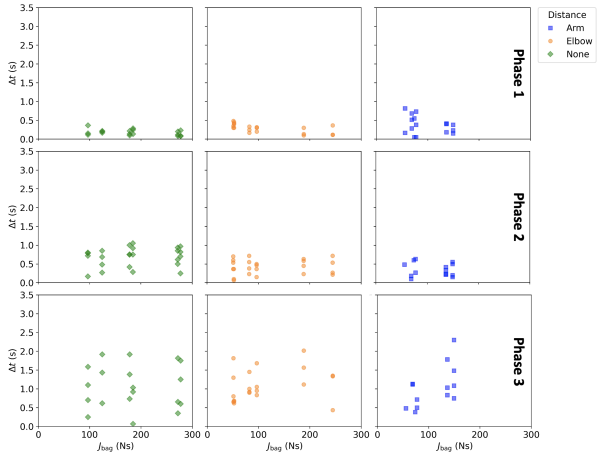

Figure S6: Duration Δt of phases 1, 2 and 3 in relation to the intensity of the impulses for the different initial inter-person distances none, elbow and arm. The arm posture of participants were up for trials without a wall.

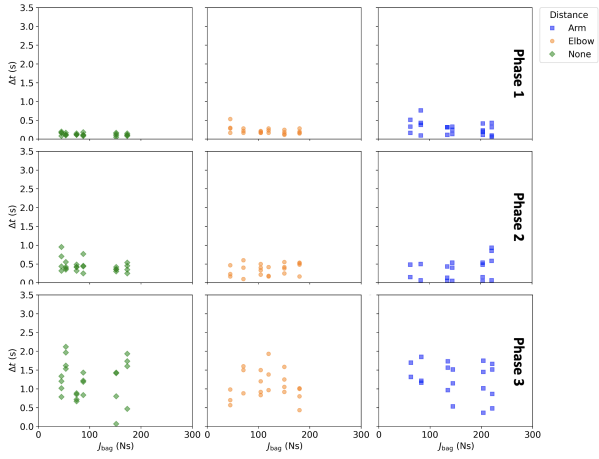

Figure S7: Duration Δt of phases 1, 2 and 3 in relation to the intensity of the impulses for the different initial inter-person distances none, elbow and arm. The arm posture of participants were up for trials with a wall.

References

[1] Thomas Chatagnon, Anne-Hélène Olivier, Ludovic Hoyet, Julien Pettré, and Charles Pontonnier. "Stepping strategies of young adults undergoing sudden external perturbation from different directions". en. In: *Journal of Biomechanics* 157 (Aug. 2023), p. 111703. ISSN: 00219290. DOI: 10.1016/j.jbiomech.2023.111703.

[2] Adrian Ramos Peon and Domenico Prattichizzo. "Reaction times to constraint violation in haptics: comparing vibration, visual and audio stimuli". In: *2013 World Haptics Conference (WHC)*. 2013, pp. 657–661. DOI: 10.1109/WHC.2013.6548486.

[3] Aditya Jain, Ramta Bansal, Avnish Kumar, and K. D. Singh. "A comparative study of visual and auditory reaction times on the basis of gender and physical activity levels of medical first year students". In: *International Journal of Applied and Basic Medical Research* 5.2 (2015). DOI: https://doi.org/10.4103/2229-516X.157168.

PUBLICATION C

Propagation of controlled frontward impulses through standing crowds

This article was published as Feldmann, S., Adrian, J., Boltes, M. (2024). Propagation of Controlled Frontward Impulses Through Standing Crowds. Collective Dynamics, 9, 1-17. doi: 10.17815/CD.2024.148

Author Contributions

Conceptualization: Sina Feldmann, Juliane Adrian and Maik Boltes
Data curation: Sina Feldmann and Juliane Adrian
Formal analysis: Sina Feldmann
Investigation: Sina Feldmann
Methodology: Sina Feldmann, Juliane Adrian and Maik Boltes
Supervision: Juliane Adrian and Maik Boltes
Validation: Sina Feldmann
Visualization: Sina Feldmann
Writing–original draft preparation: Sina Feldmann
Writing–review and editing: Sina Feldmann, Juliane Adrian and Maik Boltes

Propagation of controlled frontward impulses through standing crowds

Sina Feldmann[1 2] and Juliane Adrian[1] and Maik Boltes[1]

[1] Institute for Advanced Simulation 7: Civil Safety Research, Forschungszentrum Jülich, Jülich, Germany

[2] Faculty of Architecture and Civil Engineering, University of Wuppertal, Wuppertal, Germany

Abstract

Impulse propagation in crowds is a phenomenon that is crucial for understanding collective dynamics, but has been scarcely addressed so far. Therefore, we have carried out experiments in which persons standing in a crowd are pushed forward in a controlled manner. Variations of experimental parameters include (i) the intensity of the push, (ii) the initial inter-person distance, (iii) the preparedness of participants and (iv) the crowd formation. Our analysis links the intensity of an impulse recorded by a pressure sensor with individual movements of participants based on head trajectories recorded by overhead cameras and 3D motion capturing data.

The propagation distance as well as the propagation speed of the external impact depends mainly on the intensity of the impulse, whereas no significant effect regarding the preparedness of participants could be found. Especially the propagation speed is influenced by the initial inter-person distance. From the comparison between two methods that detect the time of motion due to the impulse, a more sensitive result is obtained when the velocity of three landmarks of the human body is taken into account and not only the forward displacement of the center of mass. Furthermore, the more intertwined participants are in relation to each other, the more the impulse is distributed to the sides. As a result, more people are affected, however with smaller individual displacements.

Keywords: External Impulse; Propagation; Pedestrian; Experiment; Motion Capturing

1 Introduction

Pedestrian models are valuable tools for understanding and managing crowd movement. Due to their flexibility and cost-effectiveness, they can be employed for a variety of applications [1]. For example, simulations enable safety to be assessed in crowded environments and help to identify potential bottlenecks, evacuation routes and areas prone to congestion [2]. This is particularly important for emergency

scenarios and large events, where many people come together. There, various collective dynamics can occur [3]. The investigation of these collective movements in crowds has become increasingly important in the context of safety, and computer-based approaches are applied more and more.

Despite recent developments in models, such as the simulation of a shock wave [4], the integration of forces in crowds [5] or the propagation of a disturbance [6], there are still limitations to overcome. Pedestrian models are often based on simplifications and assumptions about human behaviour that cannot fully capture the complexity of real interactions. For instance, people are often represented as circles or ellipses and the third dimension of movements is neglected, greatly simplifying the interactions between them. Even though there are models that attempt to simulate contact forces [7–9], the propagation of impulses is particularly lacking.

One way to mitigate this problem is the "domino model" [10]. However, people do not necessarily behave like dominoes and different movements such as steps are not considered. In tackling this complexity, understanding the advantages and disadvantages of established models is needed to better capture the complicated dynamics in dense crowds.

In order to validate and refine existing or new approaches, experimental data for comparison is crucial. Preliminary small-scale studies investigate collision dynamics [11], contact forces [12] and propagation of impulses [13], but are limited to 5 people. This makes it difficult to transfer these results to large crowds. Therefore, in the presented article, we extend the number of participants in a standing crowd that is perturbed by an external impulse up to 36. The impulse is here defined as the transmission of a force over a certain period of time. Based on recorded trajectories, pressure data and 3D motions of the participants, we propose a propagation speed, propagation distance as well as a propagation angle dependent on the initial inter-person distance. As discussed below, these quantities can directly be used for the validation of models.

2 Methods

The propagation of an external impulse has already been studied in a small scale study for a row of five people in [13]. We were able to draw first conclusions about how people regain their balance and interact with other people while transferring the impulse forward along a queue. In order to better assess how this analysis can be applied to larger groups, we extended the five-row experiments. Here, we will focus on the propagation of external impulses along a row of 20 people, as well as groups of up to 36 persons standing in different formations. This enables us to draw statistically more accurate conclusions from a larger sample size and expand the analysis to two dimensions. We vary different formations to achieve a more realistic representation of crowds and to investigate the influence of the positioning of people on the propagation of impulses.

2.1 Experiments

The experiments were conducted in Wuppertal in May 2022 as part of the EU-funded project CrowdDNA [14]. A detailed description of these experiments is summarised in the deliverable report D1.2 of the project [15]. Furthermore, the description with a complete list of conducted trials as well as the collected datasets can be accessed from the Pedestrian Dynamics Data Archive [16].

The experiments can be divided into four blocks (block 1-4) in which different volunteers between the ages of 19 and 36 were recruited. The experimental area was covered with judo mats to ensure a level of safety. All participants were facing in the same direction away from the punching bag. They were positioned either as close as possible or at elbow distance in the prescribed group formation. The tested formations (see Fig. 1) were a row of 20 people (formation A), several rows (either three or five) standing shoulder to shoulder (formation B), the rows standing shifted to the front (formation C) or standing staggered, that each person had the shoulder of 2 people in front of them (formation D). In total, there are 84 trials for formation A with 20 participants and 48 trials for each of the formations B, C and D were performed with a varying number N of participants ($N \in [20, 36]$). To achieve better comparability, the external impulses were carried out in the same way as in the five-row experiments. The same experimenter manually pushed the punching bag, that was hanging horizontally from the ceiling, towards the back of the rearmost participant in the middle row at shoulder height. The pushing intensity was again alternated from weak to medium to strong and after these three pushes, the participants were repositioned in a controlled manner. In order to manipulate the participant's preparedness, the impulse occurred either directly announced (prepared condition) or after a random waiting time in which the participants had to recite the alphabet backwards (unprepared condition). In these experiments, no instructions were given regarding the initial arm positions.

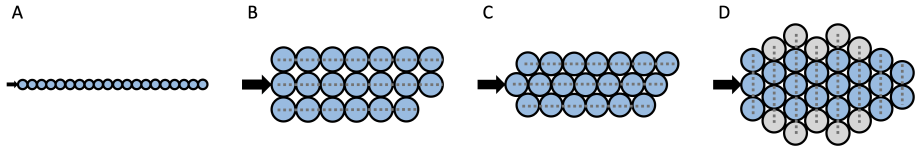

Figure 1: Participants stand in various group formations before the push. (A) 20 people line up in a queue. (B) With their shoulders next to each other, participants stand in either three or five rows. (C) Either three or five rows standing next to each other are shifted to the front so that shoulders are positioned in the gap between two people. (D) The people stand staggered so that one person has the shoulders of two people in front of them. The main group of participants wear a 3D motion capture (MoCap) suit (blue circles) and in some trials the sides are filled up with participants without a MoCap suit (grey circles). The external impulse from the punching bag is indicated as black arrow. Sketches of all investigated crowd formations can be found at [16].

2.2 Data sets

Several video cameras captured the experiments, with the overhead cameras being particularly important as they allow the orange hats of each participant to be tracked with PeTrack, collecting individual head trajectories [17, 18]. Fig. 2 shows examples of collected trajectories for each formation at none (top) and elbow distance (bottom). 3D motion data of the individual limbs for 20 people were recorded using Xsens motion capture (MoCap) suits [19] that use 17 inertial measurement units (IMU). The advantage of these sensors is that they are based on relative measurements and do not rely on a line of sight, e.g. to cameras, which means that occlusions in groups have no influence on the quality of the MoCap data. A disadvantage of these sensors is that the data is only displayed for one person at a time, which can be solved by mapping the 3D head data onto the camera trajectories [20]. As a result, the 3D data is combined into a common coordinate system of the experimental area and therefore all participants are placed and oriented with respect to each other (see Fig. 3, as well as Fig. S1 and Fig. S2 in the Supplementary Information). By attaching an Xsensor [21] pressure sensor to the front of the punching bag, the intensity of the impulses was determined.

Since the external impulse affects the whole body and participants can react with different complex movements, it is important to consider more than just head movements. The center of mass (CoM) is a suitable measure for investigating impulse propagation as it includes a wide range of movements and can be determined from the 3D MoCap data. 3D motion data were collected for the main group, i.e. 20 persons in the middle of each formation. Due to technical issues, a 3D data set for one person is missing in half of the trials. To account for boundary effects, the formations were filled up at lateral or frontal positions with participants for whom only head trajectories were recorded. In our analysis, we solely consider the combined 3D MoCap data. The experimental data including videos, head trajectories, 3D MoCap data as well as pressure data can be freely accessed from the Pedestrian Dynamics Data Archive of the Research Centre Jülich [16].

2.3 Analysis

In our analysis, we will compare the forward propagation of the external impulse of the experiments shown in Fig. 1A for 20 people in a row with the results of the five-row experiments [13], contrast the methods for motion detection from [13] and [22] and extend the analysis to the side for formations B, C and D.

For a better comparison, the same analytical methods as in [13] are applied to investigate the propagation speed and the propagation distance. This means that only the forward trajectories of the CoM, i.e. the y-direction, are examined over time as shown in Fig. 4. Based on this, the start times as well as positions of the persons affected by the external impulse are detected with elbow points (marked as black dots). The elbow point corresponds to the point at which the y-t curve bends visibly, and is often used in mathematics for optimization or cluster analysis. In order to find this point, the y-t-curves between the initial value $y_i^{\text{ini}} = y_i(t_i^{\text{ini}})$ and

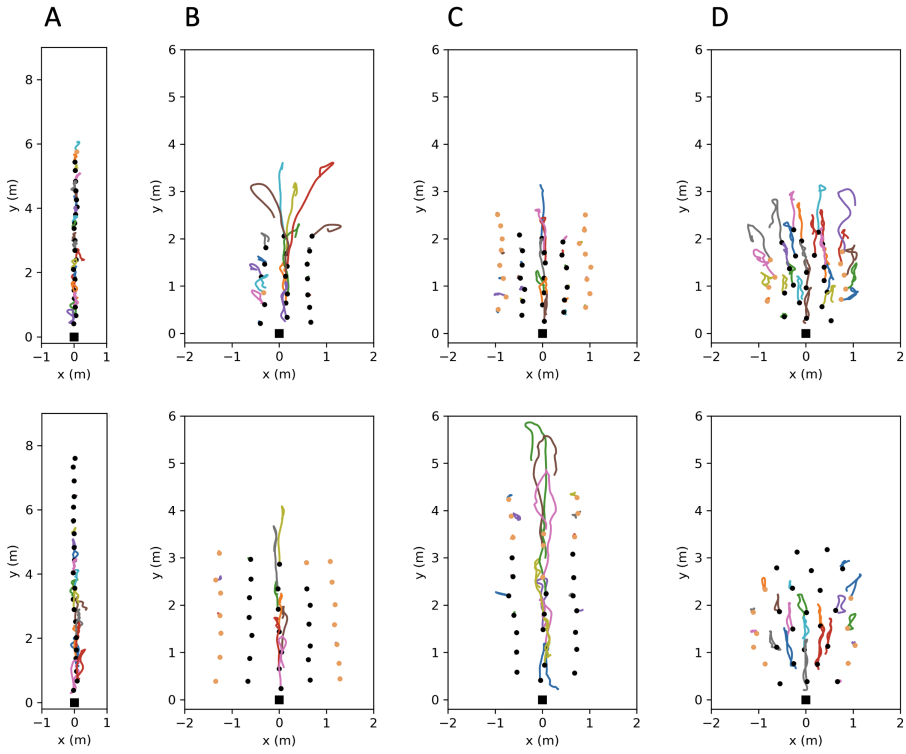

Figure 2: Exemplary representation of collected trajectories for formation A, B, C and D with strong pushes. The upper plots show trials at no distance and the bottom plots at elbow distance. The initial positions are shown as black dots for participants in a MoCap suit, as light-orange dots for participants without MoCap suit and a black square for the punching bag. The middle row was pushed along the positive y-direction.

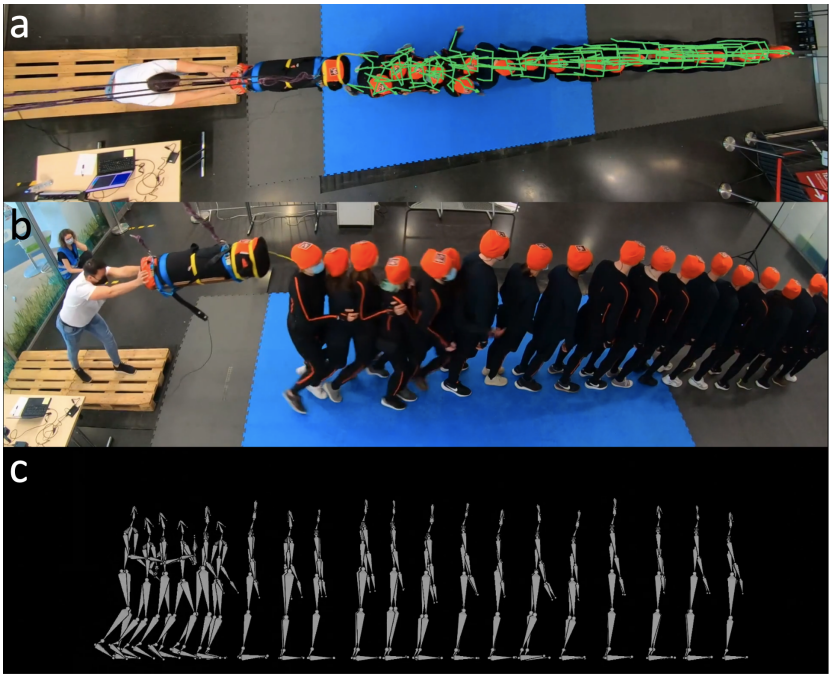

Figure 3: Example of a trial after 2 s of the push, during which 20 participants lined up in formation A at elbow distance and the rearmost person was pushed forward by the punching bag. (a) Snapshot of the overhead camera used to extract head trajectories from the orange hats. The combined 3D MoCap data with exact positioning in the experimental area are shown as green stick figures. (b) Snapshot of a side-view camera enabling a qualitative analysis. (c) Visualisation in Blender of the combined MoCap data of all 20 participants from the side. Examples of formation B, C and D can be found in the Supplementary Information (see Fig. S1 and S2)

the maximum forward displacement $y_i^{\text{end}} = y_i(t_i^{\text{end}}) = \max[y_i(t)]$ are considered. Hereby, i indicates the number of the person in the row ($i \in [1, 20]$) and the initial time is set as $t_i^{\text{ini}} = 1.5\,\text{s}$ before the push $\forall i$. The elbow point is the point of the curve that has the greatest perpendicular distance to the line $\tilde{\mathbf{g}}_i$. The line $\tilde{\mathbf{g}}_i$ passes trough the two points $\tilde{\mathbf{a}} = (y_i^{\text{ini}}, t_i^{\text{ini}})$ and $\tilde{\mathbf{b}} = (y_i^{\text{end}}, t_i^{\text{end}})$ and is defined as $\tilde{\mathbf{g}}_i = \tilde{\mathbf{a}} + k \cdot \tilde{\mathbf{h}}$ with normalized direction vector $\tilde{\mathbf{h}} = \frac{(\tilde{\mathbf{b}} - \tilde{\mathbf{a}})}{\|(\tilde{\mathbf{b}} - \tilde{\mathbf{a}})\|}$ along the line and $k \in \mathbb{R}$. The elbow point is only calculated, when person i has moved forward more than 0.065 m.

The gradient of the resulting regression line (black line) through these elbow points results in the propagation speed. First, a linear fit is selected to allow a closer comparison with [13], as the elbow points were always aligned linearly for the five-row experiments. However, an impulse could also be dampened or intensified along the row. In order to test all three hypotheses at once, a power function is fitted in a subsequent analysis (see Fig. 4 c and Fig. 4 d and Section 3.1.2)

The propagation distance of the push is calculated as the distance between the starting position of the person standing at the punching bag and the furthest forward position of j, which is the last person moving. This is represented as grey dashed lines in Fig. 4.

$$d_{\text{push}} = \max[y_j(t_j) - y_1(0)] \tag{1}$$

Using the data collected by the pressure sensor, the impulse can be determined by integrating the pressure P over the sensor area A as well as over time t.

$$J_{\text{bag}} = \int_t \int_A P \,\mathrm{d}A \,\mathrm{d}t \tag{2}$$

In a second step, the elbow-method for detecting the start of motion as result of the external impulse is compared with another method that considers the velocity of three different landmarks of the human skeleton simultaneously. This velocity-method is introduced in [22], which is an extended investigation of the five-row experiments. Hereby, individual 3D reactions of participants are separated into temporal phases and the velocity defines the start of the first phase of motion. With the velocity method, a motion as response to the external impulse is detected if the forward acceleration of the CoM exceeds $0.3\,\frac{\text{m}}{\text{s}^2}$ and if shortly afterwards the CoM, the lowest cervical vertebra C7 and the origin of the hip move forward at a velocity faster than $0.05\,\frac{\text{m}}{\text{s}}$. The actual start time of the motion is then set to the time when the forward acceleration of the CoM equals $0.15\,\frac{\text{m}}{\text{s}^2}$.

Forward velocities $v_i^p(t)$ and forward accelerations $a_i^p(t)$ for person i can be calculated from the y-position of individual body parts as follows:

$$v_i^p(t) = \left(\frac{y_i^p(t + \Delta t) - y_i^p(t - \Delta t)}{2 \cdot \Delta t} \right) \tag{3}$$

$$a_i^p(t) = \left(\frac{v_i^p(t + \Delta t) - v_i^p(t - \Delta t)}{2 \cdot \Delta t} \right) \tag{4}$$

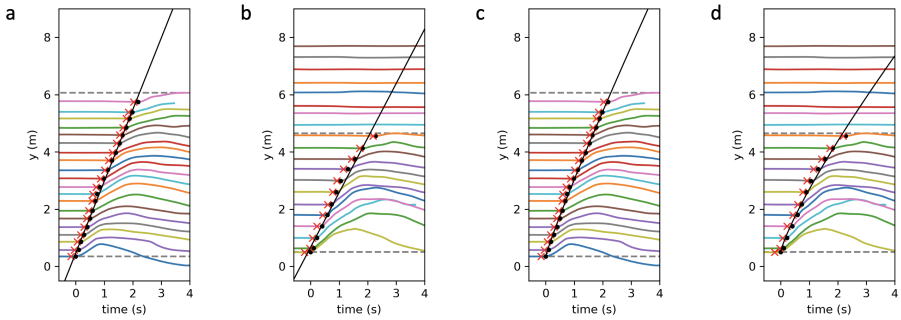

Figure 4: Changes in the y-position of the CoM over time indicate a forward motion of the participants when pushed from behind. The participants stand in formation A at no distance (a) or elbow distance (b). Using the elbow method, the start of motion (black dots) for each person is determined if they are affected by the push. The gradient of the linear regression through these points results in a forward propagation speed. The start times detected by the velocity-method (Eq. 5) are shown as red crosses. (c) and (d) show the same experimental trials as (a) and (b) with the difference that a power function is fitted to the elbow points. The coefficient b of the fitted functions indicates that (c) a linear fit is justified or (d) the impulse is dampened along the row.

Hereby, $\Delta t = 0.05\,\mathrm{s}$ was used and p corresponds to an anatomical landmark of the human body. With the velocity method, a start of motion due to a push is only calculated when the following condition is at least once true:

$$\exists\, t_1 < t_2 : a_i^{\mathrm{CoM}}(t_1) > 0.3\,\tfrac{\mathrm{m}}{\mathrm{s}^2} \wedge v_i^{\mathrm{CoM}}(t_2) > 0.05\,\tfrac{\mathrm{m}}{\mathrm{s}} \wedge v_i^{\mathrm{C7}}(t_2) > 0.05\,\tfrac{\mathrm{m}}{\mathrm{s}} \wedge v_i^{\mathrm{HIP}}(t_2) > 0.05\,\tfrac{\mathrm{m}}{\mathrm{s}}$$

The actual start time is then calculated with:

$$t_i^{\mathrm{VEL}} = \max[t_0], \quad \text{if } a_i^{\mathrm{CoM}}(t_0) > 0.15\,\frac{\mathrm{m}}{\mathrm{s}^2}, \quad \text{for } t_0 < \min[t_2] \tag{5}$$

where $t_0, t_1, t_2 \in [0\,\mathrm{s}, 5\,\mathrm{s}]$ after the push. For further details of the definition, please refer to [22].

In order to investigate the impact of the impulse to the lateral standing participants, data from formations B, C and D are also included. The start positions of the participants $\tilde{\mathbf{r}}_i^{\mathrm{CoM}}(0)$ in relation to the punching bag $\tilde{\mathbf{r}}_i^{\mathrm{BAG}}(0)$ in the xy-plane are taken into account. For $\tilde{\mathbf{r}}_i^{\mathrm{CoM}}, \tilde{\mathbf{r}}_i^{\mathrm{BAG}}, \mathbf{l}_i, \mathbf{e}_y \in \mathbb{R}^2$, a distance $l_i = \|\mathbf{l}_i\|$ as well as an angle α_i to the y-direction are determined:

$$\alpha_i = \mathrm{sgn}(\mathbf{l}_i) \cdot \arccos\left(\frac{\mathbf{l}_i \cdot \mathbf{e}_y}{\|\mathbf{l}_i\|}\right) \tag{6}$$

with $\mathbf{l}_i = \tilde{\mathbf{r}}_i^{\mathrm{CoM}}(0) - \tilde{\mathbf{r}}_i^{\mathrm{BAG}}(0)$, $\mathbf{e}_y = \binom{0}{1}$ and $\mathrm{sgn}(\mathbf{l}_i) = \begin{cases} +1, & \text{if } x_i > 0 \\ -1, & \text{otherwise} \end{cases}$.

The displacement of each participant is calculated as the distance between the starting position $\tilde{\mathbf{r}}_i^{\mathrm{CoM}}(0)$ and points on the trajectory $\tilde{\mathbf{r}}_i^{\mathrm{CoM}}(t)$ in the xy-plane. The maximum displacement ${\Delta s_i}^{\max}$ is obtained accordingly:

$$ {\Delta s_i}^{\max} = \max[\|\tilde{\mathbf{r}}_i^{\mathrm{CoM}}(t) - \tilde{\mathbf{r}}_i^{\mathrm{CoM}}(0)\|] \tag{7} $$

The analysis was executed in Python and the *ezc3d* library [23] was used for the 3D MoCap data. Statistical tests were carried out in R version 4.3.2 and the outputs can be found in the Supplementary Information (see Tables S1 - S6).

3 Results

3.1 Comparison to five-row experiments

3.1.1 Preparation

First, the influence of the preparation level of the participants (prepared or unprepared) will be examined as this aspect was not considered in the five-row experiments. Fig. 5 indicates that the preparedness of the participants has neither a significant effect on the propagation speed v_{push} nor the propagation distance d_{push} in relation to the impulse J_{bag} at the punching bag when the participants stand in a long queue of 20 people. This aspect is therefore neglected in the subsequent analysis and no distinction is made between prepared and unprepared trials.

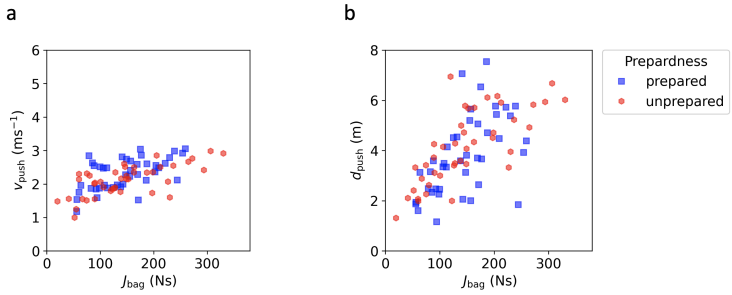

Figure 5: (a) Propagation speed and (b) propagation distance of the push through the row of 20 people (formation A) as functions of the impulse measured at the punching bag. The propagation of the external impulse is not significantly influenced by the preparedness of the participants.

3.1.2 Propagation speed

[13] come to the conclusion that the propagation speed is linearly correlated with the impulse of the push, but does not depend on the initial inter-person distance. To investigate the propagation of the external impulse in more detail, we have carried

out experiments on a larger scale. For a comparison between the two experiments, trials from the five-row experiments with a free initial arm posture at none and elbow distance are included. In the up-scaled experiments described here, all trials of formation A are evaluated and the propagation speeds through the first five persons of the long rows (A5) are calculated. A linear correlation between the propagation speed and the impulse is confirmed (see Fig. 6). However, a moderation analysis reveals a significant difference between none and elbow distance without interaction, that was previously undetected (see Table S1 in the SI). It is important to note, that the five-row experiments are comparable to A5 at no distance, but significantly differ at elbow distance (see Tables S5 and S6 in the SI).

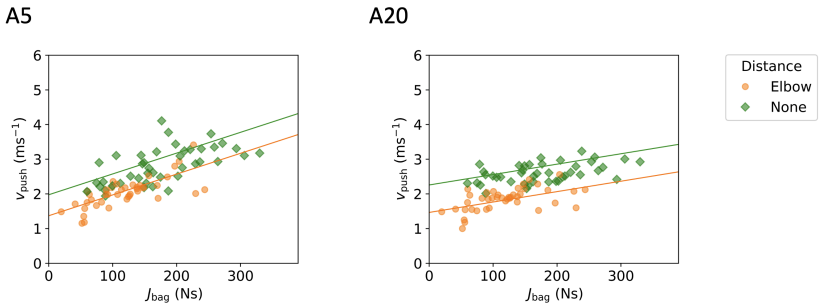

Figure 6: Propagation speed as a function of the measured impulse for the formations A5 and A20. There is a significant difference between the initial inter-person distances none and elbow. A20 differs significantly from A5, which indicates that an impulse can be absorbed along a long row.

The moderation analysis results in the following two equations for the propagation speed for formation A5:

$$\text{A5:} \quad v_{\text{push, none}} = 0.006\,\frac{\text{m}}{\text{Ns}^2} \cdot J_{\text{bag}} + 1.974\,\frac{\text{m}}{\text{s}}$$

$$\text{A5:} \quad v_{\text{push, elbow}} = 0.006\,\frac{\text{m}}{\text{Ns}^2} \cdot J_{\text{bag}} + 1.369\,\frac{\text{m}}{\text{s}}$$

These results differ significantly from the equations found for the five-row experiments [13]. In particular, the gradients across experiments vary considerably. Furthermore, it can be noted that the measured impulses are smaller in the five-row experiments compared to the up-scaled experiments.

Now, the propagation speeds are calculated for all persons in the long rows (A20) and compared to the first 5 persons in the long rows (A5). A moderation analysis also reveals a significant effect of the initial inter-person distance on the propagation speed for A20 (see S2 in SI). In addition, there are significantly lower propagation speeds at higher impulses for the long rows compared to A5 (see S5 and S6 in the SI). This results in the two equations for the propagation speed for formation A20, as follows:

$$\text{A20:} \quad v_{\text{push, none}} = 0.003\,\frac{\text{m}}{\text{Ns}^2} \cdot J_{\text{bag}} + 2.256\,\frac{\text{m}}{\text{s}}$$

$$\text{A20:} \quad v_{\text{push, elbow}} = 0.003 \, \frac{\text{m}}{\text{Ns}^2} \cdot J_{\text{bag}} + 1.464 \, \frac{\text{m}}{\text{s}}$$

This could indicate that the impulses are being dampened along the rows of 20 people. To investigate this, we fitted a power function $y(t) = a \cdot t^b + c$ to the elbow points of A20 instead of the linear fit. Two examples of the power function fit can be found in Fig. 4 c and Fig. 4 d. The coefficient b is of particular interest here, as it specifies whether a linear fit is justified ($b \approx 1$), whether the impulse is absorbed ($b < 1$) or whether the impulse is intensified ($b > 1$). Fig. 7 shows the distribution as well as the kernel density estimate of b for all A trials. It can be seen that all three cases occur. However, the maximum of the distribution lies below 1, indicating that on average pushes are dampened when they propagate through the long row.

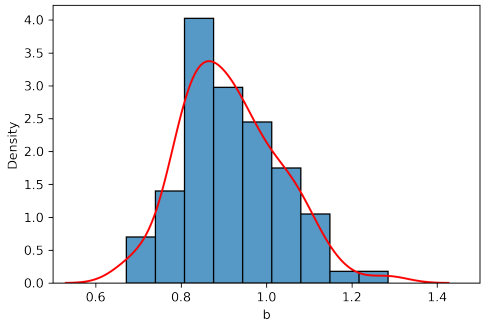

Figure 7: Distribution of the coefficient b obtained from a power function fit of the elbow points for A trials. The maximum is less than 1, which suggests an absorption effect along the row of 20 participants.

3.1.3 Propagation distance

Fig. 8 shows the propagation distance (Eq. 1) as a function of the measured impulse (Eq. 2). A linear correlation between the propagation distance and the impulse is further supported by this analysis and no effect of the initial inter-person distance on the propagation distance can be found.

These results are difficult to compare with the five-row experiments, as the push propagates through the entire row of 5 people starting at $J = 110\,\text{N}$ and therefore, the propagation distance reaches a maximum of approx. 3 m. However, the distance is also bounded in the large experiments, as the impulse sometimes passes through the entire row of 20 people (see Fig. 4 a). This indicates, that the distance should be investigated using even more people.

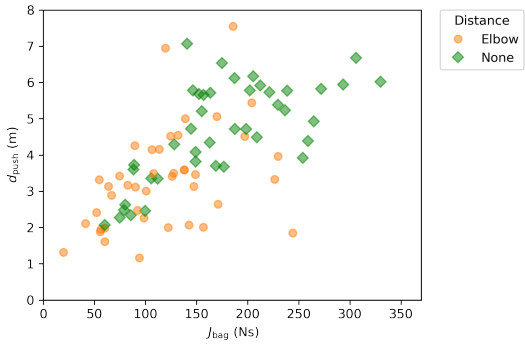

Figure 8: Propagation distance for the long rows A20 increases with stronger impulses. There is no difference between none and elbow distance.

3.2 Comparison of the two detection methods

We proposed two different methods (see section Sec. 2.3) to detect whether a participant is affected by the external impulse and to determine the time the motion starts. In Fig. 4, the elbow-method is shown as black dots and the velocity method derived from Eq. 5 as red crosses. It can be seen that the two methods are well comparable with each other, whereby the velocity method sets a slightly earlier point in time. A qualitative comparison of both methods for all A trials with the recorded videos shows that the velocity method is more sensitive than the elbow method. The number of falsely detected persons are listed in Tab. 1.

Table 1: Comparison of the elbow method as well as the velocity method with the recorded videos for A trials.

method	false -positive	false-negative	total
velocity	29	13	1644
elbow	8	90	1680

3.3 Extension to side

The formations B, C and D are included to extend the analysis to the side. First, we want to investigate the effect of lateral standing rows on the propagation speed of the middle rows for formations B and C. Therefore, the same analysis as discussed in Section Sec. 3.1.2 is carried out for the middle row, which stands directly in front of the punching bag. The moderation analyses show no significant difference between the initial inter-person distances for both formations (see Tables S3 and S4 in the SI). For the propagation speed, the equations $v_{\text{push}} = 0.005\,\frac{\text{m}}{\text{Ns}^2} \cdot J_{\text{bag}} + 1.658\,\frac{\text{m}}{\text{s}}$ and $v_{\text{push}} = 0.004\,\frac{\text{m}}{\text{Ns}^2} \cdot J_{\text{bag}} + 1.666\,\frac{\text{m}}{\text{s}}$ are obtained for formations B and C respectively.

In order to investigate the impact of the impulse to the lateral standing participants, the velocity method (Eq. 5) is used to detect the start positions of participants that are affected by the push. For these participants, the distance l_i as well as the angle α_i to the start position of the punching bag are calculated with Eq. 6. The angle becomes negative if the person stands on the left of the punching bag and positive when standing on the right side. Fig. 9 shows a heat map of the determined angles as a function of distance for formations A, B, C and D. The different colours of the points represent the maximum displacement $\Delta s_i^{\max}$ of the participant. This is calculated as the distance between the starting position and the furthest point on the trajectory in the xy-plane (see Eq. 7).

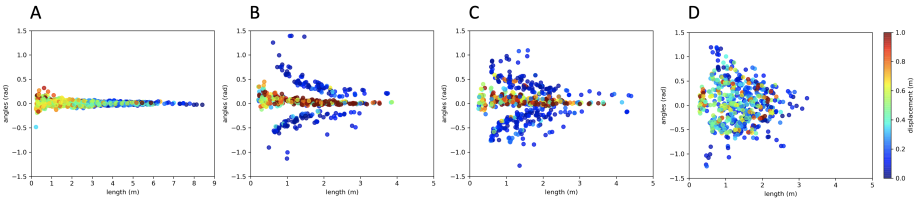

Figure 9: Heat map of the individual displacement of the initial position for formations A, B, C and D. Angles α_i are shown as function of the distance l_i from the punching bag to the initial positions of participants that are affected by the external impulse (Eq. 6). The color indicates the maximum displacement $\Delta s_i^{\max}$ of the participant (Eq. 7).

The more intertwined the participants are standing in relation to each other, the more lateral components occur. The external impulse is distributed over a larger area and therefore propagates less to the front and more to the sides. As a result, the individual displacements are smaller for participants standing in formation D compared to B or C.

4 Discussion

This article investigates the propagation of external impulses through standing crowds. For this purpose, experiments were carried out that illustrate a simplified representation of real crowds. First, only one row of people is analysed, which is then extended to multiple rows and a group formation.

4.1 Limitations

One limitation of this study is manual pushing and the pressure sensor. The perceived strength of the pusher can differ from the measured values, so the categorisation is not clear. Besides, the pressure sensor only records a normal component of the pushing force which does not fully correspond to reality. The experiments are also restricted in comparison to real life scenarios. Since we are mainly investigating rows here, this analysis could mainly be applied to queuing systems. In real dense crowds, people probably do not stand as uniformly as in these experiments. Therefore, it would be interesting to investigate what happens when people are not standing

evenly distributed and what effect a gap in the crowd can have on the propagation of impulses. Another aspect contrary to reality is that the impulses only come from one direction and therefore other pushing directions could be investigated in the future. Additional factors, that could be considered for a further and more realistic analysis are uneven ground or the awareness level of participants.

4.2 Conclusion

In this study, we find that the propagation speed of an impulse depends on the intensity of the push and the initial inter-person distance. A significant difference regarding the preparation of participants on the propagation could not be found. Here it is particularly interesting to note that the initial inter-person distance actually causes a significant difference in the propagation speed, which could not be shown in the preceding five-row experiments [13]. We assume that this could be explained by a small number of repetitions for the same conditions and the same participants.

Furthermore, a row of five people is quite short, so that there may be boundary effects and certain phenomena remain unrecognized. Along the row of 20 people, an absorption effect of the impulse is observed. When using a power function fit to investigate the damping of the push through the row, one assumes that there is a constant coefficient b for the complete range of the propagation. This might be improved to a position-dependent absorption coefficient since we observe a linear propagation speed for the first part of the row. The damping only starts for the last few participants affected by the push, resulting in a J-shaped propagation speed curve. One explanation for this would be that persons behave similar to the non-Newtonian mixture of starch and water in the well-known popular experiment: They react more stiff to stronger impacts whereas with decreasing impact strength, muscles have time to counteract and dissipate the external force. This implies that the absorption coefficient is rather a function of the intensity than the position. On the other hand, of course, the intensity itself depends on the distance from the initial impact. These findings underline the fact that the domino model is not a good choice for modelling impulse propagation through crowds. In addition, it should be noted that people are not physical particles, but individuals with different characteristics (e.g. height, weight) who can use different strategies to regain balance. All of this may have an impact on the variables we are investigating.

On the other hand, it could also be possible that an impulse is intensified along the row, which is indicated by a few cases when the coefficient $b > 1$. We assume that different reactions of participants can be the reason for this. The exact circumstances of this, however, require further investigation. In addition, the propagation speed is only defined for one row and should be extended to 2 dimensions in the future.

A big advantage of this evaluation is that we use 3D data to draw a 2D illustration of the propagation. Especially, the investigation on how strong the impulses

affect people, depending on their position within a crowd. This heat map can be particularly helpful for models that rely on 2D representations of people.

Acknowledgements

This study was funded by the European Unions Horizon 2020 research and innovation program within the project CrowdDNA [grant number 899739]. We would like to thank Jernej Čamernik, Thomas Chatagnon, Helena Lügering, Armin Seyfried and Anna Sieben who supported us in the conception, planning and realisation of the experiments. Furthermore, we are grateful to Alica Kandler for her help in setting up the experiments and curating the data.

Ethics Statement

The experiments were approved by the ethics board of the University of Wuppertal in April 2022 (Reference: MS/AE 220330).

References

[1] Mohcine Chraibi, Antoine Tordeux, Andreas Schadschneider, and Armin Seyfried. "Modelling of Pedestrian and Evacuation Dynamics". en. In: *Encyclopedia of Complexity and Systems Science*. Ed. by Robert A. Meyers. Berlin, Heidelberg: Springer Berlin Heidelberg, 2018, pp. 1–22. ISBN: 978-3-642-27737-5. DOI: 10.1007/978-3-642-27737-5_705-1.

[2] Raphael Korbmacher and Antoine Tordeux. "Review of Pedestrian Trajectory Prediction Methods: Comparing Deep Learning and Knowledge-Based Approaches". In: *IEEE Transactions on Intelligent Transportation Systems* 23.12 (Dec. 2022), pp. 24126–24144. ISSN: 1524-9050, 1558-0016. DOI: 10.1109/TITS.2022.3205676.

[3] Maik Boltes, Jun Zhang, Antoine Tordeux, Andreas Schadschneider, and Armin Seyfried. "Empirical Results of Pedestrian and Evacuation Dynamics". en. In: *Encyclopedia of Complexity and Systems Science*. Ed. by Robert A. Meyers. Berlin, Heidelberg: Springer Berlin Heidelberg, 2018, pp. 1–29. ISBN: 978-3-642-27737-5. DOI: 10.1007/978-3-642-27737-5_706-1.

[4] Wouter van Toll, Cédric Braga, Barbara Solenthaler, and Julien Pettré. "Extreme-Density Crowd Simulation: Combining Agents with Smoothed Particle Hydrodynamics". en. In: *Motion, Interaction and Games*. Virtual Event SC USA: ACM, Oct. 2020, pp. 1–10. ISBN: 978-1-4503-8171-0. DOI: 10.1145/3424636.3426896.

[5] Jingni Song, Feng Chen, Yadi Zhu, Na Zhang, Weiyu Liu, and Kai Du. "Experiment Calibrated Simulation Modeling of Crowding Forces in High Density Crowd". In: *IEEE Access* 7 (2019), pp. 100162–100173. ISSN: 2169-3536. DOI: 10.1109/ACCESS.2019.2930104.

[6] Cuiling Li, Rongyong Zhao, Yan Wang, Ping Jia, Wenjie Zhu, Yunlong Ma, and Miyuan Li. "Disturbance Propagation Model of Pedestrian Fall Behavior in a Pedestrian Crowd and Elimination Mechanism Analysis". In: *IEEE Transactions on Intelligent Transportation Systems* (2023), pp. 1–11. ISSN: 1524-9050, 1558-0016. DOI: 10.1109/TITS.2023.3314072.

[7] Sujeong Kim, Stephen J. Guy, Karl Hillesland, Basim Zafar, Adnan Abdul-Aziz Gutub, and Dinesh Manocha. "Velocity-based modeling of physical interactions in dense crowds". en. In: *The Visual Computer* 31.5 (May 2015), pp. 541–555. ISSN: 0178-2789, 1432-2315. DOI: 10.1007/s00371-014-0946-1.

[8] Wouter Van Toll, Thomas Chatagnon, Cédric Braga, Barbara Solenthaler, and Julien Pettré. "SPH crowds: Agent-based crowd simulation up to extreme densities using fluid dynamics". en. In: *Computers & Graphics* 98 (Aug. 2021), pp. 306–321. ISSN: 00978493. DOI: 10.1016/j.cag.2021.06.005.

[9] Chongyang Wang, Liangchang Shen, and Wenguo Weng. "Modelling physical contacts to evaluate the individual risk in a dense crowd". en. In: *Scientific Reports* 13.1 (Mar. 2023), p. 3929. ISSN: 2045-2322. DOI: 10.1038/s41598-023-31148-z.

[10] Chongyang Wang, Shunjiang Ni, and Wenguo Weng. "Modeling human domino process based on interactions among individuals for understanding crowd disasters". en. In: *Physica A: Statistical Mechanics and its Applications* 531 (Oct. 2019), p. 121781. ISSN: 0378-4371. DOI: 10.1016/j.physa.2019.121781.

[11] Chongyang Wang and Wenguo Weng. "Study on the collision dynamics and the transmission pattern between pedestrians along the queue". en. In: *Journal of Statistical Mechanics: Theory and Experiment* 2018.7 (July 2018), p. 073406. ISSN: 1742-5468. DOI: 10.1088/1742-5468/aace27.

[12] Xudong Li, Weiguo Song, Xuan Xu, Jun Zhang, Long Xia, and Congling Shi. "Experimental study on pedestrian contact force under different degrees of crowding". en. In: *Safety Science* 127 (July 2020), p. 104713. ISSN: 09257535. DOI: 10.1016/j.ssci.2020.104713.

[13] Sina Feldmann and Juliane Adrian. "Forward propagation of a push through a row of people". en. In: *Safety Science* 164 (Aug. 2023), p. 106173. ISSN: 09257535. DOI: 10.1016/j.ssci.2023.106173.

[14] CrowdDNA Project. *Website CrowdDNA Project*. https://crowddna.eu/. July 3, 2022. URL: https://crowddna.eu/ (visited on 07/03/2024).

[15] CrowdDNA Project. *D1.2: Laboratory dataset on large groups*. http://crowddna.eu/d1-2-laboratory-dataset-on-large-groups/. Dec. 18, 2023. URL: http://crowddna.eu/d1-2-laboratory-dataset-on-large-groups/ (visited on 12/18/2023).

[16] Sina Feldmann, Juliane Adrian, Maik Boltes, Jernej Čamernik, Thomas Chatagnon, Marc Comino-Trinidad, Alica Kandler, and Armin Seyfried. *Impulse propagation through a small standing crowd*. Pedestrian Dynamics Data Archive, Institute for Advanced Simulation 7: Civil Safety Research, Forschungszentrum Jülich. 2024. DOI: 10.34735/ped.2022.6.

[17] Maik Boltes and Armin Seyfried. "Collecting pedestrian trajectories". In: *Neurocomputing* 100 (2013). Special issue: Behaviours in video, pp. 127–133. ISSN: 0925-2312. DOI: https://doi.org/10.1016/j.neucom.2012.01.036.

[18] Maik Boltes, Ann Katrin Boomers, Juliane Adrian, Ricardo Martin Brualla, Arne Graf, Paul Häger, Daniel Hillebrand, Deniz Kilic, Paul Lieberenz, Daniel Salden, and Tobias Schrödter. *PeTrack*. Version v0.9. July 2021. DOI: 10.5281/zenodo.5126562.

[19] Martin Schepers, Matteo Giuberti, and Giovanni Bellusci. "Xsens MVN: Consistent Tracking of Human Motion Using Inertial Sensing". en. In: (2018). DOI: 10.13140/RG.2.2.22099.07205.

[20] Maik Boltes, Juliane Adrian, and Anna-Katharina Raytarowski. "A Hybrid Tracking System of Full-Body Motion Inside Crowds". en. In: *Sensors* 21.6 (Mar. 2021), p. 2108. ISSN: 1424-8220. DOI: 10.3390/s21062108.

[21] Xsensor LX210:50.50.05. *Datasheet: Xsensor SENSORS LX210:50.50.05*. 2019. URL: https://www.xsensor.de/wp-content/uploads/2015/11/LX210_50_50_05-2500-Sensoren-508mm-Aufl%C3%B6sung-Gr%C3%B6sse-25x25cm-Messbereich-014-11Ncm2-Anwendung-Sitze_Rollst%C3%BChle.pdf (visited on 10/13/2022).

[22] Sina Feldmann, Thomas Chatagnon, Juliane Adrian, Julien Pettré, and Armin Seyfried. "Temporal segmentation of motion propagation in response to an external impulse". en. In: *Safety Science* (Jan. 2024). DOI: underreview.

[23] Benjamin Michaud and Mickaël Begon. "ezc3d: An easy C3D file I/O cross-platform solution for C++, Python and MATLAB". In: *Journal of Open Source Software* 6.58 (Feb. 2021), p. 2911. ISSN: 2475-9066. DOI: 10.21105/joss.02911.

S Supplementary Information

S1 Experimental Data

The experiments were recorded with several video cameras. The top-down videos are used to collect individual head trajectories of each participant with PeTrack and the sideview camera enable a qualitative analysis. The 3D motion of 20 participants recorded with MoCap suits from Xsens are combined with the trajectories to integrate them into a common coordinate system of the experimental area.

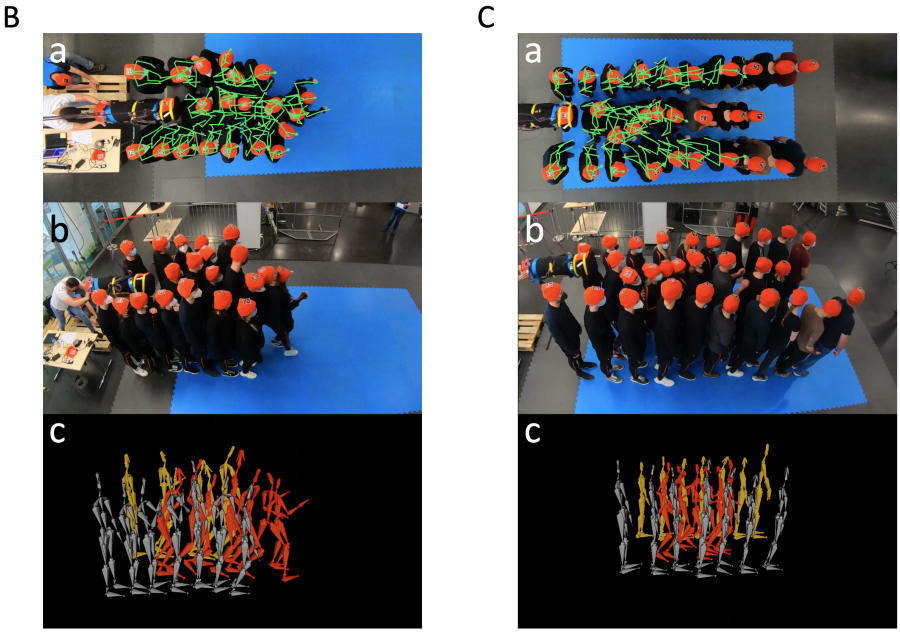

Figure S1: Examples of formation B and C. (a) Snapshot of the overhead camera with combined 3D MoCap data visualised as green stick figures. (b) Snapshot of a side-view camera enabling a qualitative analysis. (c) Visualisation in Blender of the combined MoCap data of 20 participants from the side. The front row is coloured in grey, the middle row in red and the back row in yellow.

S2 Moderation analysis

All moderation analyses were conducted in R version 4.3.2. First, we compare the effect of initial inter-person distance for each formation A5, A20, B and C individually. In doing so, only the middle row, which stands directly in front of the punching bag, is taken into account. The results are shown in Tables S1, S2 , S3 and S4 for the comparison of no and elbow distance.

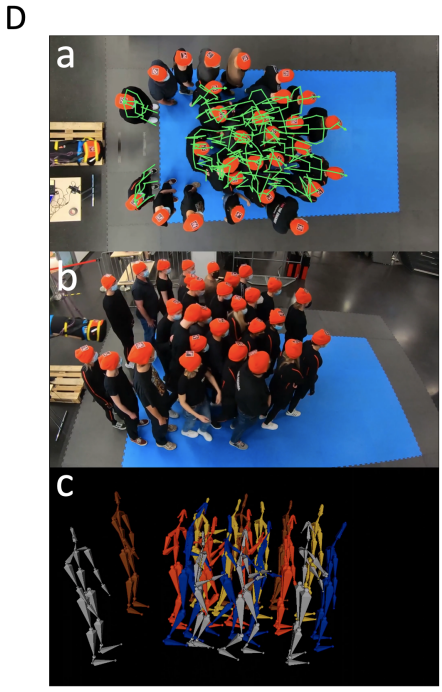

Figure S2: Example of formation D (a) Snapshot of the overhead camera with combined 3D MoCap data visualised as green stick figures. (b) Snapshot of a side-view camera enabling a qualitative analysis. (c) Visualisation in Blender of the combined MoCap data of 20 participants from the side. The skeletons are coloured from front to back (x-position) as follows: grey, blue, red, yellow, brown.

Table S1: Results of the moderation analysis comparing no and elbow distance for A5.

Residuals:	Min	1Q	Median	3Q	Max
	-0.78745	-0.21077	-0.01897	0.19585	1.28502

Coefficients	Estimate	Std. Error	t	p	Signif.
intercept	1.3691	0.1361	10.056	7.5e-16	***
impulse of push	0.0057	0.0010	5.415	6.26e-07	***
distance none	0.6052	0.2071	2.923	0.0045	**
impulse : distance none	-0.0009	0.0013	-0.668	0.5058	

Signif. codes: 0 '***' 0.001 '**' 0.01 '*' 0.05 '.' 0.1 ' ' 1

Residual standard error: 0.3636 on 80 degrees of freedom
Multiple R-squared: 0.6621, Adjusted R-squared: 0.6494
F-statistic: 52.25 on 3 and 80 DF, p-value: $<$ 2.2e-16

Table S2: Results of the moderation analysis comparing no and elbow distance for A20.

Residuals:	Min	1Q	Median	3Q	Max
	0.63112	-0.15951	0.01043	0.16122	0.50499
Coefficients	Estimate	Std. Error	t	p	Signif.
intercept	1.4637	0.0971	15.080	< 2e-16	***
impulse of push	0.0032	0.0007	4.326	4.34e-05	***
distance none	0.7921	0.1476	5.365	7.68e-07	***
impulse : distance none	-0.0013	0.0010	-1.338	0.185	
Signif. codes: 0 '***' 0.001 '**' 0.01 '*' 0.05 '.' 0.1 ' ' 1					
Residual standard error: 0.2592 on 80 degrees of freedom Multiple R-squared: 0.7206, Adjusted R-squared: 0.7101 F-statistic: 68.78 on 3 and 80 DF, p-value: < 2.2e-16					

Table S3: Results of the moderation analysis comparing no and elbow distance for formation B.

Residuals:	Min	1Q	Median	3Q	Max
	-0.55682	-0.21081	-0.00706	0.14132	0.84558
Coefficients	Estimate	Std. Error	t	p	Signif.
intercept	1.6225	0.1573	10.314	2.55e-13	***
impulse of push	0.0042	0.0011	3.808	0.0004	***
distance none	0.2405	0.2285	1.053	0.2983	
impulse : distance none	0.0010	0.0015	0.648	0.5206	
Signif. codes: 0 '***' 0.001 '**' 0.01 '*' 0.05 '.' 0.1 ' ' 1					
Residual standard error: 0.3218 on 44 degrees of freedom Multiple R-squared: 0.6176, Adjusted R-squared: 0.5915 F-statistic: 23.69 on 3 and 44 DF, p-value: 2.801e-09					

In the one row experiments A5 and A20, a significant difference can be observed between no and elbow distance. However, no significant distance was found for multiple rows B and C.

Table S4: Results of the moderation analysis comparing no and elbow distance for formation C.

Residuals:	Min	1Q	Median	3Q	Max
	-0.73434	0.30283	-0.00189	0.25902	1.04705
Coefficients	Estimate	Std. Error	t	p	Signif.
intercept	1.5211	0.1973	7.711	1.05e-09	***
impulse of push	0.0049	0.0015	3.264	0.0021	**
distance none	0.2523	0.3088	0.817	0.4184	
impulse : distance none	-0.0019	0.0019	-1.008	0.3191	
Signif. codes: 0 '***' 0.001 '**' 0.01 '*' 0.05 '.' 0.1 ' ' 1					
Residual standard error: 0.3975 on 44 degrees of freedom Multiple R-squared: 0.3343, Adjusted R-squared: 0.289 F-statistic: 7.367 on 3 and 44 DF, p-value: 0.000419					

In a next step, we compared formation A5 to formation A20 and the five-row experiments. The results are listed in Tables S5 and S6 for no and elbow distance respectively.

Table S5: Results of the moderation analysis comparing formations A5, A20 and five-row experiment at no distance.

Residuals:	Min	1Q	Median	3Q	Max
	-0.78745	-0.22060	-0.03223	0.18316	1.28502
Coefficients	Estimate	Std. Error	t	p	Signif.
intercept	1.9744	0.1444	13.671	< 2e-16	***
impulse of push	0.0048	0.0008	6.213	1.74e-08	***
formation A20	0.2814	0.2042	1.378	0.1718	
formation five-row	0.0140	0.2624	0.053	0.9576	
impulse : formation A20	-0.0028	0.0011	-2.595	0.0111	*
impulse : formation five-row	0.0020	0.0021	0.942	0.3489	
Signif. codes: 0 '***' 0.001 '**' 0.01 '*' 0.05 '.' 0.1 ' ' 1					
Residual standard error: 0.3365 on 87 degrees of freedom Multiple R-squared: 0.4297, Adjusted R-squared: 0.397 F-statistic: 13.11 on 5 and 87 DF, p-value: 1.626e-09					

Table S6: Results of the moderation analysis comparing formations A5, A20 and five-row experiment at elbow distance.

Residuals:	Min	1Q	Median	3Q	Max
	-0.66271	-0.13221	0.01054	0.15693	0.75765

Coefficients	Estimate	Std. Error	t	p	Signif.
intercept	1.3691	0.1108	12.358	< 2e-16	***
impulse of push	0.0057	0.0009	6.654	2.43e-09	***
formation A20	0.0946	0.1567	0.604	0.5476	
formation five-row	-0.3296	0.2178	-1.514	0.1337	
impulse : formation A20	-0.0024	0.0012	-2.025	0.0459	*
impulse : formation five-row	0.0124	0.0028	4.412	2.92e-05	***

Signif. codes: 0 '***' 0.001 '**' 0.01 '*' 0.05 '.' 0.1 ' ' 1

Residual standard error: 0.2959 on 87 degrees of freedom
Multiple R-squared: 0.5715, Adjusted R-squared: 0.5468
F-statistic: 23.2 on 5 and 87 DF, p-value: 9.791e-15

Sina Feldmann

Address: Am Hahnberg 25, 65529 Waldems, Germany
Mobile: +49 176 3449 1750
E-Mail: sina_feldmann@brown.edu

Education

since 08 2020 **PhD student, University of Wuppertal, Germany**
Towards Improved Civil Safety: Experimental Insights into Impulse Propagation through Crowds
Supervisor: Prof. Dr. Armin Seyfried

09 2018 – 11 2019 **M.Sc. Environmental Science, University of Aberdeen, UK**
Topic of Master thesis: Biosphere – Atmosphere Interactions in the Daisyworld Model
Class: With Commendation

10 2014 – 03 2018 **B.Sc. Physics, Karlsruhe Institute of Technology, Germany**
Topic of Bachelor thesis: Production of Nanostructured Layers by Electrospinning
Average grade: Good (2.3)

06 2013 **Higher Education Entrance Qualification, Pestalozzischule Idstein, Germany**
Average grade: Good (1.6)

Work Experience

since 01 2024 **Research Associate in Cognitive, Linguistic, and Psychological Sciences, Brown University, USA**
Comparative simulations of models of collective crowd motion
Examination of an assistive technology to control locomotion

08 2020 – 10 2023 **Research Assistant, Civil Safety Research, Forschungszentrum Jülich, Germany**
Planned and conducted experiments with pedestrians
Processed and analyzed collected data
Participated in the project *CrowdDNA*

01 2023 – 03 2023 **Visiting Scientist, VirtUs, INRIA, Rennes, France**
Investigated how experimental results can be incorporated into simulation models

07 2013 – 07 2014 **Full time volunteer work with artefact, International Centre for Sustainable Development, Glücksburg, Germany**
Supervised projects on renewable energies for children

Schriften des Forschungszentrums Jülich
IAS Series

Band / Volume 57
Plasma Breakdown and Runaway Modelling in ITER-scale Tokamaks
J. Chew (2023), xv, 172 pp
ISBN: 978-3-95806-730-1

Band / Volume 58
Space Usage and Waiting Pedestrians at Train Station Platforms
M. Küpper (2023), ix, 95 pp
ISBN: 978-3-95806-733-2

Band / Volume 59
Quantum annealing and its variants: Application to quadratic unconstrained binary optimization
V. Mehta (2024), iii, 152 pp
ISBN: 978-3-95806-755-4

Band / Volume 60
Elements for modeling pedestrian movement from theory to application and back
M. Chraibi (2024), vi, 279 pp
ISBN: 978-3-95806-757-8

Band / Volume 61
Artificial Intelligence Framework for Video Analytics:
Detecting Pushing in Crowds
A. Alia (2024), xviii, 151 pp
ISBN: 978-3-95806-763-9

Band / Volume 62
The Relationship between Pedestrian Density, Walking Speed and Psychological Stress: Examining Physiological Arousal in Crowded Situations
M. Beermann (2024), xi, 117 pp
ISBN: 978-3-95806-764-6

Band / Volume 63
Eventify Meets Heterogeneity: Enabling Fine-Grained Task-Parallelism on GPUs
L. Morgenstern (2024), xv, 110 pp
ISBN: 978-3-95806-765-3

Band / Volume 64
Dynamic Motivation in Crowds: Insights from Experiments and Pedestrian Models for Goal-Directed Motion
E. Üsten (2024), ix, 121 pp
ISBN: 978-3-95806-773-8

Schriften des Forschungszentrums Jülich
IAS Series

Band / Volume 65
Propagation of Stimuli in Crowds:
Empirical insights into mutual influence in human crowds
H. Lügering (2024), xi, 123 pp
ISBN: 978-3-95806-775-2

Band / Volume 66
Classification of Pedestrian Streams: From Empirics to Modelling
J. Cordes (2024), vii, 176 pp
ISBN: 978-3-95806-780-6

Band / Volume 67
Optimizing Automated Shading Systems in Office Buildings by Exploring Occupant Behaviour
G. Derbas (2024), 9, x, 168, ccxxiii
ISBN: 978-3-95806-787-5

Band / Volume 68
Speed-Density Analysis in Pedestrian Single-File Experiments
S. Paetzke (2025), XIII, 107 pp
ISBN: 978-3-95806-818-6

Band / Volume 69
Proceedings of the 35th Parallel Computational Fluid Dynamics International Conference 2024
A. Lintermann, S. S. Herff, J. H. Göbbert (2025), xv, 321 pp
ISBN: 978-3-95806-819-3

Band / Volume 70
Towards Improved Civil Safety: Experimental Insights into Impulse Propagation through Crowds
S. Feldmann (2025), xi, 99 pp
ISBN: 978-3-95806-828-5

Weitere ***Schriften des Verlags im Forschungszentrum Jülich*** unter
http://wwwzb1.fz-juelich.de/verlagextern1/index.asp

IAS Series
Band / Volume 70
ISBN 978-3-95806-828-5

Mitglied der Helmholtz-Gemeinschaft

JÜLICH
Forschungszentrum